MODELING AND SIMULATION IN PROCESS HAZARD ANALYSES

Júlia Pinto Athanázio de Azevedo

Dissertação de Mestrado apresentada ao Programa de Pós-graduação em Engenharia Química, COPPE, da Universidade Federal do Rio de Janeiro, como parte dos requisitos necessários à obtenção do título de Mestre em Engenharia Química.

Orientadores: José Carlos Costa da Silva Pinto
Maurício Bezerra de Souza Jr.

Rio de Janeiro
Dezembro de 2019

MODELING AND SIMULATION IN PROCESS HAZARD ANALYSES

Júlia Pinto Athanázio de Azevedo

DISSERTAÇÃO SUBMETIDA AO CORPO DOCENTE DO INSTITUTO ALBERTO LUIZ COIMBRA DE PÓS-GRADUAÇÃO E PESQUISA DE ENGENHARIA (COPPE) DA UNIVERSIDADE FEDERAL DO RIO DE JANEIRO COMO PARTE DOS REQUISITOS NECESSÁRIOS PARA A OBTENÇÃO DO GRAU DE MESTRE EM CIÊNCIAS EM ENGENHARIA QUÍMICA.

Examinada por:

_____
Prof. José Carlos Costa da Silva Pinto, D.Sc.

_____
Prof. Maurício Bezerra de Souza Jr., D.Sc.

_____
Dr. Rafael Raoni Lopes Britto, D.Sc.

_____
Prof. Paulo Fernando Ferreira Frutuoso e Melo, D.Sc.

_____
Dr. Normando José Castro de Jesus, D.Sc.

RIO DE JANEIRO, RJ - BRASIL
DEZEMBRO DE 2019

Azevedo, Júlia Pinto Athanázio de

Modeling and simulation in process hazard analyses / Júlia Pinto Athanázio de Azevedo. – Rio de Janeiro: UFRJ/COPPE, 2019.

XXIV, 186 p.: il.; 29,7 cm.

Orientadores: José Carlos Costa da Silva Pinto

Maurício Bezerra de Souza Jr.

Dissertação (mestrado) – UFRJ/ COPPE/ Programa de Engenharia Química, 2019.

Referências Bibliográficas: p. 140 - 149.

1. Identificação de Perigos. 2. Modelagem e Simulação. 3. LIPP-SHAC. I. Pinto, José Carlos Costa da Silva *et al*. II. Universidade Federal do Rio de Janeiro, COPPE, Programa de Engenharia Química. III. Título.

Agradecimentos

Primeiramente, agradeço a Deus, pois no meu caminho sempre houve meios de lembrar que não estou só, alimentando a minha força para seguir frente aos desafios.

Agradeço à minha família: Fabricio, meu marido, pelo companheirismo, parceria e amor, que me fortalecem e foram fundamentais durante o período deste trabalho; meu pai, Roberto, pela dedicação, amor e inspiração de disciplina e boa vontade; e minha Vó, Maria, pelo carinho e cuidado, que nunca faltaram.

Agradeço aos meus orientadores: Zé e Maurício, pela paciência, dedicação e disponibilidade durante o processo de construção desta dissertação. Ao Zé, pela presença descontraída e leve, aliada à vasta experiência, com a qual pôde acolher minha personalidade e anseios; e ao Maurício pela motivação e constante incentivo.

Agradeço aos amigos do mestrado: Daniel, amigo de longa data, pela parceria sem igual (tens minha eterna gratidão!); Pedro, por sempre manter o bom humor e, mesmo em meio ao fogo, ter a serenidade de estender a mão; Lucas, por compartilhar sua sensibilidade e genialidade; Aninha, pela doçura, força e coragem; e os queridos Danillo, Sâmia e Tet por tornarem o dia-a-dia mais agradável e divertido.

Agradeço às minhas amigas de vida: Clara, Rebeca, Júlia e Thais por nutrirem minhas raízes e, especialmente, Alice, companheira de profissão, por enriquecer minha formação como pessoa e engenheira. Agradeço a Glaucia, por disponibilizar seu tempo para contribuir com o trabalho, e também pela referência de profissional que é para mim.

Agradeço aos meus padrinhos: Mônica e Tuca, pela confiança depositada em mim e pela presença alegre, que sempre me enche de energia!

Agradeço aos professores do PEQ, que contribuíram para uma formação de excelência; e aos colegas do programa, Thamires, Carol, Jonildo, Sergio e Ataíde, que compartilharam suas experiências de bom grado e, certamente, tornaram o caminho menos difícil.

Agradeço à secretaria acadêmica, especialmente à Vera, pela disponibilidade e presteza em nos atender. E por fim, mas não menos importante, às instituições de fomento à pesquisa do Brasil, Cappes e CNPq, pelas bolsas de estudo oferecidas ao programa.

Resumo da Dissertação apresentada à COPPE/UFRJ como parte dos requisitos necessários para a obtenção do grau de Mestre em Ciências (M.Sc.)

MODELAGEM E SIMULAÇÃO EM ANÁLISES DE PERIGOS DE PROCESSOS

Júlia Pinto Athanázio de Azevedo

Dezembro/2019

Orientadores: José Carlos Costa da Silva Pinto
Maurício Bezerra de Souza Jr.

Programa: Engenharia Química

O presente trabalho tem como alvo desenvolver um caminho sistemático para aplicação de simulação computacional para identificação de perigos de processos, objetivando minimizar problemas referentes aos métodos tradicionais, e propõe uma metodologia baseada na associação dos principais pontos de trabalhos anteriores, e contribui com aspectos relacionados à preparação de simulações e à determinação do conjunto mínimo de variáveis de processo que viabilizam a posterior interpretação dos resultados. Para ilustrar, a etapa de reação do propeno para formação de polipropileno (processo LIPP-SHAC) foi usada como estudo de caso. Como resultado, obteve-se uma análise de perigos totalmente baseada em modelagem e simulação - complementada por um estudo de frequência baseado no método de Monte Carlo - que foi comparada a um estudo de HAZOP tradicional independente, discutindo-se as principais diferenças e vantagens de cada método. Além disso, aspectos de modelagem foram avaliados por meio de simulação de modelos com diferentes níveis de detalhamento, visando a investigar o efeito das premissas e dos parâmetros, quando o modelo é submetido a uma ampla faixa de condições operacionais. Finalmente, recomendações para o uso de modelagem e simulação aliadas à identificação de perigos foram propostas, buscando potencializar o emprego dessas ferramentas no contexto da análise e gerenciamento de riscos.

Abstract of Dissertation presented to COPPE/UFRJ as a partial fulfillment of the requirements for the degree of Master of Science (M.Sc.)

MODELING AND SIMULATION IN PROCESS HAZARD ANALYSES

Júlia Pinto Athanázio de Azevedo

December/2019

Advisors: José Carlos Costa da Silva Pinto
Maurício Bezerra de Souza Jr.

Department: Chemical Engineering

The present work aims to develop a systematic way to use computational simulations for hazard identification, in order to tackle drawbacks related to the traditional methods, and proposes a methodology that is based on the association of the main points of previous works, with new contributions regarding the preparation for the simulations and the characterization of the minimum set of process variables that can enable appropriate interpretation of the results. In order to illustrate the proposed procedure, the propene polymerization process (LIPP-SHAC process) was used as a case study. As a result, hazard analyses based on modeling and simulation - complemented by a frequency study based on the Monte Carlo method - was compared to an independent traditional HAZOP study, in order to highlight the main differences and advantages of each method. Besides, additional modeling aspects were evaluated with the help of simulation performed with different models, in order to investigate the effects of model assumptions and parameter values when the model is used in a wide range of operating conditions. Finally, recommendations for use of models and simulations for hazard identification are proposed, aiming to encourage the use of these tools for risk analysis.

Contents

Agradecimentos iv

List of Figures x

List of Tables xv

List of Symbols xvii

List of Abbreviations xxiii

Chapter 1 1

Introduction 1

1.1. Motivation 1

1.2. Objectives 2

1.3. Dissertation Structure 3

Chapter 2 5

Literature Review 5

2.1. Risk Assessment 5

2.2. Hazard Identification Methodologies 6

2.2.1. Traditional Tools 8

2.2.2. Some Recent Advances 12

2.3. Cause-Consequence Relation: Frequency Estimation 26

2.3.1. Assessment of Scenario Likelihood 26

2.3.2. Traditional Strategies 27

2.3.3. Technological Advances 27

2.4. Polymerization Main Hazards 34

2.4.1. Runaway Reaction 34

Chapter 3 38

Case-Study: Bulk Polymerization of Propene 38

3.1. Propene Polymerization Chemistry 38

3.1.1. Types of Propene Polymerization Process 41

3.2. Case Study Description 43

3.3. Case Study Modeling 45

3.3.1. Assumptions 45

3.3.2. The Kinetic Model 47

3.3.3. The Reaction Rates 48

3.3.4. Moments Method 49

3.3.5. Material Balances 51

3.3.6. Energy Balance 55

3.3.7. Controllers 57

3.3.8. Physical Properties 58

3.3.9. Polymer Properties 59

3.3.10. Parameters and Nominal Conditions 60

3.4. Analysis of Model Implementation 63

3.4.1. Simulation Environment 63

3.4.2. Sensitivity Analysis 63

3.5. Model Adaptation 66

Chapter 4 73

Hazard Identification Method 73

4.1. Proposed Approach 73

Chapter 5 80

Results and Discussion 80

5.1. Device Malfunction Identification 80

5.2. Simulations 81

5.2.1. Normal Condition 81

5.2.2. Malfunction Simulation 82

5.3. Analysis of the Single Failure Approach 118

5.4. Safety Considerations after Simulation Results 127

5.5. Comparison with Traditional HAZOP 128

Chapter 6 136

Conclusions 136

Bibliography 140

Appendix A Verification of Model Implementation 150

Appendix B Thermodynamic Parameters for Model Development 155

Appendix C Possible Failure Modes of Process Devices 159

Appendix D Failure rates of devices 163

Appendix E Hazard Analysis from Simulation Results 169

Appendix F Traditional HAZOP Discussion 173

List of Figures

Figure 2.1-1 - Risk assessment steps. Adapted from (PASMAN, 2015). 6

Figure 2.2.2-1 – Hazard identification research areas from 1974 to 2007. Adapted from DUNJÓ et al (2010)..... 12

Figure 3.2-1 - Process Flow Chart..... 44

Figure 3.4.2-1 - Process variables behavior for different setpoints of monomer purity in the recycled stream: (a) Monomer purity in the recycled stream (left) and purge mass flowrate (right); (b) Monomer mass flowrate to reactor (left) and monomer make-up mass flowrate (right); (c) Propane mass inside the reactor (left) and Productivity (right)..... 65

Figure 3.4.2-2 - Process variables behavior for different setpoints of monomer mass flowrate in the recycled stream: (a) Monomer purity in the recycled stream (left) and purge mass flowrate (right); (b)Monomer mass flowrate to reactor (left) and monomer make-up mass flowrate (right); (c) Propane mass inside reactor (left) and Productivity (right)..... 66

Figure 3.5-1 – Strategy for numerical simulations..... 67

Figure 3.5-2 – Hierarchical structure of Developed Models..... 67

Figure 3.5-3 –Adjustment of the kinetic factor. 68

Figure 3.5-4 – Densities of the saturated liquid near the critical temperature..... 72

Figure 3.5-5 – Comparison of heat capacity near the critical temperature..... 72

Figure 4.1-1 – Characteristics of the HAZOP and the Malfunction Device procedures. 74

Figure 4.1-2 - Generic Process View..... 74

Figure 4.1-3 - Systematic Approach for Device Malfunction Identification. 77

Figure 4.1-4 - Generic Master Logic Diagram. Adapted from PAPAZOGLOU and ANEZIRIS, (2003). 78

Figure 5.1-1 – Possible candidates for process malfunctions. 80

Figure 5.2.1-1 - (—) Normal conditions of the most critical variables for safety. 81

Figure 5.2.2-1 - General disturbance representation: (a) (- - -) (- - -) (- - -) (- - -) decreasing steps; (b) (—) (—) (—) (—) increasing steps; (—) normal steady state 82

Figure 5.2.2-2 – Behavior of critical variables in scenarios S-1 and S-2 with Models 1 and 2. 83

Figure 5.2.2-3 – Behavior of critical variables in scenarios S-1 and S-2 with Model 3. 84

Figure 5.2.2-4 – Behavior of liquid fraction of monomer in scenarios S-1 and S-2 with Model 3 85

Figure 5.2.2-5 – (a) Make-up flow disturbance (10% increase) and (b) Behavior of other mass flowrates with Model 1. 86

Figure 5.2.2-6 – Behavior of critical variables in scenario S-3 with Model 1 87

Figure 5.2.2-7 – Behavior of critical variables in scenario S-3 with Model 2. 88

Figure 5.2.2-8 - Mass flowrates after disturbance of +10% on the monomer make-up stream with Model 2. 88

Figure 5.2.2-9 – Behavior of critical variables in scenario S-3 with Model 3. 89

Figure 5.2.2-10 – Behavior of critical variables in scenario S-4 with Model 1. 90

Figure 5.2.2-11 –Temperature disturbances in scenario (a) S-5; and (b) S-6. 90

Figure 5.2.2-12 - Behavior of critical variables in scenarios S-5 and S-6 with Model 1. 91

Figure 5.2.2-13- Behavior of critical variables in scenarios S-7 and S-8 with Model 1. 92

Figure 5.2.2-14- Behavior of critical variables in scenarios S-7 and S-8 with Model 3. 92

Figure 5.2.2-15 – Behavior of critical variables in scenario S-9 with Model 1. 93

Figure 5.2.2-16- Behavior of critical variables in scenarios S-10 and S-11 with (a) Model 1; and (b) Model 2. 94

Figure 5.2.2-17 – Behavior of critical variables in scenario S-12 with Model 1. 95
Figure 5.2.2-18 – Behavior of critical variables in scenarios S-13 and S-14 with Model 1. 96
Figure 5.2.2-19 – Behavior of critical variables in scenarios S-13 and S-14 with Model 2. 97
Figure 5.2.2-20 – Behavior of critical variables in scenarios S-13 and S-14 with Model 3. 97
Figure 5.2.2-21 – Behavior of critical variables in scenario S-15 with Model 1. 98
Figure 5.2.2-22 – Behavior of critical variables in scenarios S-16, S-17 and S-19 with Model 1. 99
Figure 5.2.2-23 – Behavior of critical variables in scenario S-18 with Model 1. 100
Figure 5.2.2-24 – Mass flowrates after +50% of the inlet catalyst rate with Model 1. 101
Figure 5.2.2-25 – Behavior of critical variables in scenario S-18 with Model 2. 101
Figure 5.2.2-26 – Behavior of critical variables in scenario S-18 with Model 3. 102
Figure 5.2.2-27 – Behavior of critical variables in scenarios S-20 and S-21 with (a) Model 1; and (b) Model 3. 103
Figure 5.2.2-28 – Behavior of critical variables in scenario S-22 with Model 2. 105
Figure 5.2.2-29 – Behavior of critical variables in scenario S-23 with Model 1. 106
Figure 5.2.2-30 – Behavior of critical variables in scenarios S-24 and S-25 with Model 1. 107
Figure 5.2.2-31 – Behavior of critical variables in scenarios S-24 and S-25 with Model 3. 108
Figure 5.2.2-32 – Effects of temperature disturbance with Model 1. 108
Figure 5.2.2-33 - Behavior of critical variables in scenario S-26 with Model 1. 109

Figure 5.2.2-34 – (a) Behavior of critical variables in scenarios S-27 and S-28 with Model 1; (b) Effects of temperature disturbance in scenario S-27; (b) Effects of temperature disturbance in scenario S-28. 110
Figure 5.2.2-35 – Behavior of critical variables in scenarios S-29 and S-30 with Model 1. 112
Figure 5.2.2-36 – Behavior of critical variables in scenarios S-29 and S-30 with Model 2. 112
Figure 5.2.2-37 – (a) Behavior of critical variables in scenarios S-29 and S-30 with Model 3; (b) Pressure dynamics for interruption of the slurry mass flowrate; (c) Polymer fraction dynamics for interruption of slurry mass flowrate. 113
Figure 5.2.2-38 – (a) Behavior of critical variables in scenario S-31 with Model 3. ... 114
Figure 5.2.2-39 – Behavior of critical variables in scenarios S-33 and S-34 with Model 1. 115
Figure 5.2.2-40 – (a) Behavior of critical variables in scenario S-35 with Model 1; (b) Effects of the polymer fraction; (c) Effects of the inlet monomer mass flowrate, mM 116
Figure 5.2.2-41 – (a) Effect of the polymer fraction behavior for $\tau c = 0.1$; (b) Effect of the monomer inlet mass rate, mM for $\tau c = 0.1$ with Model 1. 117
Figure 5.2.2-42 – Behavior of critical variables in scenarios S-36 and S-37 with Model 1. 118
Figure 5.3-1 – Representation of the simulation history. 123
Figure 5.3-2 – Flowchart of the proposed Monte Carlo algorithm. 125
Figure 5.5-1 – Stratified comparison between the standard and the computational based methods. 133
Figure A-1 – Effect on process variables caused by changing input conditions: (a) Melting Index ($g.10min-1$); (b) Productivity; (c) Xylene Soluble content (%p/p) 151

Figure A-2 - Effect on the controlled and manipulated variables caused by changing catalyst mass feed rate 152
Figure A-3 - Effect on the process variables caused by changing input conditions: (a) Melting Index ($g.10min-1$); (b) Productivity; 153

List of Tables

Table 2.2.1-1 – Techniques for hazard analysis Techniques with estimated effort and associated plant lifecycle phase. Adapted from CENTER FOR CHEMICAL PROCESS SAFETY (1992). 8

Table 3.3.2-1 - Polymerization Mechanism and Reaction Rates. 47

Table 3.3.7-1 –Control Strategies (SILVA, 2018). 57

Table 3.3.7-2 – Additional Control Strategies. 58

Table 3.3.10-1 - Parameters of the process model (MATTOS NETO; PINTO, 2001; SILVA, 2018). 60

Table 3.3.10-2 – Nominal conditions of the process model (MATTOS NETO; PINTO, 2001; SILVA, 2018). 61

Table 3.3.10-3 - Kinetics parameters required to perform the simulations (MATTOS NETO; PINTO, 2001; SILVA, 2018). 61

Table 3.3.10-4 –Tuning Parameters of the controllers. 62

Table 3.3.10-5 – Operational ranges of manipulated variables. 62

Table 4.1-1 – Typical Failure Modes of general process streams. 75

Table 4.1-2 - Failure Modes of boundaries and interfaces of process nodes. 76

Table 5.2.2-1 - Polymerization rate term before and after interruption of the condensate flowrate. 104

Table 5.3-1 – Failure data for different devices. 119

Table 5.3-2 – Probability of simultaneous failure after running 1×104 histories per MC simulation. 124

Table 5.3-3 - Probability of simultaneous failure after running 1×105 histories per MC simulation. 124

Table 5.3-4 – Analyzer contribution for simultaneous failure (1×104 histories per MC simulation). 126

Table 5.3-5 – Analyzer contribution for simultaneous failure (1×105 histories per MC simulation). 126

Table 5.5-1 –Comparison of results obtained with different hazard identification methodologies. 129

Table B-1 – Numerical Values and Contributory terms of the equation of state for calculation of properties. 155

Table B-2 – Auxiliary Terms 158

Table C-1– Possible Failure Modes. 159

Table D-1 – Failure rates for device malfunctions as considered in the simulations... 163

Table E-1 – Hazard Analysis Table from Simulation Results. 169

Table F-1 – HAZOP Discussion Results. 173

List of Symbols

a_l	Constant l of propagation adjustment factor	$[dimensionless]$
b_i	Constant i of vapor pressure equation	$[dimensionless]$
C_{AS}	Molar concentration of active site	$[mol/L]$
C_{cat}	Total Molar concentration of catalyst	$[mol/L]$
C_{H_2}	Molar concentration of Hydrogen	$[mol/L]$
c_i	Constant i of liquid density equation	$[dimensionless]$
C_{Pe}	Molar concentration of Propene	$[mol/L]$
C_{PEEB}	Molar concentration of PEEB	$[mol/L]$
Cp_{fluid}	Global heat capacity	$[cal/(kg\,°C)]$
C_{P_i}	Molar concentration of live polymer of chains of size i	$[mol/L]$
Cp_{liq}	Heat capacity of liquid at saturated condition	$[cal/(kg\,°C)]$
Cp_{orig}	Heat capacity curve used for original models	$[cal/(kg\,°C)]$
Cp_{Pol}	Heat capacity of Polymer	$[cal/(kg\,°C)]$
Cp_{Pe}	Heat capacity of propene	$[cal/(kg\,°C)]$
C_{TEA}	Molar concentration of TEA	$[mol/L]$
Cp_{vap}	Heat capacity of vapor at saturated condition	$[cal/(kg\,°C)]$
Cp_w	Heat capacity of Water	$[cal/(kg\,°C)]$
d_i	Constant i of vapor density equation	$[dimensionless]$
E_j	Activation energy of the reaction step j	$[cal/mol\ ]$
E_p	Activation energy of propagation	$[cal/mol\ ]$
f	Adjustment factor of propagation rate	$[dimensionless]$
k_c	Kinetic rate constant for initiation	$[L\ mol/h]$
k_d	Kinetic rate constant for deactivation	$[1/h]$
k_j	Kinetic rate constant for reaction step j	$[variable]$
k_{j0}	Pre-exponential factor for reaction step j	$[variable]$
k_p	Kinetic rate constant for propagation	$[L\ mol/h]$

k_{p0}	Pre-exponential factor of propagation	$[L\ mol/h]$
$k_{p,\dot{m}M}$	Proportional gain of inlet monomer mass flow controller	$[dimensionless]$
$k_{p,T}$	Proportional gain of reactor temperature controller	$[kg/(h\ K)]$
k_{p,T_C}	Proportional gain of condenser temperature controller	$[kg/(h\ K)]$
k_{tH}	Kinetic rate constant for hydrogen chain transfer	$[L\ mol/h]$
k_{tM}	Kinetic rate constant for monomer chain transfer	$[L\ mol/h]$
k_{tS}	Kinetic rate constant for spontaneous chain transfer	$[1/h]$
$k_{p,V}$	Proportional gain of reactor level controller	$[kg/(h\ L)]$
$k_{p,wM}$	Proportional gain of recycled monomer purity controller	$[kg/h]$
k_{xs}	Empirical quality parameter	$[dimensionless]$
$\dot{m_{gas}}$	Mass flowrate of gas	$[kg/h]$
MI	Melting index	$[dimensionless]$
$\dot{m}_l$	Inlet mass flowrate of component l (l = Propene, Propane, H_2, Cat, PEEB, TEA, make-up, recycle)	$[kg/h]$
$\dot{m_{M,c}}$	Mass flowrate of vapor from the reactor to the condenser	$[kg/h]$
$m_{M,c}$	Total mass of monomer inside condenser	$[kg]$
$\dot{m_{M,c,bias}}$	Bias of the manipulated variable $\dot{m_{M,c}}$	$[kg/h]$
$\dot{m_{M,mkup,bias}}$	Bias of the manipulated variable $\dot{m_{M,mkup}}$	$[kg/h]$
$\dot{m_{M,mkup}}$	Mass flowrate of monomer at the make-up stream	$[kg/h]$
$\dot{m_{M,sp}}$	Set point of monomer inlet mass flowrate	$[kg/h]$
$\dot{m_{M,Rec}}\|_{max}$	Maximum mass flowrate of monomer at recycle stream	$[kg/h]$
MM_{H_2}	Molar mass of hydrogen	$[g/mol]$
MM_{Cat}	Molar mass of catalyst	$[g/mol]$
MM_{Pe}	Molar mass of propene	$[g/mol]$
M_n	Number average molecular weight	$[g/mol]$
$\dot{m_{purge,bias}}$	Bias of the manipulated variable $\dot{m_{purge}}$	$[kg/h]$
$\dot{m_{purge}}$	Mass flowrate of purge	$[kg/h]$
m_{PEEB}	Mass of PEEB	$[kg]$

m_{Pol}	Mass of polymer inside reactor	$[kg]$
$m_{s,bias}$	Bias of the manipulated variable $\dot{m}_s$	$[kg/h]$
$\dot{m}_s$	Mass flowrate of Slurry	$[kg/h]$
m_{TEA}	Mass of TEA	$[kg]$
$M_{total,liq}$	Total mass of liquid inside reactor	$[kg]$
$\dot{m}_w$	Mass flowrate of water through the condenser	$[kg/h]$
M_w	Weight average molecular weight	$[g/mol]$
$m_{w,bias}$	Bias of the manipulated variable $\dot{m}_w$	$[kg/h]$
$m_{w,c}$	Total mass of water inside condenser	$[kg]$
N_{Cat}	Number of catalysts mols	$[mol]$
N_h	Total number of histories	$[dimensionless]$
N_n	Number of mols of component n	$[mol]$
N_{Pe}	Number of propene mols	$[mol]$
n_{sf}	Number of histories with simultaneous failures	$[dimensionless]$
P_{avg}	Average probability of failure between tests	$[dimensionless]$
P_{crit}	Critical pressure of Propylene	$[bar]$
PD	Polidispersion index	$[dimensionless]$
PFD_{backup}	Probability of failure on demand of the backup system	$[dimensionless]$
P_M^{SAT}	Vapor pressure of monomer	$[bar]$
$P_{reactor}$	Reactor pressure	$[bar]$
P_{sf}	Probability of simultaneous failure	$[dimensionless]$
Q_C	Heat of condensation	$[cal]$
Q_E	Heat exchanged in the condenser	$[cal]$
Q_{Pol}	Heat of polymerization	$[cal]$
q_s	Volumetric flow of slurry	$[L/h]$
R	Universal gas constant	$[cal/(mol\ K)]$
R_n	Reaction rate of component n	$[mol/(h\ L)]$
R_{pol}	Rate of polymer formation	$[mol/(h\ L)]$

R_{λ_κ}	Rate of generation of the κ^{th} moment of the live polymer size distribution	$[mol/(h\ L)]$
R_{μ_κ}	Rate of generation of the μ^{th} moment of the dead polymer size distribution	$[mol/(h\ L)]$
T	Reactor temperature	$[K]$
T_c	Temperature of condenser	$[K]$
$T_{c,sp}$	Set point of T_c	$[K]$
T_{crit}	Critical temperature of Propylene	$[K]$
T_{in}	Temperature of reactor inlet streams	$[K]$
t_k	Time to failure of the k^{th} failure along the one-year time interval, among n total failures	$[h]$
T_{ref}	Referential temperature	$[K]$
T_{sp}	Set point of T	$[K]$
$T_{w,in}$	Temperature of the water inlet stream to condenser	$[K]$
T_w	Temperature of water in the condenser	$[K]$
UA	Global heat exchange coefficient	$[cal/(K\ h)]$
V	Volume of the reaction mass	$[L]$
V_{crit}	Critical molar volume of Propylene	$[L]$
V_l	Volume of liquid inside reactor	$[L]$
$V_{reactor}$	Reactor volume capacity	$[L]$
V_{sp}	Set point of reactor volume	$[L]$
w_M	Mass fraction of monomer	$[dimensionless]$
$w_{M,mkup}$	Mass fraction (purity) of monomer at make-up stream	$[dimensionless]$
$w_{M,rec}$	Mass fraction (purity) of monomer at recycle stream	$[dimensionless]$
$w_{M,Rec_{sp}}$	Set point of monomer purity at recycle stream	$[dimensionless]$
w_{Pa}	Mass fraction of propane inside reactor	$[dimensionless]$
w_{Pe}	Mass fraction of propene inside reactor	$[dimensionless]$
w_{Pol}	Mass fraction of polymer	$[dimensionless]$
$(X)_i$	General term of the equation of state for the calculation of properties	$[dimensionless]$

$(XC)_i$	Term of the equation of state for calculation of properties regarding heat capacity	$[dimensionless]$
x_{liq}	Liquid fraction of propene	$[dimensionless]$
XS^R	Parameter of XScalculation	$[\%p/p]$
XS	Xylene soluble content	$[\%p/p]$
$(XT)_i$	Term of the equation of state for calculation of properties regarding temperature	$[dimensionless]$
$(X\rho)_i$	Term of the equation of state for calculation of properties regarding density	$[dimensionless]$
Z_{crit}	Propylene critical compressibility factor	$[dimensionless]$
$-\Delta H$	Enthalpy of polymerization	$[cal/kg]$
$\zeta(\chi)$	Generic distribution	$[dimensionless]$
η_κ	κ^{th} order moment	$[variable]$
θ	Dimensionless number given by $1 - T/T_c$	$[dimensionless]$
Θ	Equipment or device test interval	$[h]$
λ_M	Latent heat of monomer condensation	$[cal/kg]$
λ_{device}	Failure rate of the operating device	$[1/h]$
λ_{ie}	Initiating event rate	$[1/h]$
λ_κ	κ^{th} order moment of live polymer chains	$[mol/L]$
λ	Failure rate	$[1/h]$
μ_κ	κ^{th} order moment of dead polymer chains	$[mol/L]$
ρ_M	Density of monomer	$[kg/L]$
$\rho_{Pe,c}$	Critical density of propene	$[kg/L]$
$\rho_{Pe,liq}$	Density of liquid propylene at saturated conditions	$[kg/L]$
$\rho_{Pe,vap}$	Density of vapor propene at saturated conditions	$[kg/L]$
ρ_{Pol}	Density of polymer	$[kg/L]$
ρ_{liq}	Density of liquid propane	$[kg/L]$
ρ_{orig}	Density used for original models	$[kg/L]$
ρ	Slurry density	$[kg/h]$
τ_{T_C}	Integral time of condenser temperature controller	$[h]$

$\tau_{\dot{m}M}$	Integral time of monomer inlet mass flow controller	$[h]$
τ_T	Integral time of reactor temperature controller	$[h]$
τ_V	Integral time of reactor level controller	$[h]$
τ_{wM}	Integral time of recycled monomer purity controller	$[h]$
τ	Temperature term of state equation	$[dimensionless]$
ψ_i	Auxiliary coefficients	$[dimensionless]$
ω	Propene density term of state equation	$[dimensionless]$
Ω	Dimensionless temperature	$[dimensionless]$

List of Abbreviations

AC: Controller of monomer purity (analytical controller)…….. 44

BN: Bayesian networks…….. 27

CSTR: Continuous Stirred Tank Reactors……... 44

CV: Controlled Variables…… 56

DAG: Directed Acyclic Graphs……... 27

DBN: Dynamic Bayesian Networks…… 28

ET: Event Tree…… 26

FC: Controller of flow……. 44

FMEA: Failure Mode and Effect Analysis…….. 8

FT: Fault Tree…….. 26

HAZID: Hazard Identification…… 18

HAZOP: Hazard and Operability Analysis……. 8

ICI: Imperial Chemical Industries……... 29

LC: Controller of level…… 44

LIPP-SHAC: Liquid Polymerization of Polypropylene with Super High Activity Catalyst…… 42

LOC: Loss of Containment…….. 7

LOPA: Layer of Protection Analysis…….. 12

LOPC: Loss of Primary Content…….. 76

MAWP: Maximum Allowed Working Pressure…….. 80

MCMC: Markov-Chain Monte-Carlo…… 30

MI: Melting Index……... 41

MV: Manipulated Variables…… 56

MMD: Molar Mass Distribution…….. 41

NDFs: Numerical Differentiation Formulas……... 62

P&IDs: Process and Instrumentation Diagrams…….. 10

PEEB: Para-Ethyl 4-EtoxyBenzoate……... 43

PP: Polypropylene……... 37

SDG: Signed Directed Graphs……. 17

SIF: Safety Instrumented Function…….. 34

SIL: Safety Integrity Level…….. 13

SIS: Safety instrumented System…… 14

TEAL: Triethyl Aluminum ……. 43

TC: Controller of temperature …… 44

VSVO: Variable-step, Variable-order……. 62

XS: Xylene Soluble Content…… 41

Chapter 1

Introduction

1.1.Motivation

Chemical and oil processes are intrinsically sources of potential hazards due to the necessity of dealing with toxic compounds, higher energetic substances and large-scale equipment. History has shown that if these processes are not properly managed, the results can be catastrophic (BOWONDER, 1987; GORDON, 1998; VENART, 2004).

For instance, one can remember the Bophal accident, when thousands of people died and many more were injured due to the contamination with a toxic gas that was released from an over-pressurized reactor under a runaway reaction (JOSEPH; KASZNIAK; LONG, 2005).

The causes of major accidents have been mainly related to lack of knowledge about process and system safety (PASMAN, 2015). However, accidents [such as the ones in Bophal (1984) and Seveso (1976)] called society's attention for the need to improve industrial safety (JOSEPH; KASZNIAK; LONG, 2005; KLETZ, 2009). As a matter of fact, many efforts have been made to develop and regulate the safe operation of industrial plants (CENTER FOR CHEMICAL PROCESS SAFETY, 1992). The field of safety engineering has been organized since then and became more accessible, conveying industry to a new level of maturity on safety (PASMAN, 2015).

In a first moment, the lack of knowledge about process safety was usually compensated by introduction of safety margins (PASMAN, 2015). However, the availability of new tools and methods, has made it possible to reduce and sometimes

eliminate these margins - when not safe vital - looking for efficiency on costs and operation (PASMAN, 2015). The main challenge for the industry, nowadays, is making processes more competitive without compromising safety (PASMAN, 2015).

At this new stage, the accident causes often are more related to cost considerations and pressure on decision-making - present in all hierarchy levels – rather than to lack of knowledge. Therefore, assessment of process risks, development of cost and time-saving tools and application of systematic approaches for process safety management are crucial to allow efficient risk-informed decision making and, thus, to avoid accidents and losses (PASMAN, 2015).

1.2.Objectives

In the context of risk assessment and risk-based decision, the hazard identification step is crucial because it is the starting point for further and more involving analyses that compose a robust process safety management system. When hazardous scenarios are overlooked or underestimated, a false safety perception can be created. On the other hand, the overestimation of hazards can result in the misuse and waste of resources.

Based on that, the main objective of the present work is to study how chemical engineering and computational technologies can be combined to enhance hazard identification procedures. Particularly, the use of modeling and simulation tools for competitive hazard assessment is investigated, in order to understand the main challenges, advantages and limitations of their application.

To achieve the proposed goal, the following subsidiary objectives are pursued:

- Identification of the main lines of investigation related to the development of hazard identification tools aiming to understand the drawbacks and advantages of each tool;

- Proposal of a method for hazard identification based on the analyzed tools, particularly with the use of phenomenological modeling and computational simulation;
- Application of the proposed method to a case study in order to:
    - Characterize the modeling features that enable the hazard study;
    - Identify difficulties and drawbacks for generic use;
    - Discuss the performance of the proposed method based on the case study.
- Comparison of the performance of the proposed method with the performance of a traditional one, aiming to uncover benefits and challenges for applications of novel tools.

1.3.Dissertation Structure

This dissertation is divided into six chapters. In Chapter 2, the main issues related to risk analysis and hazard identification are reviewed and discussed. The progress made to quantify accident frequencies is also reviewed. Chapter 3 describes the case study selected to evaluate the proposed hazard analysis methodology and presents the process modeling. Chapter 4 introduces the bases of the proposed hazard methodology and Chapter 5 applies the proposed method to the selected case study. Also in Chapter 5 the model is adapted to allow for safety analyses and simulations are presented. Particularly, results obtained with different models are discussed and compared to results obtained with a traditional hazard identification approach. In order to validate the single failure approach used for the analysis of the case study, a Monte Carlo simulation procedure was implemented and discussed. Chapter 6 presents the main conclusions obtained in the present study and recommendations for use of modeling and simulation tools for hazard identification, aiming to enhance the use of these tools in the context of risk analyses. Finally, six appendices have been attached to the present document in order to record the performed

hazard analyses, aiming to support the reader comprehension of the main text without disturbing the fluidity of reading.

The present work was performed at the Laboratory of Process Modeling, Simulation and Control (LMSCP) of the Chemical Engineering Program (PEQ) of Alberto Luiz Coimbra Engineering Research and Postgraduate Institute (COPPE), Federal University of Rio de Janeiro, Brazil.

Chapter 2

Literature Review

2.1.Risk Assessment

A risk assessment systematic comprises a set of analytical tools and methods that can provide the overall evaluation of the process safety and support management based on user-defined criteria of acceptable risk (CENTER FOR CHEMICAL PROCESS SAFETY, 2000; CROWL; LOUVAR, 2002; PASMAN, 2015).

The development of risk assessment tools has been boosted by many factors: (i) the impact of major accidents, (ii) the establishment of process safety and health regulations, and, of course, (iii) the perception that working safely can improve plant operations and profitability (CENTER FOR CHEMICAL PROCESS SAFETY, 1992).

Conceptually, risk can be defined as the combination of the estimated frequency and the estimated consequence of an accidental scenario. In other words, risk can be understood as the measure of the damage based on its magnitude and likelihood. Aerospace and, mainly, nuclear industries pioneered the development of methods for quantitative risk analyses, with extensive studies published in the early 1980s. (CENTER FOR CHEMICAL PROCESS SAFETY, 2000)

Risk assessment can be performed with various levels of detail, depending on the objectives, tools and applied methodology. However, the following steps are normally needed for a proper risk assessment (PASMAN, 2015):

1 – Identification of hazards: which scenarios can cause potential upset effects?

2 – Quantification of consequences: what is the extension of the accidental effect?

3 – Quantification of frequencies: how often can the accidental scenario occur?

4 – Quantification of risk: how many deaths/how much cost can the damage cause?

5 – Risk Reduction: what are the necessary safeguards and management procedures needed to achieve an acceptable risk?

6 – Risk Management: what is the cost-effective decision to keep the plant into the tolerable risk region?

A systematic view of the described steps is shown in Figure 2.1-1, with examples of common related analytical tools.

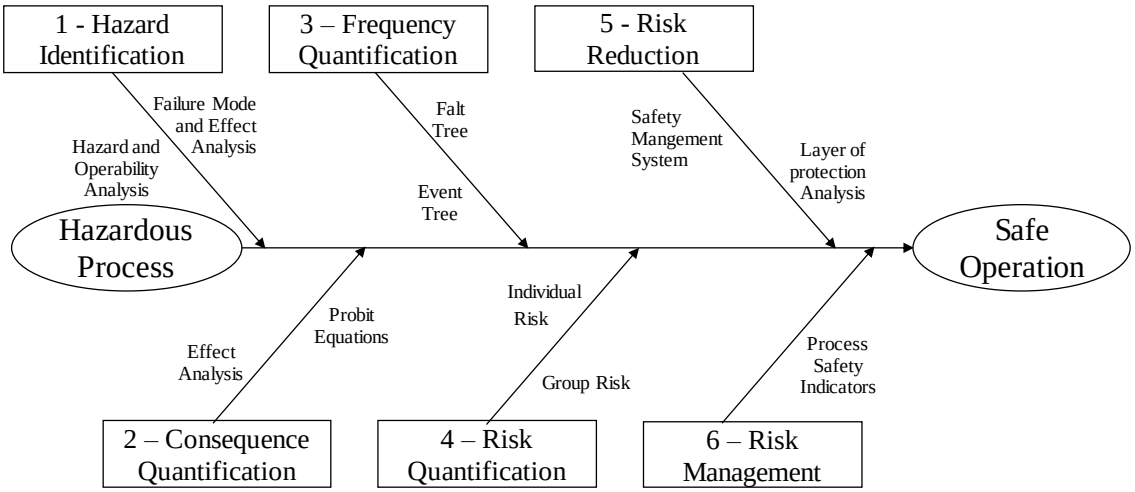

Figure 2.1-1 - Risk assessment steps. Adapted from (PASMAN, 2015).

The present text focuses on hazard identification methodologies and frequency estimation, reviewing the most traditional methods used by oil and chemical companies and the computational advances reported by scientific organizations and academia.

2.2.Hazard Identification Methodologies

Effective hazard evaluation programs constitute the heart for fruitful process safety management systems. To be successful, hazard identification studies must provide clear information for further risk assessment steps; must provide high quality information to support decision-making; and must employ the minimum amounts of resource to achieve

the first two goals (CENTER FOR CHEMICAL PROCESS SAFETY, 1992). Particularly, it is necessary not only to identify scenarios but also understand the potential severity that they can have (DUNJÓ et al., 2010).

According to Pasman (2015), the hazard identification step is the major cause of uncertainty in risk assessment process. Although hazard identification seems to be the "easiest" step, when compared to the complexity of remaining steps, differences observed when different analysts or tools are involved worry experts and responsible parts.

Hazard identification techniques aim to identify the hazardous situations related to inherent weaknesses in design and operation of a given process and generally present a qualitative nature (CENTER FOR CHEMICAL PROCESS SAFETY, 1992).

When performing hazard identification studies, one should look for potential mechanisms of loss of containment (LOC), which means the release of chemical substances beyond the designed boundaries (PAPAZOGLOU; ANEZIRIS, 2003). Besides, hazard identification analyses should be performed throughout the whole plant lifecycle, including design, operation and decommissioning. For each process phase and depending on the available information, characteristics of the analyzed process and demanded results, distinct hazard identification tools can be selected (CENTER FOR CHEMICAL PROCESS SAFETY, 1992). Although hazard identification constitutes a fundamental step of the risk assessment process, it can be performed independently from frequency estimation and risk analyses (CROWL; LOUVAR, 2002).

The present text focus on hazard identification tools that can be applied to the design (last phases) and operation, when detailed information about equipment and operation of chemical processes are already available.

2.2.1. Traditional Tools

The most employed techniques for hazard identification are based on expert and/or multidisciplinary skilled team knowledge applied to a systematic procedure. Checklists and Surveys, What-If, Failure Mode and Effect Analysis (FMEA), Hazard and Operability Analysis (HAZOP), among others, are usually applied to perform this task (GRAF; SCHMIDT-TRAUB, 2000). Table 2.2.1-1 shows commonly used techniques, according to the required level of detail (measured according to the estimated time to perform a study) and the associated plant lifecycle phase:

Table 2.2.1-1 – Techniques for hazard analysis Techniques with estimated effort and associated plant lifecycle phase. Adapted from CENTER FOR CHEMICAL PROCESS SAFETY (1992).

	Checklist	**Preliminary Hazard Analysis**	**What-if**	**HAZOP**	**FMEA**	**Fault Tree**	**Event Tree**
	10 h	52 h	52 h	80 h	50 h	216 h	144 h
Research and Development		x	x				
Conceptual Design							
Detailed Engineering	x	x	x	x	x	x	x
Construction and Start-up	x		x				
Routine Operation	x		x	x	x	x	x
Decommissioning	x		x				

The main limitations of traditional hazard identification methods are related to: (i) reproducibility (each group may achieve a different result); (ii) possibility of incompleteness (there is no indication that all scenarios are necessarily covered); (iii) inscrutability (sometimes it is hard to understand the registered discussions and to use them); (iv) subjectivity and experience-based (it depends on human judgment to determine scenarios) (CENTER FOR CHEMICAL PROCESS SAFETY, 1992).

Among the traditional hazard identification methods, special importance can be assigned to HAZOP, due to its worldwide application, legislation approval and effectiveness in identifying hazards (DUNJÓ et al., 2010). For example:

> *"The HAZOP technique has been widely adopted and is the centerpiece of the hazard identification system in many companies." (MANNAN, 2014)*

> *"The HAZOP method is the main classical hazard identification tool used in risk analysis, on which scenarios can be based." (PASMAN, 2015)*

HAZOP was originally developed to identify hazards in the design phase of new installations, in the early 1970s (PASMAN, 2015). Nevertheless, it is a useful tool for almost all plant lifecycle phases, including operation (CENTER FOR CHEMICAL PROCESS SAFETY, 1992), being able to simultaneously identify hazards and operability problems (DUNJÓ et al., 2010).

LAWLEY (1974) (apud DUNJÓ et al., 2010) was the first to publish the minimum requirements and steps needed to perform operability and hazard studies based on process parameters rather than on process equipment. HAZOP is an inductive (PAPAZOGLOU; ANEZIRIS, 2003) and disciplined procedure (DUNJÓ et al., 2010) based on brainstorming activity that uses the creativity that results from the interaction between participants and their experience (PASMAN, 2015). Imperial Chemical Industries (ICI) was the first to establish that HAZOP should be performed by an interdisciplinary team

with the necessary skills to identify potential hazards (CENTER FOR CHEMICAL PROCESS SAFETY, 1992).

The popularity and strengths of HAZOP is related to the fact that it is an "opened-ended" and "thinking-together among members" approach (PASMAN, 2015). Although HAZOP is a well-established technique and known worldwide, each company and organization has adjusted the technique to fulfill its particular necessities (CENTER FOR CHEMICAL PROCESS SAFETY, 1992).

The HAZOP procedure consists initially in reviewing the plant drawings (process and instrumentation diagrams, P&IDs) and, complementarily, the associated logic diagrams and procedures, in order to define study nodes, which are sections of the P&ID that can include equipment, lines and/or operation steps (CROWL; LOUVAR, 2002). After defining the study nodes, the normal operation condition must be presented, including process parameters, substances, sequential operation, among other relevant pieces of information. Then, a systematic approach is applied to identify deviations from the normal design intention: guide words (no, more, as well as, other than) are combined to process variables/parameters to characterize operation scenarios (CENTER FOR CHEMICAL PROCESS SAFETY, 1992).

For every process deviation (guide words + process variable), the group should speculate about the associated consequences and list all possible causes. The existing safeguards to prevent the deviation should also be recorded and, finally, additional recommendations should be provided, if necessary (CENTER FOR CHEMICAL PROCESS SAFETY, 1992). Generally, the need of additional safeguards must be decided based on the team's experience and/or based on some sort of risk acceptability criteria (PASMAN, 2015). The procedure is repeated until all relevant combinations of guide

words and process variables/parameters are analyzed for all process nodes (CENTER FOR CHEMICAL PROCESS SAFETY, 1992).

Due to its popularity, HAZOP applications have been extended to other fields of knowledge, as medical diagnostic systems, road-safety and photovoltaic facilities (DUNJÓ et al., 2010). However, although recent studies recognize the importance and applicability of HAZOP, they also reinforce the intrinsic limitations and drawbacks of the technique, as follows:

- Subjected to human factor: safety relevant scenarios may be forgotten; for complex plants, consequence discussion may be inaccurate and unclear (GRAF; SCHMIDT-TRAUB, 1999; TIAN; DU; MU, 2015);
- Depends on team skill and experience (ŠVANDOVÁ et al., 2005);
- Time-consuming and labor-intensive (DUNJÓ et al., 2010; PAPAZOGLOU; ANEZIRIS, 2003; VENKATASUBRAMANIAN; VAIDHYANATHAN, 1994) ;
- Expensive (LABOVSKÁ et al., 2014);
- Depends on heuristic knowledge (BAYBUTT, 2015; RAONI; SECCHI; DEMICHELA, 2018);

BAYBUTT (2015) presented a comprehensive critique about HAZOP, aiming to guide multidisciplinary teams on how to compensate the intrinsic HAZOP weaknesses. Besides, as many companies and regulations require periodic revalidations of the hazard identification studies, different research lines have been developed to deal with HAZOP drawbacks and increase its efficiency (PASMAN, 2015).

2.2.2. Some Recent Advances

Due to drawbacks of traditional hazard identification methods, efforts have been made to develop computational tools that are able to minimize them (GRAF; SCHMIDT-TRAUB, 1999). For instance, DUNJÓ et al. (2010) investigated more than 150 journals and books published from 1974 to 2010, related to hazard identification analyses. Figure 2.2.2-1 groups the analyzed papers into distinct research areas. These numbers emphasize the importance of hazard identification for risk assessment and show the safety community's interest in tackling its main limitations.

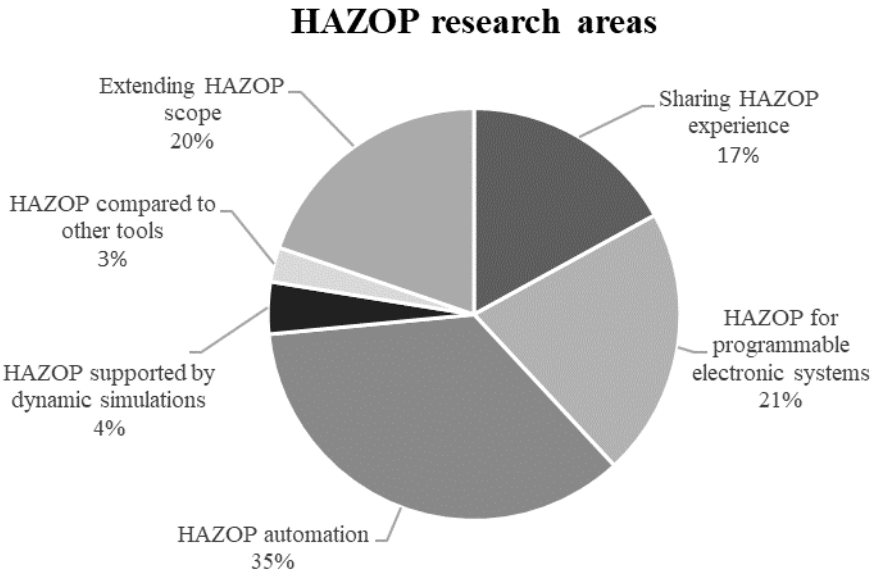

Figure 2.2.2-1 – Hazard identification research areas from 1974 to 2007. Adapted from DUNJÓ et al (2010).

The research group "HAZOP compared to other tools" roughly aims to compare the HAZOP to other tools, discussing the coverage, scopes and limitations of the analyzed techniques. As identified by different authors, HAZOP lacks on covering accident causes related to organization factors (DUNJÓ et al., 2010). Regarding the group "Extending" HAZOP scope", studies propose hybrid methods that combine HAZOP with other methodologies, including combination of HAZOP with Failure Mode and Effect Analysis

(FMEA) (to improve quality), HAZOP with Layer of Protection Analysis (LOPA) and HAZOP with Fault Tree Analysis (FTA) (to support quantification of risk and minimize uncertainty), HAZOP with Check-list (to prioritize process areas and identify accident mechanisms) (DUNJÓ et al., 2010). For example:

> *"No single technique can support all the aspects of safety/risk, so the process of safety/risk assessment is best achieved through a systematic approach using combinations of the (...) techniques"* (RAMZAN; COMPART; WITT, 2007).

The need to embrace features related to management attitudes, organization culture, operational training, among other human factors, constitutes another line of investigation to extend the HAZOP scope. Human error is related to 50% to 90% of the operational risk (DUNJÓ et al., 2010). Therefore, new guide words and new parameters related to human aspects (for example, missing information or action) or deviations based on specific human failure have been proposed by different authors. Attempts to take into consideration aspects of safety-management failures have also been put in practice (DUNJÓ et al., 2010). The particularities of batch processes, where the human interference is more active than in continuous processes, constitute another topic of interest to increase the HAZOP scope (DUNJÓ et al., 2010).

Subjectivity, inherent to most of hazard analysis techniques, may be regarded as positive because it allows creativity and captures human experience; on the other hand, it introduces dependency on human judgment to define the relevance and mechanism of different scenarios. Many authors have studied critical quality aspects of a "gold hazard analysis" and shared their experiences. The relevance of this research line comes from the fact that expertise can be acquired from knowledge sharing and data stored on data bases (DUNJÓ et al., 2010).

Connecting HAZOP results with Safety Integrity Level (SIL) provided by a Safety Instrumented Function (SIF) constitutes another research line identified by DUNJÓ et al. (2010). Particularly, the rapid advances of process automation have introduced the necessity of implementing dedicated Safety Instrumented System (SIS) to take care of the process safety. Combinations of HAZOP with LOPA and HAZOP with FTA (for more complex systems) have been presented as useful combinations to specify the SIL requirement (DUNJÓ et al., 2010).

According to Figure 2.2.2-1, research work related to hazard identification automation concentrated most publications in the last decade regarding the evolution of hazard identification methods. The implementation of the so-called "expert systems" focuses on hazard identification automation to reduce the analysis time and to facilitate the application of the procedure (DUNJÓ et al., 2010).

PARMAR and LEES (1987) (apud GRAF; SCHMIDT-TRAUB, 2000) reported the first research regarding the automation of hazard identification methods. These authors proposed a computational-based tool, programmed to automatically generate causes and effects of a process deviation, based on a fault-propagation model (PARMAR; LEES, 1987a, 1987b). This type of approach, named qualitative modeling, improves the precision of hazard analysis and enables re-usage of the obtained results (GRAF; SCHMIDT-TRAUB, 1999). However, similar proposals bring an important challenge related to the inexistence of a "universal model" that can be used for all processes introducing a preliminary preparation step that can take time and require expertise.

PARMAR and LEES (1987a) highlighted four features that must be considered by a general hazard identification expert system: (i) it must be based on a plant model (the model consists of rules and plant configuration information that define the interconnection between process states, not necessarily a detailed phenomenological

model; (ii) it must provide a control strategy to transfer the model information to the hazard identification table; (iii) it must facilitate the comprehension of the cause-effect relation; (iv) and it must also allow for increasing knowledge data-bases (learning mechanism).

VENKATASUBRAMANIAN and VAIDHYANATHAN (1994) developed an expert system, called HAZOPExpert, aiming to reduce time and effort, increase level of detail and minimize human error related to the HAZOP analyses. HAZOPExpert is a knowledge-based system, that depends on two types of information: process-specific (material characteristics, reaction nature, etc.) and process-independent models (equipment type, common causes and consequences, propagation method). These two groups can interact with each other in the system framework, through an objected-oriented architecture, creating process-specific descriptions for a HAZOP study. Efforts have been made to identify common causes and consequences of common groups of equipment that are present in most chemical process units. However, some specific equipment require complex automatization because they differ significantly from process to process (VENKATASUBRAMANIAN; VAIDHYANATHAN, 1994).

Digraph-based models have been developed for general processes to facilitate and expand the user interface. In the HAZOP automation context, this kind of model has been used to provide graphical representation of causal models with qualitative cause-effect relation resulting from the propagation of a process variable deviation through the flowsheet. Digraphs were first used for fault tree construction and to support fault diagnostics. They consist of graphical boxes that contain the qualitative states of process variables (node values) and are interconnected by directed arcs that increase or reduce the node value through arc gain (model gain) (VAIDHYANATHAN; VENKATASUBRAMANIAN, 1995).

GRAF and SCHMIDT-TRAUB (1999) proposed a qualitative hazard assessment method based on state chart modeling and simulation, applied on the early phases of the process design, when detailed plant information is not available. Instead of using continuous numerical variables, the method consists of describing the process variables in terms of discrete states. The transition between states is triggered by events or conditions included in the model. The methodology was applied to an ethyl acetate plant, generating seven hundred qualitative states that could be trigged by more than 15,000 identified events and conditions. The simulation starts from the normal operating scenario and then a single deviation is imposed. The model is capable of generating the chain of effects in the whole plant and providing a consistent view of the system behavior and interdependent hazard. The methodology was compared to the traditional HAZOP procedure and it was possible to notice that the results were not significantly different. However, the traditional method boosted human creativity and identification of complex risks, while the second method was more systematic and allowed for better documentation of hazards. It was understood that the computational-based tool can be a strong allay of the traditional method, being able to enhance its quality (GRAF; SCHMIDT-TRAUB, 1999).

One year later, a detailed review of the previous work was published and provided reflections about qualitative modeling in a state-chart form, demanding the development of hazard assessment tools that consider the mechanism and likelihood of hazardous scenarios (GRAF; SCHMIDT-TRAUB, 2000).

SHACHAM; BRAUNER and CUTLIP (2000) reported an open architecture simulator, consisting of model equations that can be modified for further analysis. The authors considered this to be important in order to allow for faster simulations in case of abnormal conditions and identification of the possible hazard causes. The method was

applied to a batch propylene oxide polymerization reactor and the results confirmed that, depending on the case, the process behavior depended on the analyzed failure and respective time of occurrence. Consequently, accessible simulations constitute important tools to predict the process behavior and support decision-making.

PAPAZOGLOU and ANEZIRIS (2003) proposed a structured and deductive methodology for identification of causes of loss of primary content, called Master Logic Diagram (MLD). The proposed methodology was similar to the event tree approach, although the quantification of event probability in each branch was not the key focus. Instead, physical deviations related to structural failures (which reduce the design capacity of the process containment barrier or increasing the process load against the containment barrier) were identified: high temperature; overpressure; under pressure; corrosion; erosion; vibration; external loading among others. Based on identified failures, team effort should be made to identify the immediate causes or the initiating events of the failures. The method was applied to an ammonia storage unit and the results were compared to real accident causes, showing that the main initiating events could indeed be identified by the method. Besides, the MLD procedure was compared to the HAZOP methodology and the results showed MLD advantages on identifying initiating events with more detailed consequence analyses. (PAPAZOGLOU; ANEZIRIS, 2003).

(MCCOY, ZHOU and CHUNG (2006) reported that signed directed graphs (SDG) were the most used method for semi-automated hazard identification analyses. The main advantages of SDG pointed by the authors were the simplicity and efficiency on simulating the chain of events after a failure in a process plant. On the other hand, this kind of model is based on linear and “blind” chain of events, which generally does not consider time evolution and tends to exaggerate the number of process hazard scenarios, as the technique is not able to distinguish reasonable scenarios from unrealistic ones.

(MCCOY, ZHOU and CHUNG (2006) considered that SDF should be improved to consider better models and better description of events transition in a process plant, detailing process states, adding process constraints and taking into account degradation and other realistic process conditions.

Many other studies have been developed to automatize hazard analysis, resulting on the creation of OPHAZOP, containing a library of facts, rules and information of process plants, which was upgraded as TOPHAZOP; EXPERTOP equipped with a knowledge-based structure and an inference tool; STOPHAZ (Support Tool for Process Hazard Analysis); HAZOPtool; COMHAZOP among others (DUNJÓ et al., 2010). Particularly, PASMAN (2015) highlighted the innovative character of the method proposed by SELIGMANN et al. (2012): Blended Hazard Identification (HAZID). BLHAZID combined features of a function-driven method with a component-driven approach, aiming to detail the failure causes, extend the hazard coverage and provide a framework for reuse, fault diagnosis and semiquantitative examinations (SELIGMANN et al., 2012). Finally, attempts have also been made to use artificial intelligence hazard identification automation and to automatize hazard identification preparation steps and estimation of the analysis duration (DUNJÓ et al., 2010).

DUNJÓ et al. (2010) also reported the use of dynamic simulations to support hazard identification analyses. The use of dynamic simulations can improve hazard identification methods and support for design of effective risk reduction measure for instance, providing safety response times (BERDOUZI et al., 2018) and improve operational training. According to DUNJÓ et al. (2010), however, the application of dynamic simulations to support hazard analysis has been used mainly for teaching purposes.

DUNJÓ et al. (2010) concluded that researches that intend to adapt hazard identification methods to new technologies are essential to keep it up to date. Besides, researches related to sharing of experience can be very relevant for training purposes. Although many attempts have been made to automatize hazard identification procedures, it is important to emphasize that most hazard identification analyses are still being conducted with the traditional HAZOP method, based on human expert teams.

Five years after the remarkable literature review provided by DUNJÓ et al. (2010), the understanding about the development of hazard identification methods, was divided into two main classes: theoretical methods, based on expert knowledge and using qualitative modeling, and computational methods, which make use of modeling and simulation to reveal cause-effect relation (LABOVSKÁ et al., 2014; PASMAN, 2015) The present text focuses on the computational approaches.

- **Modeling and Simulation Tools Applied for Hazard Analyses**

ŠVANDOVÁ et al. (2005) proposed a new hazard assessment approach by integrating the traditional HAZOP methodology with well-established modeling and simulation tools. Based on the combination of strategies, multiplicity of steady states, process stability and non-linear dynamics could be included into the analysis. The method was applied in propylene and higher glycol production processes. This process, under certain operation conditions, presents multiple steady-states, which can directly affect the hazard study. Modeling and simulation results showed that the consequences of some process deviations (originating from the HAZOP guide words) were complex to evaluate without the support of the computational tool, because the duration of the failure played an important role on the process behavior and final attained steady-state, leading in some cases to unexpected accidental scenarios and reaffirming the importance of the proposed approach to understand process behavior and implement robust protection measures.

The quantitative HAZOP, described as the use of dynamic simulations in a traditional hazard identification procedure, can constitute a useful tool for quantifying the magnitude of the effects of process variable deviations on operation conditions. This type of information can complement and improve the quality of the HAZOP method and be used for educational and operational training purposes (EIZENBERG; SHACHAM; BRAUNER, 2006).

The use of process simulations in safety-related studies had been explored little until the last decade. A systematic procedure, called Extended HAZOP, was proposed to include disturbance simulations into the hazard identification framework, associated with new documenting procedures, that separate the physical effects (quantitative simulation results) from the related risk consequences (evaluation of the physical effects) (RAMZAN; COMPART; WITT, 2007). RAMZAN, COMPART and WITT (2007a) believe that most HAZOP qualitative questions do not bring much new information to the analysis, so that simulations can add value to the analytical procedure. An application was performed for a distillation column unit proving the benefits of the method.

Although many commercial simulators are available, they are normally applied to examine process operability and control aspects, so that extrapolations that describe process malfunctions may not be realistic. Therefore, RAMZAN, COMPART and WITT (2007a) highlighted that the success of the method is linked to the model quality, so that the analyst should be careful about model constraints and assumptions before using the simulation results, which should be validated with actual process data (RAMZAN; COMPART; WITT, 2007).

LABOVSKÝ et al. (2007a) discussed some basic principles of using mathematical models to support the hazard identification of multiphase exothermic reactors. Due to the specificity of most chemical reactions, a general software for chemical simulation of

reactors is not available. When modeling this kind of unit, it is necessary to use adequate numerical algorithms for integration of the differential balance equations and to estimate the model parameters properly. The model should describe the important process variables and count on accurate parameters so that the selection of the model, the model assumptions and the model parameters are all crucial for a reliable prediction of the process behavior.

LABOVSKÝ et al. (2007b) performed a model-based HAZOP analysis for a complex ether plant. The existence of multiple steady states was confirmed through model simulations. Particularly, the presence of multiple steady states affected the process operation point during and after the occurrence of the process deviation. This non-expected behavior could not be identified qualitatively and indeed allowed for improvement of the quality of the proposed hazard analysis.

Other works discussed the influence of multiple steady states on process safety. The application of a mathematical model both for steady state and dynamic simulations can significantly improve the level of detail during the hazard identification study. Steady-state simulations can be used to investigate the possible occurrence of multiple operation values and the stability along a wide range of parameter values, while dynamic simulations can provide the time-dependent behavior of the process variables in presence of a certain disturbance (LABOVSKÁ et al., 2014).

Attempts to integrate qualitative knowledge-based modeling with quantitative dynamic simulations have been made to increase the level of detail and the quality of HAZOP analyses, mainly for the identification of hazardous consequences. The proposed procedure was applied to a three-phase separation process and showed that the use of quantitative simulations can validate the qualitative cause-effect relationships (WU et al., 2014).

DynSim-HAZOP is a method that combines dynamic simulation in HAZOP studies, where deviations are converted into parameter disturbances and the effects are obtained as simulation outputs. Two case studies (an extractive distillation column and an ammonia production plant) were simulated with Aspen Plus and Aspen Dynamics to validate the method and the results successfully provided quantitative time-dependent reliable information about the processes (TIAN; DU; MU, 2015).

A dynamic HAZOP, based on process simulations, was proposed to replicate the sequence of events of the Texas City refinery explosion, which started with the overfilling of a distillation column. As the accident occurred during the plant start-up, the mathematical model did not focus on the dynamics of the separation, since the vessel was not distilling the product yet, but only filling with liquid streams (ISIMITE; RUBINI, 2016). Vapor-liquid equilibrium, heating and filling phenomena were modeled with ASPEN HYSIS and the distillation column was represented as a tank separator. With the performed simulations, it was possible to reproduce the most acceptable version of the accident and find a second pathway for the accident mechanism (ISIMITE; RUBINI, 2016), showing that simulations could be applied to represent normal operating conditions and transient responses during plant start-up and shutdown. The authors reported that Dynamic HAZOP reduced subjectivity improving the accuracy of consequence identification and saving HAZOP team time.

SOARES, PINTO and SECCHI (2016) studied the employment of a safety-based control layer that uses periodic simulations of failure conditions to define the control strategy and variable setpoints. During normal condition, a single-input single-output model-based control, using updated parameters obtained through a reconciliation strategy, is used. Periodically, the updated data is sent to the failure simulator in order to predict the process behavior and check if the operations is safe based on model predictions

and failure scenarios. If the forecasted behavior exceeds the safety limit, the control strategy must be reconfigured to a multiple-input multiple-output controller that uses an optimization algorithm to find a safety set of operating parameters that will drive the process to a safe operation zone and prevent the risk of process shutdown.

JANOŠOVSKÝ et al. (2017) discussed the role of commercial process simulators to support hazard identification analyses. The pre-defined packages and models of the analyzed software can indeed save time and facilitate the simulation task. Nevertheless, some modifications may be necessary in order to accurately describe the system behavior in a wide range of process deviations.

The application of process simulation was also used to identify thermal runaway in a semi-batch oxidation reactor. Actual experimental data were used to validate the accuracy of the model simulations. Simulation results were quantitatively categorized into different classes of severity allowing for reduction of subjectivity (BERDOUZI et al., 2018). As concluded by the authors, dynamic simulations constitutes an important prediction tool for risk analysis, especially during transient operations of non-linear complex processes (BERDOUZI et al., 2018).

Parametric sensitivity and continuation algorithms were applied to analyze an ammonia production plant and evaluate the effects of deviations of process variables and the existence of multiple steady states. Both behaviors are difficult to consider during conventional hazard identification studies and confirm the relevance of using simulations to investigate safety issues (JANOŠOVSKÝ et al., 2018).

BRITTO (2018) showed that modern computational tools can enhance traditional methods of risk assessment. The author proposed the use of simulation tools to understand the process behavior during process malfunctions and to quantify scenarios probabilities

using Monte Carlo simulations. Finally, the author proposed the use of a risk surface that takes into account severity, frequency and time of failure.

The use of process simulations for hazard identification allows for precise cause (malfunction)-effect (process deviation) understanding taking into account the dynamic and non-linear information of the process behavior. Besides, although it does not eliminate the necessity of heuristic knowledge to define the possible process deviations, the technique simplifies the hazard identification session and thus can be used as a time saving tool (BRITTO, 2018). This quantitative assessment of process variable deviations allows for more precise identification of hazardous scenarios and constitutes a powerful tool for identification of alarm activation, supporting a robust alarm management. (BRITTO, 2018)

The proposed method, named Malfunction Procedure, initially performs simulations of normal operation condition, in order to validate the phenomenological model and to obtain relevant normal process values. Then, simulations of malfunctions, identified previously by a first heuristic hazard identification step, are performed to understand the process dynamics and the consequent deviations. The robustness of the procedure is based on the fact that a complete map of process deviations can be made considering the proposed malfunctions. On the other hand, the results depend on the quality of the identification step of plausible process malfunction. (RAONI; SECCHI; DEMICHELA, 2018). Although process deviations can be obtained by simulation, the safety-relevant consequences must be assessed through a second heuristic hazard analysis performed by a multidisciplinary group. Through the effort of the previous simulation study, precise process data can be obtained for each malfunction scenario and deviations can be analyzed by the team with less time and higher quality (RAONI; SECCHI; DEMICHELA, 2018). The choice of the software and model depends on node complexity

and availability of process and design information. Sometimes, simulations performed during the design phase can be used to feed the hazard analysis (RAONI; SECCHI; DEMICHELA, 2018).

The number of controlled variables in a process can be numerous, depending on the process complexity, and quality and productivity demands. The presence of control protocols can substantially complicate the hazard analysis and the identification of critical consequences, since they affect the propagation of disturbances (DANKO et al., 2019).

DANKO et al. (2019) observe that process simulations are one of many tools that can be used to support traditional HAZOP. In their work, the effect of a classical feedback control system was evaluated, when integrated to the raw process model. The results showed that control systems can introduce or increase hazards into a process.

According to the LOPA concept, control systems are the first protection layers of the process after process design. The application of disturbances to a simulation-based hazard identification method should be performed both in the presence and absence of control loops. This leads to better identification of consequence root causes and facilitates the more accurate design of safety barriers (DANKO et al., 2019).

Besides discussing the importance of segregating control loops from the raw-process, DANKO et al. (2019) also compared the roles of dynamic and steady-state simulations for the hazard analyses. Dynamic simulations were used to perform parametric sensitivity analyses which are useful to provide start-up and shutdown hazards and changes of process parameters and device conditions. Steady-state simulations were used to perform continuation and bifurcation analyses to identify runaway conditions and number and stability of steady-states.

In summary, many works have evaluated the application of dynamic process simulations to support hazard identification analyses in the last decades. The main

reported advantages were the possibility to quantify deviations, clarify the cause-effect mechanism and identify complex behaviors (due to process non-linearities and the possible existence of multiple steady states). The use of commercial simulation tools has been widely reported in the references, mainly due to the facility of using pre-existing models, although concerns about model coverage and extrapolation capacity when applied to wide ranges of process deviations have also been expressed.

Recently, PASMAN, ROGERS and MANNAN (2017, 2018) surveyed the hazard identification methods, highlighting their important role for risk assessment context, in spite of their intrinsic weaknesses and incompleteness. Having based their studies on accident investigation reports to look for opportunities to improve hazard identification methods, the authors confirmed that the computational advances can be of great relevance. However, they also highlighted the necessity to integrate equipment features with human factors and transient operations (as start-up and shut-down), because those components are commonly associated with accident causes and are merged into a socio-technical system that if properly modeled, will be able to predict the potential hazards better.

2.3. Cause-Consequence Relation: Frequency Estimation

> *"Central in risk analysis are cause-effect relations of probabilistic nature"* (PASMAN, 2015).

2.3.1. Assessment of Scenario Likelihood

When the assessment of scenario probabilities is compared to advances made on consequence analysis, the probabilistic branch has found more difficulties to progress. This fact is related to the industry resistance to share data of failures and "near misses" and detailed accident information (PASMAN, 2015). The probabilistic estimation of risks

consists in modeling the expected frequency of safety relevant consequences, generally involving a chain of low probability events (SIU; KELLY, 1998).

2.3.2. Traditional Strategies

Fault Tree (FT) and Event Tree (ET) analyses are the methods used most often to estimate frequency of events occurrence (BRITTO, 2018). Particularly, Layer of Protection Analysis (LOPA) is a method that starts with an initiating event frequency and investigates how many and how reliable the protection measures must be to prevent undesired event (CENTER FOR CHEMICAL PROCESS SAFETY, 2001).The main drawback regarding the use of these methods is the multiplication of the many estimated frequencies that convey the initiating event to the undesired scenario (causal model) carrying a level of uncertainty accumulation that makes the final estimate considerably unreliable (FENTON; NEIL, 2013; PASMAN, 2015).

The lower the frequency of occurrence of a particular scenario, the less available the respective statistics will be. In some cases, a potential hazardous event may have never been experienced before. Therefore, the estimation of rare events frequency constitutes a challenging task that requires deep study of the causal model in order to satisfactorily describe cause-consequence relations and obtain the most reliable data collection and failure frequency estimates (FENTON; NEIL, 2013).

Consequently, it is desirable that the causal model is able to correlate events and deal with data variability, updating to the existing conditions and being flexible, among other features to achieve an optimum result (PASMAN, 2015).

2.3.3. Technological Advances

Bayesian statistics has been used widely to support engineering systems and allow for probabilistic risk assessment (KELLY; SMITH, 2009). The fundamentals of Bayesian

statistics have been applied to build Bayesian networks, BNs, which can be useful to model the relationship between causes and final consequences because they take into account the available statistical data and expert judgment, updating the data during the operation time (FENTON; NEIL; MARQUEZ, 2008; SIU; KELLY, 1998). BNs can be represented by directed acyclic graphs, also known as DAG (KELLY; SMITH, 2009). Depending on the application, BNs or causal models (FENTON; NEIL; MARQUEZ, 2008) can be assembled in terms of discrete or continuous probabilities of occurrence for each event that constitutes the chain of events that may convey to the final scenario (PASMAN, 2015).

Bayesian statistics and the concept of conditional probability enable some peculiar modeling aspects, such as common events causes and interdependence, and allow the revision of probability of certain events based on new observations and inferences, which can be very useful to assess risks (FENTON; NEIL, 2013). It is interesting to observe that an existing fault tree and event tree can be turned into a Bayesian Network, or even a LOPA study. This gives the model some benefits, such as precise calculation and the possibility to describe states more in detail (FENTON; NEIL, 2013)

To handle more complex process structures and continuous problems, Monte Carlo simulations and discretization can be helpful. In all cases, the future probabilities are based on the Markov assumption that each event in the stochastic process depends only on the current state and is memoryless (or, in other terms, is not linked to previous events) (PASMAN, 2015).

BNs can be time dependent or not. Omitting time is very common in process risk evaluations when the main goal is understanding the final state probability. Time varying applications, also called Dynamic Bayesian Networks, DBN, are generally used when it is desired to model equipment degradation and domino effects (PASMAN, 2015). DBNs

are able to represent how a certain variable changes its state in time, through a stochastic model (FENTON; NEIL, 2013).

The use of evidences to improve the estimation of a catastrophic event in combination with distribution probabilities constitute an important advance on estimating frequency of a cause-effect relation (PASMAN, 2015). Hierarchical Bayesian approaches are based on the occurrence of accident precursor events, which are defined as events that signalize the process potential to damage (KHAKZAD; KHAN; PALTRINIERI, 2014), such as “near misses”, activation of safety devices and intermediate events that take place before the undesired consequence (PASMAN, 2015).

Applications of Bayesian approaches to financial, health and ecological problems indicate the popularization of Bayesian statistics fundamentals and the advent of tools and computational resources that enable the implementation of Bayesian strategies in risk and uncertainty analysis (KELLY; SMITH, 2009).

As discussed before, the main concern about catastrophic event probabilities is the uncertainty related to multiple precursor events. In this context, the use of fuzzy sets seems attractive because they use the distribution of probabilities related to the occurrence of single events. Thus, this strategy somehow provides information about the chain of uncertainty of a major event (PASMAN, 2015). Understanding probability as a subjective measurement of an event likelihood is crucial when the risk information is used as reference to support decision under uncertainty (SIU; KELLY, 1998).

Bayesian networks have been applied to characterize the reliability of software systems, enabling the prediction of defects through incorporation of qualitative and quantitative measurements. However, using BNs that involve continuous nodes led to imprecision due to use of static discretization methods. Advances on BNs solution strategies and development of dynamic discretization procedures allowed overcoming of

this drawback and increase of accuracy of this statistical tool (FENTON; NEIL; MARQUEZ, 2008).

The application of a Hybrid-Bayesian networks (with both discrete and continuous variables) to dependable systems showed that dynamic discretization can constitute a successful alternative for stochastic risk analyses (NEIL et al., 2008). According to NEIL et al. (2008), BNs are relevant modeling tools for probabilistic inference when it is possible to observe some of the variables of the model, providing input information to update the current process status.

KELLY and SMITH (2009) discussed the main advances related to applications of Bayesian statistics for risk assessment, which included “Hierarchical modeling of variability”, “Modeling of time-dependent reliability” and “Treatment of uncertain and missing data”. The authors assigned the advances on existence of open software, increasing computational capacity and availability of techniques Markov-Chain Monte-Carlo (MCMC) sampling methods as the main factors for increase of the popularity of these statistical tools.

In order to support predictive maintenance activities, avoiding the usual blind maintenance approach, an integration of HAZOP and DBN was proposed used to provide a model for maintenance optimization, considering costs and safety issues simultaneously. HAZOP provides the causal relation between equipment and the process while DBN allows to predict how the system can failure (HU; ZHANG; LIANG, 2012). Virtual age models and DBNs were combined to predict the system performance and support life extension assessment (RAMÍREZ; UTNE, 2015).

A method to embody accident precursor data, based on hierarchical Bayesian networks, was developed to support the risk estimation of offshore blowouts. As this kind of estimation lacks representative frequency data, the use of the Bayesian approach was

proposed to integrate specific data into the analysis and then it was compared to other non-Bayesian estimators based on the maximum occurrence probabilities strategy, which included the support of an event tree method, in order to systematize the relation between the accident and the respective contributing events. Different probability distribution functions were applied in order to compare how they could affect the prior distribution function and hence the accuracy of the accident prediction (KHAKZAD; KHAN; PALTRINIERI, 2014).

The advantages of integrating phenomenological process simulations with probability modeling were shown in a management of change application. It was demonstrated that the combination of tools enhance risk-based decision making and enables a clearer view of the accident chain of events (DEMICHELA; BALDISSONE; CAMUNCOLI, 2017).

The integration of hazard identification methods with frequency estimation approaches was also applied to support maintenance strategies. The combination of a modified FMEA approach, used to identify and rank failure modes and adjusted to rank it criticality, with Monte Carlo simulations to randomly generate possible sets of risk numbers enabled the identification of the most critical machines of an electrical power plant (BEVILACQUA; BRAGLIA; GABBRIELLI, 2000).

The uncertainty related to hazard identification and frequency and severity estimation of accidental scenarios, inherent to safety process analysis, has also been discussed. The use of fuzzy sets was shown to constitute an alternative for determination of the probability distribution functions with the help of a risk correction index (MARKOWSKI et al., 2010).

The inaccuracy of parameters, due to the inherent random variability of the system behavior, can be represented by the probabilistic approach. However, for some cases,

when dealing with lack of information or knowledge, the use of possibilistic distributions based on a Fuzzy Logic seem more appropriate (BARALDI; ZIO, 2008).

Each step of the safety analysis routine carries different uncertainties. Regarding hazard identification, which is usually qualitative, the main uncertainty is related to the extent and scope of the analysis (Have all the potential scenarios been correctly identified?) This kind of uncertainty was called “The completeness uncertainty”. The severity estimation step also brings a level of uncertainty related to the expert knowledge to judge the scenario, which was entitled as the “Modeling uncertainty”. Finally, the uncertainty and inaccuracy of available data, typical of frequency estimation, was called the “Parameter uncertainty” (MARKOWSKI et al., 2010).

In order to combine the different types of uncertainty and generate a representative final risk index, different approaches have been proposed. The stochastic variability has been studied with Monte Carlo simulations; whose main limitation is related to the representativeness of the probability density function. The knowledge variability is the most difficult to handle, although the fuzzy logic provides a path to deal with all categories of uncertainty simultaneously despite the fact that most studies applied frequency analyses (MARKOWSKI et al., 2010).

The purely probabilistic and fuzzy approaches were compared with a hybrid technique that combined possibilistic and probabilistic distribution functions, using Monte Carlo sampling and fuzzy interval analyses (BARALDI; ZIO, 2008).

Monte Carlo simulations were applied for safety risk assessment in a highly distributed interaction system in the air traffic industry. Due to the significant severity of the scenarios and the high complexity of the operation, the air traffic industry development of safety evaluation tools constitutes an important reference for the chemical and oil industries. The estimation of top event probabilities can be represented as the

combination of conditional events probability. The experience of operational experts can be integrated with frequency data from the aviation safety databases. The more severe will be the outcome, the more complex the interaction between multiple agents will be, so that Monte Carlo simulations can support risk estimates (BLOM; STROEVE; DE JONG, 2006).

Dynamic fault trees are used when it is desired to model dependent failures, redundancy and other behaviors that cannot be properly represented by traditional fault trees. For small systems, the solution of the fault tree can be obtained by Markov Models using state space approaches. However, when system complexity increases or when the failure probability distribution cannot be represented by an exponential function, other methods are needed to solve the dynamic fault tree. Monte Carlo simulations are able to deal with these limitations and have been applied to solve fault tree dynamic gates with satisfactory results (DURGA RAO et al., 2009).

The Monte Carlo approach has also been used to solve problems considering human factors. The human factor model can be developed and consists of a frequency modifier based on organizational features related to skills, knowledge and behavior. The uncertainty range of the human based factors can be obtained from questionnaires regarding the organizational culture. The probability density function is assumed to be uniform, since the human factor behavior the behavior is not known. The application to real plants showed that the detailed consideration of human factors to the probability assessment study resulted in more conservative risks (GONZÁLEZ DAN et al., 2016).

BRITTO (2018) proposed a different manner to model the occurrence probability of an event by using Monte Carlo simulations. Roughly, the simulation was performed with the perspective of a deterministic process variable and not from the perspective of the device conditions. The methodology allowed the integration of the deterministic

process behavior with the stochastic behavior. Unlike conventional resolutions of the probabilistic dynamic system, the described method, instead of modeling a certain time interval where a stochastic set of events may happen, proposed to simulate an entire sequence of events (until the end of the chain of events) to obtain the cumulative consequence. With this strategy, the discrete probabilistic variable is used to change the number of activated events. Then the drawback of carrying out numerous simulations to obtain a representative result from the Monte Carlo approach can be partially overcome.

In conclusion, through the examples shown before, one can see that many different approaches have been used to deal with failure data accuracy, uncertainty related to human knowledge and complex interactions between the events that compose the accident occurrence mechanism. Due to computational advances, the solution of dynamic and complex problems has become possible, leading to advances of the results obtained with more traditional methods. Nevertheless, although the technological advances have been applied to real cases, they have not completely replaced traditional methods, although they clearly indicate the main limitations of the traditional risk assessment process.

2.4. Polymerization Main Hazards

2.4.1. Runaway Reaction

Exothermic reactions are characterized by the release of heat during the reaction course. This kind of reaction can be subjected to a phenomenon called runaway, that consists of fast and self-sustained overheating when the reaction rate of heat release is higher than the cooling rate capacity. This occurs because, in general terms, the rate of heat release depends exponentially on the reactor temperature, while the cooling rate increases linearly with the reaction temperature. Therefore, from a certain reactor temperature level,

an uncontrolled thermal hazard may take place, resulting from the uncontrolled increase of the reaction rate, and hence of the rate of heat release (BARTON; NOLAN, 1989).

This phenomenon is worsened by the combined effect on the reactor pressure, that increases with the increase of temperature. The increase of vapor pressure of the components, with possible evolution of gas can be aggravated when a component is subject to thermal decomposition. Those effects may exceed the reactor design conditions and lead to loss of containment (BARTON; NOLAN, 1989). To better understand runaway reactions, it is necessary to obtain knowledge about the kinetics and thermodynamic behavior of the reaction, about the heat transfer dynamics and also about the thermal stability and physical properties of the reactor components (BARTON; NOLAN, 1989).

The main causes of this loss of control are side reactions, inadequate cooling and accumulation of reagents and intermediates, leading to heat accumulation and temperature increase (CASSON MORENO; SALZANO; KHAN, 2016). Inadequate design, substandard operational procedures, low quality raw-material control, temperature control failure, agitation failures and mischarging of reactants are also relevant factors that may contribute to thermal runaway (GYENES; CARSON, 2017). Batch processes are more likely to accumulate heat; hence runaway reactions are more frequent in this kind of processes, although they can also take place in continuous processes (CASSON MORENO; SALZANO; KHAN, 2016).

Polymerization reactions are intrinsically exothermic. Due to their usual high activation energy, the reaction rate is very sensitive to temperature changes. The combination of these factors makes polymer production processes prone to runway reactions when subject to inefficient heat removal (SILVA, 2018).

Barton and Nolan (1989) investigated more than 120 incidents related to runaway reactions, reported between 1962 and 1982. Ranking these incidents according to the process technology, polymerization processes contributed to most of the incidents, totalizing 45 events. Following the rank, incidents in nitration processes (with 35 events); and incidents in sulfonation processes (with 12 events). Although the data is not recent, the statistics highlight the runaway risk associated with polymerization reactions.

Although important lessons can be available after numerous incidents of the chemical industry, exothermic runaway reactions are still cause of major accidents (ICHEME, 2016). In Germany, 1993, a failure in the agitator system of a batch reactor led to thermal runaway causing the release of more than 10 tons of a dangerous product. In USA, 1994, a polymerization facility was destroyed after a runaway reaction in a polymerization reactor due to excess dosage of butadiene monomer ("Accident Report Detail | Occupational Safety and Health Administration", [s.d.]). In USA, 2007, an insufficient cooling triggered a runaway reaction that caused an explosion that killed 4 people and injured 13 others (ICHEME, 2016). In Japan, 2012, a runaway polymerization of acrylic acid (FUJITA et al., 2019) caused a pressure rise due to decomposition reactions that started after the bypass of a safety interlock, leading to an explosion that killed 1 person and injured many others. In 2014, 1 person was killed due to an explosion in a German facility that produced flame retardants for textile (ICHEME, 2016).

Different polymerization processes (such as processes with vinyl acetate monomer (GUSTIN; LAGANIER, 2005), acrylic acid monomer (FUJITA et al., 2019) and propylene (LUO; SU; WU, 2010) have been investigated in order to evaluate causes of thermal runaway, clarify thermal hazards and simulate emergency situations. Therefore, the development of tools and studies that can clarify hazard mechanisms can

be a relevant line of research in the context of prevention of losses and accidents of processes associated with polymerization reactions.

Chapter 3

Case-Study: Bulk Polymerization of Propene

3.1.Propene Polymerization Chemistry

Propene is an unsaturated hydrocarbon, classified as an olefin. The presence of the double bound in the molecule increases its reactivity, allowing the application in many different processes, including polymerization (SILVA, 2018).

The polymerization of propene to produce polypropylene, PP, is well established in the industry, after the consolidation of the catalyst process discovered by Giulio Natta comprising the chemical interaction between organometallic compounds and chloride salts of titanium (SHAMIRI et al., 2014). According to POSCH (2017), polypropylene is the second most important commercial polyolefin. In modern society, polypropylene can be found in furniture, medical utensils, coatings, and other plastic objects (SILVA, 2018).

Although polypropylene had been synthesized before Natta's discovery, in the mid-1950 (VEN, 1990), only low molar mass polymer chains could be produced, without commercial value. The catalyst route brought to this product a stereospecific reaction able that was to generate isotactic and crystalline macromolecules, with attractive properties for many useful applications for everyday life (SILVA, 2018).

When it comes to polypropylene, the stereochemistry plays an important role to understand the final product properties. Due to the existence of a methyl group bounded to the ethylenic chain, when the monomer molecule is repeated in the macromolecular

structure, the methyl groups can be positioned on for the same side of the molecule (isotactic polymer); they can be positioned on alternate sides of the molecule (syndiotactic polymer); or they can be randomly positioned in the molecule (atactic polymer) (OUELLETTE; RAWN, 2014).

The isotactic molecule provides a crystalline polymer material and adds valuable commercial properties to the final product. Therefore, processes that are able to convert propene into highly isotactic polymers are the ones most frequently found in industry. The control of the stereochemistry of the polymer is related to the proper selection of the catalyst (MADDAH, 2016; SILVA, 2018).

When Natta conducted the first reactions, the isotactic content was below 50%, which was still too low to justify the large-scale application (MALPASS; BAND, 2012). In that time, the catalyst used was prepared through the reaction between $TiCl_4$ and $TEAL$(triethyl aluminum), which is known as the Ziegler Natta catalyst system (SILVA, 2018). The evolution of the catalyst systems used to produce highly isotactic form of polypropylenes started from the perception about the influence of the catalyst structure on the reaction selectivity and product stereochemistry (CERRUTI, 1999). Despite the advances made in terms of catalyst structure, the first generation of Ziegler-Natta catalysts presented some limitations regarding productivity and isotactic contents, not justifying its application in industry (MALPASS; BAND, 2012; SILVA, 2018).

The second generation of Ziegler-Natta catalysts, developed by Solvay, was based on the increase of specific area, which made the catalysts more selective and active, when compared to first-generation catalysts. Although the use of these catalysts still required application of complementary separation steps for removal of catalyst and of non-isotactic chain, some commercial processes became feasible (SILVA, 2018).

The advance of catalyst systems applied to the polymerization of olefins proceeded then with the development of catalyst supports, which increased substantially the catalyst activity (CERRUTI, 1999). The increase of catalyst activity brought two main gains to olefin polymerization processes: the increase of productivity and, thus, the elimination of separation steps for catalyst removal, although the problem of reaction selectivity and low isotactic content was still relevant (SILVA, 2018).

The third generation of Ziegler-Natta catalysts was consolidated with the use of Lewis bases, which increased the selectivity and the isotactic content of the final product. Two Lewis bases compounded the system: one known as the internal electron donor, and the second known as the external electron donor. The first Lewis bases increased the isotactic content by 10%; however, purification steps to remove atactic polymer chains, were still necessary (SILVA, 2018).

The fourth generation of Ziegler-Natta catalysts was related to the use of new Lewis bases, which provided catalyst systems with higher selectivity and higher productivity that finally led to satisfactory isotactic contents and eliminated the necessity of further purification steps to remove atactic polymer chains consolidating the application for bulk polymerization processes, where the monomer constitutes the reaction medium. Although these catalysts brought significant gains regarding the isotactic contents of the product, the fourth-generation catalysts introduced a new problem related to the high catalyst activity: the overheating of catalyst particles, which can cause operational problems due to polymer agglomeration and modification of the physical properties. This problem was overcome through the addition of further process step named as pre-polymerization (MALPASS; BAND, 2012).

The discovery of new Lewis bases made it possible the use of a single base (the internal donor), instead of a pair of bases as originally applied. This concept allowed the

consolidation of the fifth-generation of Ziegler-Natta catalysts, which increased the catalyst activity, narrowed the molar mass distribution (KAMINSKY, 2013) and improved the thermal stability, which affects the final product properties (SILVA, 2018). The commercial use of these catalysts is increasing because they offer operating and quality benefits (LYONDELLBASELL, [s.d.])

Finally, a new family of catalysts was developed by Sinn and Kaminsky, based on metallocene compounds (a transition metal coordinated by cyclic unsaturated hydrocarbons) with methyl-aluminoxane. The main advantages of this catalyst class, known as single site catalysts, is the high selectivity for polypropylene formation, producing high isotactic contents with high productivity (SILVA, 2018). However, the commercial use of these catalysts is still under development.

3.1.1. Types of Propene Polymerization Process

The advances in the chemistry of propene polymerization enabled the large-scale production processes. The process design is based mainly on the following process demands:

- heat removal: due to the high exothermic nature of the reaction nature, the design of the cooling strategy is critical (VEN, 1990);
- polymer yield: this variable affects the catalyst cost (per mass of polymer) and determines the catalyst residues, and consequently the necessity of additional removal steps. The polymer yield is influenced by the catalyst activity, propylene partial pressure/concentration, temperature and residence time (VEN, 1990);
- product quality:

- Isotacticity (indirectly related to the xylene soluble content, XS): influenced by the catalyst, co-catalyst and Lewis bases (SILVA, 2018; VEN, 1990).
- Molar Mass Distribution (MMD, which is indirectly measured by the melting index, MI): controlled by the actuation of chain transfer agents, normally hydrogen (SILVA, 2018).

Industrial propene homo polymerization processes are typically continuous (VEN, 1990) and can be grouped into four different types, as described below:

- The slurry process:

This was the first type of industrial process, when low-activity catalysts were available. The process uses an inert hydrocarbon as a suspending medium, so that downstream solvent purification unities are required. The process typically operated with low reactor temperatures (50 – 70°C), and the polymerization interrupted with a catalyst killer at the outlet stream of the main reactor. In the 1990s, these were the most common types of process. Nowadays these processes are considered obsolete although many plants are still in operation (SILVA, 2018; VEN, 1990).

- The liquid propylene process:

Also referred as bulk-phase or liquid-pool processes, the liquid propylene process is similar to the slurry process, with the fundamental difference that they use the monomer as the suspending medium, implying on higher monomer concentrations and thus higher reaction rates, making downstream solvent purification steps unnecessary and reducing the operation costs. The pressure must be high enough to keep propene in the liquid phase and, as it operates with boiling propene, the removal of the heat of evaporation represents an effective way to cool the reactor. Nevertheless, due to the high reaction rates, the

intense heat release requires the proper design of the cooling system (SILVA, 2018; VEN, 1990).

- The solution process:

The solution polypropylene process differs from the slurry process because the polymer can dissolve in the solvent at higher temperatures (between 175 to 250 °C). The high heat off reaction can be used as a heat source to integrate the energy balance of the plant. However, the operation of this kind of process is expensive and, hence, this commercial operation is not common (SILVA, 2018; VEN, 1990).

- The gas phase process:

In the gas phase process, no solvent is used; hence there is no need for downstream separation processes. The reaction takes place in fluidized bed reactors or stirred bed reactors with continuous feeding of propylene gas (SILVA, 2018; VEN, 1990). The commercial use of propylene gas phase polymerization processes is increasing but slurry and mass processes are still the ones applied most often in the industry (MATTOS NETO; PINTO, 2001).

3.2.Case Study Description

The case study is based on the Liquid Polymerization of Polypropylene with Super High Activity Catalyst, LIPP-SHAC, process. It consists of a bulk polymerization process (the suspending medium is the monomer) in a single continuous three-phase stirred tank reactor, to produce PP powder suspended in liquid propylene (DUTRA et al., 2014; MATTOS NETO; PINTO, 2001; PRATA et al., 2009). A fourth-generation Ziegler–Natta catalyst system ($TiCl_4/MgCl_2 + PEEB + TEAL$) is used in the considered process. Due to its high activity, catalyst removal and polymer purifications are not necessary (SILVA, 2018).

The model used to perform simulations is based on the work of DUTRA et al., (2014), MATTOS NETO and PINTO (2001), PRATA et al. (2009) and SILVA (2018) with some new aspects that will be discussed in the sequence. The described process is represented in Figure 3.2-1.

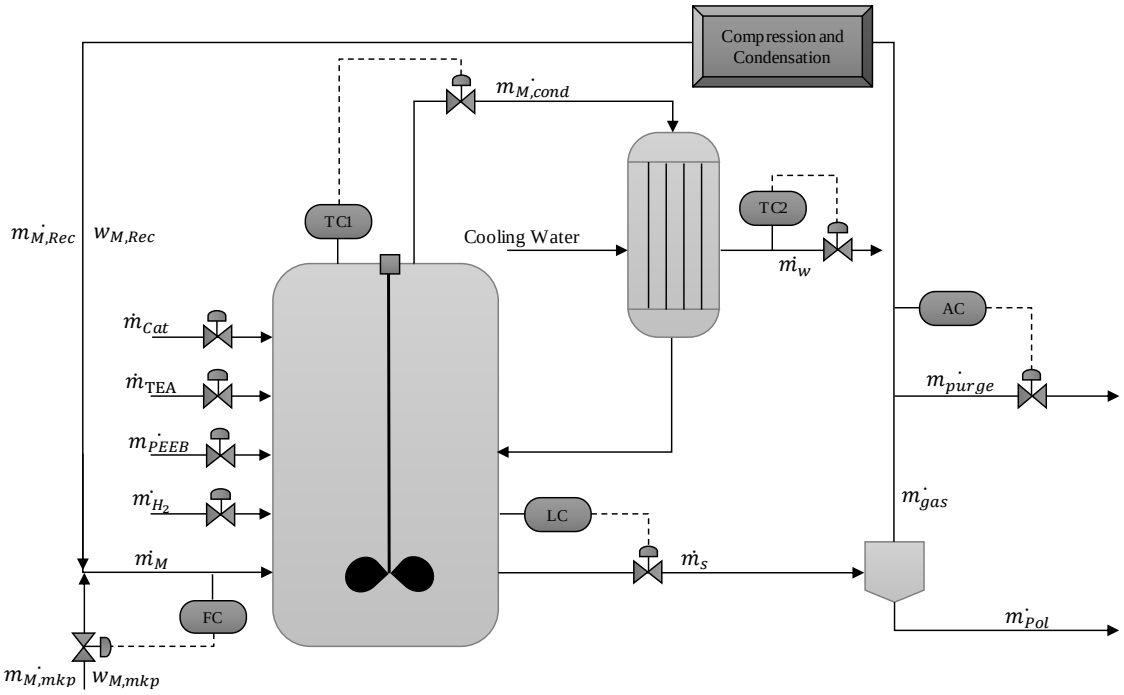

Figure 3.2-1 - Process Flow Chart.

The reactor is fed by five continuous fresh streams: catalyst ($\dot{m_{Cat}}$); 2 additive streams of PEEB (Para-Ethyl 4-etoxybenzoate), the electron donor used to improve the polymer quality ($\dot{m_{PEEB}}$) and TEAL, the co-catalyst ($\dot{m_{TEA}}$); hydrogen (chain transfer agent) ($\dot{m_{H_2}}$); and monomer (liquid propylene) ($\dot{m_M}$). The addition of hydrogen is necessary to adjust the molar mass distribution of the polymer. Hydrogen interrupts the growth of the polymer chain and restores the activity of the original catalyst sites.

The reactor temperature is controlled by condensation of the vapor phase ($\dot{m_{M,cond}}$) (boiling propylene) in top condenser refrigerated with cooling water. The temperature of cooling water is controlled through the manipulation of the cooling

water flow ($\dot{m}_w$). The reactor level is controlled through manipulation of the automatic valve placed at the outlet stream of the reactor ($\dot{m}_s$), which contains essentially non-reacted monomer and polymer (SILVA, 2018).

The non-reacted monomer is recovered in a gas separator by pressure reduction. The vapor phase ($\dot{m}_{gas}$), carries the monomer and volatile impurities, while the solid phase carries the polymer ($\dot{m}_{Pol}$), solid additives and catalyst, which are incorporated to the PP product with no need of further purification.

The impurities in the monomer feed contain mostly propane (inert), so that the recirculation of non-reacted monomer leads to accumulation of propane, which must be purged (MATTOS NETO; PINTO, 2001; PRATA et al., 2009). In order to control the propane accumulation inside the reactor, a control loop manipulates the valve placed at the purge stream ($\dot{m}_{purge}$), according to the monomer purity measured in the recirculation stream ($\dot{m}_{M,Rec}$). Besides that, the monomer feed rate is controlled through manipulation of the monomer make-up flow ($\dot{m}_{M,mkup}$) to keep constant the monomer concentration inside the reactor.

TC, LC, FC and AC are, respectively, controllers of temperature, level, flow and purity (analytical).

3.3.Case Study Modeling

3.3.1. Assumptions

To describe the process, the following assumptions and simplifications were considered:

- The reactor behaves as an ideal CSTR:
    - CSTR ideal exponential residence time distribution.
    - Perfect mixing (lumped model).
    - Ideal mixing (agitation heat can be neglected).

- Dynamics of pipes and connections are neglected;
- Dynamics of condenser and gas separator can be neglected;
- Dynamics of compression and condensation of the recycled stream can be neglected.
- The solid, liquid and vapor phases inside reactor are in thermodynamic equilibrium.
- Contributions of hydrogen vapor pressure to the reactor pressure can be neglected.
- Molecular interactions for computation of mixture properties can be neglected:
    - The total volume of the mixture is the sum of volumes of pure individual species (volume additivity).
    - The heat capacity and density of the liquid phase is the mass-weighted average of the properties of individual components.
- The reaction takes place only in the solid phase and diffusive effects can be neglected;
- Long Chain Assumption:
    - Reactivity of polymer chains does not depend on chain length and, thus, can be represented by single propagation kinetic constant.
    - Monomer consumption in the initiation step can be neglected when compared to propagation step.
- Perfect efficiency of gas separation:
    - Monomer and propane can be completely separated from the solid.
    - Catalyst and additives remain in the polymer mass during the separation step.

3.3.2. The Kinetic Model

The propene bulk homopolimerization with a fourth-generation Zigler-Natta catalyst can be represented by the polymerization mechanism in the solid phase (catalyst active site) that considers initiation, propagation, chain transfer and active site deactivation steps as described in Table 3.3.2-1. The reactions follow first order kinetics in respect to the reactants (ROSA, 2013):

Table 3.3.2-1 - Polymerization Mechanism and Reaction Rates.

Step	**Reaction**	**Rate**
Initiation	$AS + Pe \overset{k_c}{\rightarrow} P_1$	$k_c . C_{Pe} . C_{AS}$
Propagation	$P_i + Pe \overset{k_p}{\rightarrow} P_{i+1}$	$k_p . C_{P_i} . C_{Pe}$
Chain Transfer to Monomer	$P_i + Pe \overset{k_{tM}}{\longrightarrow} D_i + P_1$	$k_{tM} . C_{P_i} . C_{Pe}$
Chain Transfer to Hydrogen	$P_i + H_2 \overset{k_{tH}}{\longrightarrow} D_i + P_1$	$k_{tH} . C_{P_i} . C_{H_2}$
Spontaneous Chain Transfer	$P_i \overset{k_{tS}}{\longrightarrow} D_i + P_1$	$k_{tS} . C_{P_i}$
Deactivation	$P_i \overset{k_d}{\rightarrow} D_i$	$k_d . C_{P_i}$

In Table 3.3.2-1, AS, Pe and H_2 represent the active site, propene and hydrogen, respectively, and C_{AS}, C_{Pe} and C_{H_2} are the respective molar concentrations. P_i and D_i are live and dead polymer chains of size i, respectively, and C_{P_i} is the molar concentration of live polymer chains of size i.

The kinetic constants for initiation, chain transfer to monomer, chain transfer to hydrogen, spontaneous chain transfer and deactivation, denoted as k_j $(j = \mathrm{c, tM, tH, tS, d})$ can be expressed in terms of the reactor temperature (T), according to the Arrhenius Law:

$$k_j(T) = k_{j0}.e^{-\frac{E_j}{R}\left(\frac{1}{T}-\frac{1}{T_{Ref}}\right)} \quad (1)$$

k_{j0} and E_j are the pre-exponential factor and the activation energy of reaction step j, respectively. R is the universal gas constant and T_{ref} is a reference temperature.

For the kinetic constant for propagation, k_p, two other important effects must be taken into account: the hydrogen concentration dependence, which can reduce the propagation rate, decreasing the Ziegler-Natta catalyst activity; and the effect of additives concentration ratio, $\frac{C_{TEA}}{C_{PEEB}}$, which leads to an optimum value of maximum catalyst activity. Those dependencies can be modeled through an adjustment factor, f, that multiplies the kinetic constant, as follows (SILVA, 2018):

$$f = \left[1 + a_1.\left(\frac{C_{H_2}}{a_2 + C_{H_2}}\right) + a_3.\left(\frac{m_{TEA}}{m_{PEEB}} + a_4\right)^2\right] \quad (2)$$

$$k_p\left(T, C_{H_2}, C_{TEA}, C_{PEEB}\right) = f.k_j(T) = k_{p0}.e^{-\frac{E_p}{R}\left(\frac{1}{T}-\frac{1}{T_{Ref}}\right)} \quad (3)$$

m_{TEA} and m_{PEEB} are the TEA and PEEB masses in the reactor and a_l $(l = 1,2,3,4)$ are the propagation adjustment factor constants.

3.3.3. The Reaction Rates

The kinetic model provides the necessary rate equations for the individual consumption or formation rates (ROSA, 2013). In Equations (4 – 9), R_n $(n = M, AS, H_2, P_i, D_i)$ are the consumption or formation rates for monomer, catalyst active sites, hydrogen, live polymer chains and dead polymer chains, respectively.

i. Propene Reaction Rate:

$$R_{Pe} = -k_c.C_{Pe}.C_{AS} - \left(k_p + k_{tM}\right).C_{Pe}.\left(\sum_{i=1}^{\infty} C_{P_i}\right) \quad (4)$$

ii. Active Site Reaction Rate:

$$R_{AS} = -k_c.C_{Pe}.C_{AS} + \left(k_{tH}.C_{H_2} + k_{tS}\right).\left(\sum_{i=1}^{\infty} C_{P_i}\right) \quad (5)$$

iii. Active Site Reaction Rate:

$$R_{H_2} = -k_{tH}.C_{H_2}.\left(\sum_{i=1}^{\infty} C_{P_i}\right) \quad (6)$$

iv. Live Polymer Reaction Rate:

$$R_{P_1} = k_c.C_{Pe}.C_{AS} + k_{tM}.C_{Pe}.\left(\sum_{i=1}^{\infty} C_{P_i}\right) - (k_p.C_{Pe} + k_{tM}.C_{Pe} + k_{tH}.C_{H_2} + k_{tS} + k_d).C_{P_1};\ (i = 1) \quad (7)$$

$$R_{P_i} = k_p.C_{P_{i-1}}.C_{Pe} - \left(k_p.C_{Pe} + k_{tM}.C_{Pe} + k_{tH}.C_{H_2} + k_{tS} + k_d\right).C_{P_i};\ (i > 1) \quad (8)$$

v. Dead Polymer Reaction Rate:

$$R_{D_i} = \left(k_{tM}.C_{Pe} + k_{tH}.C_{H_2} + k_{tS} + k_d\right).C_{P_i} \quad (9)$$

3.3.4. Moments Method

The moments technique can be applied to the polymerization model to reduce the number of equations. This simplification transforms the detailed information about the individual polymer chains into average properties, but facilitates the numerical solution of the set of differential equations (ROSA, 2013). For the purposes of the present text, only general information about the average polymer is necessary, so that the moments method is

appropriate for the proposed study. Therefore, the κ^{th} order moment (η_κ) of a generic distribution $\zeta(\chi)$ can be defined as:

$$\eta_\kappa = \sum_{\chi=1}^{\infty} \chi^\kappa . \zeta(\chi) \tag{10}$$

Applying Equation (10) to the polymerization model, Equations (11) and (12) can be obtained representing the κ^{th} order live and dead polymer moments, respectively:

$$\lambda_\kappa = \sum_{i=1}^{\infty} i^\kappa . C_{P_i} \tag{11}$$

$$\mu_\kappa = \sum_{i=1}^{\infty} i^\kappa . C_{D_i} \tag{12}$$

With those definitions, the rates of polymer moments rates can be obtained as described below:

i. Rates of Live Polymer Moments:

Multiplying both sides of Equation (8) by i^κ and applying the operator $\sum_{i=2}^{\infty}$, and then summing to Equation (7), it can be proven that the generic rates of live polymer moments, R_{λ_κ}, can be given by (ROSA, 2013):

$$\begin{aligned} R_{\lambda_\kappa} = {} & k_c . C_{Pe} . C_{AS} + k_p . C_{Pe} . \left(\sum_{j=1}^{\infty} (j+1)^\kappa C_{P_j} \right) + k_{tM} . C_{Pe} . \lambda_0 \\ & - k_p . C_{Pe} . \lambda_\kappa - k_{tH} . C_{H_2} . \lambda_\kappa - k_{tM} . C_{Pe} . \lambda_\kappa - k_{tS} . \lambda_\kappa \\ & - k_d . \lambda_\kappa \end{aligned} \tag{13}$$

Making $\kappa = 0,1,2$, the rates of zero, first and second-order of live polymer moments become:

$$R_{\lambda_0} = k_c . C_{Pe} . C_{AS} + (-k_{tH} . C_{H_2} - k_{tS} - k_d) . \lambda_0 \tag{14}$$

$$R_{\lambda_1} = k_c.C_{Pe}.C_{AS} + k_p.C_{Pe}.\lambda_0 + k_{tM}.C_{Pe}.(\lambda_0 - \lambda_1) + (-k_{tH}.C_{H_2} - k_{tS} - k_d).\lambda_1 \quad (15)$$

$$R_{\lambda_2} = k_c.C_{Pe}.C_{AS} + k_p.C_{Pe}.(2\lambda_1 + \lambda_0) + k_{tM}.C_{Pe}.(\lambda_0 - \lambda_2) + (-k_{tH}.C_{H_2} - k_{tS} - k_d).\lambda_2 \quad (16)$$

ii. Rates of Dead Polymer Moments:

Applying analogous mathematical transformations, the rates of dead polymer moments, R_{μ_κ}, become (ROSA, 2013):

$$R_{\mu_\kappa} = \left(k_{tM}.C_{Pe} + k_{tH}.C_{H_2} + k_{tS} + k_d\right).\lambda_\kappa \quad (17)$$

Making $\kappa = 0, 1, 2$, the rates of the zero, first and second-order dead polymer moments become:

$$R_{\mu_0} = \left(k_{tM}.C_{Pe} + k_{tH}.C_{H_2} + k_{tS} + k_d\right).\lambda_0 \quad (18)$$

$$R_{\mu_1} = \left(k_{tM}.C_{Pe} + k_{tH}.C_{H_2} + k_{tS} + k_d\right).\lambda_1 \quad (19)$$

$$R_{\mu_2} = \left(k_{tM}.C_{Pe} + k_{tH}.C_{H_2} + k_{tS} + k_d\right).\lambda_2 \quad (20)$$

3.3.5. Material Balances

The process flow chart, shown in Figure 3.2-1 can guide the material balances of the process.

i. Reactor Mass Balance

$$\frac{d(\rho.V)}{dt} = \dot{m_{Pe}} + \dot{m_{Pa}} + \dot{m_{H_2}} + \dot{m_{Cat}} + \dot{m_{PEEB}} + \dot{m_{TEA}} - \dot{m_s} \quad (21)$$

$$\dot{m_{Pa}} = \dot{m_{mkup}}.\left(1 - w_{M,mkup}\right) + \dot{m_{Rec}}.(1 - w_{M,rec}) \quad (22)$$

$$\frac{1}{\rho} = \frac{w_M}{\rho_M} + \frac{w_{Pol}}{\rho_{Pol}} \quad (23)$$

Feed flowrates of propene, propane, hydrogen, catalyst, PEEB, TEA, make-up and recycle are given by $\dot{m}_l (l = Pe,\ Pa,\ H_2,\ Cat,\ PEEB,\ TEA,\ mkup,\ Rec)$,

respectively. $\dot{m}_s$ is the outlet mass flowrate of slurry and V is the volume inside the reactor. The inlet mass flowrate of propane, $\dot{m_{pa}}$, depends on the purities of the monomer make-up and recycled streams, $w_{M,mkup}$ and $w_{M,rec}$, and respective flowrates, $\dot{m_{mkup}}$ and $\dot{m_{Rec}}$, respectively. The slurry density, ρ, can be written in terms of the major components inside the reactor, the monomer and the polymer, and their respective mass fractions w_M and w_{Pol}, and individual densities ρ_M and ρ_{Pol}.

ii. Total concentration of active species

According to MELO JUNIOR (2000) (apud DUTRA, 2012), the concentration of catalytically active species, also referred as total catalyst, is given by:

$$C_{cat} = C_{AS} + \sum_{i=1}^{\infty} C_{P_i} = C_{AS} + \lambda_0 \tag{24}$$

However, $\lambda_0 \gg C_{AS}$, so that a simplification can be made:

$$C_{cat} \approx \lambda_0 \tag{25}$$

Besides that, in polymerization reactions the initiation step is much less frequent than propagation, which enables to neglect the rate of initiation when the rate of propagation also affects the analyzed component rate.

Therefore, the molar balances of individual species can be written as follows.

iii. Monomer Molar Balance:

$$\frac{dN_{Pe}}{dt} = \frac{d(V.C_{Pe})}{dt} = \frac{\dot{m_{Pe}}}{MM_{Pe}} - C_{Pe}.q_s + R_{Pe}.V \tag{26}$$

where $R_M \approx -\left(k_p + k_{tM}\right).C_{Pe}.\lambda_0$.

The number of propene mols is N_{Pe} and MM_{Pe} is the monomer molar mass. The outlet volumetric flowrate of slurry and inlet flowrate of monomer are given, respectively, by:

$$q_s = \frac{\dot{m}_s}{\rho} \tag{27}$$

$$\dot{m_{pe}} = w_{M,mkup}.\dot{m_{M,mkup}} + w_{M,mkup}.\dot{m_{M,Rec}} \tag{28}$$

iv. Catalyst Molar Balance:

From Equation (25), the reaction rate for catalyst can be simplified as:

$$R_{cat} \approx R_{\lambda_0} \tag{29}$$

Therefore, the molar balance of catalyst can be written as:

$$\frac{dN_{Cat}}{dt} = \frac{\dot{m_{Cat}}}{MM_{Cat}} - \lambda_0.q_s + R_{\lambda_0}.V \tag{30}$$

where the number of catalyst mols is N_{Cat} and MM_{Cat} is the catalyst molar mass.

v. Hydrogen Molar Balance:

$$\frac{dN_{H_2}}{dt} = \frac{\dot{m_{H_2}}}{MM_{H_2}} - C_{H_2}.q_s + R_{H_2}.V \tag{31}$$

where MM_{H_2} is the hydrogen molar mass.

vi. Polymer Mass Balance:

The polymer formation rate, R_{Pol}, can be regarded equal to the propagation rate for all live polymer species. In agreement with the long chain assumption, it is possible to write:

$$R_{Pol} = k_p.C_{Pe}.\lambda_0 \tag{32}$$

$$\frac{dm_{Pol}}{dt} = -\dot{m_{Pol}} + R_{pol}.MM_{Pe}.V \tag{33}$$

where m_{Pol} and $\dot{m_{Pol}}$ are respectively the polymer mass inside the reactor and the output mass flowrate of polymer from gas separator.

vii. Additives Mass Balance:

Based on the assumption that additives remain incorporated in the final polymer, the mass balance can be written as:

$$\frac{dm_{TEA}}{dt} = \dot{m_{TEA}} - \left(\frac{m_{TEA}}{m_{Pol}}\right).\dot{m_{Pol}} \quad (34)$$

$$\frac{dm_{PEEB}}{dt} = \dot{m_{PEEB}} - \left(\frac{m_{PEEB}}{m_{Pol}}\right).\dot{m_{Pol}} \quad (35)$$

where m_{TEA} and m_{PEEB} are respectively the TEA and $PEEB$ masses inside the reactor.

viii. Moments Balance of Live Polymer Chains:

$$\frac{d(V.\lambda_0)}{dt} = \frac{dN_{Cat}}{dt} \quad (36)$$

$$\frac{d(V.\lambda_1)}{dt} = -q_s.\lambda_1 + R_{\lambda_1}.V \quad (37)$$

$$\frac{d(V.\lambda_2)}{dt} = -q_s.\lambda_2 + R_{\lambda_2}.V \quad (38)$$

Based on the assumption that the propagation step is considerably more frequent than initiation and that $\lambda_0 \gg C_{AS}$, Equations (14), (15) and (16) can be rewritten as follows, after neglecting the initiation step term:

$$R_{\lambda_0} = (-k_{tH}.C_{H_2} - k_{tS} - k_d).\lambda_0 \quad (39)$$

$$R_{\lambda_1} = k_p.C_{Pe}.\lambda_0 + k_{tM}.C_{Pe}.(\lambda_0 - \lambda_1) + (-k_{tH}.C_{H_2} - k_{tS} - k_d).\lambda_1 \quad (40)$$

$$R_{\lambda_2} = k_p.C_{Pe}.(2\lambda_1 + \lambda_0) + k_{tM}.C_{Pe}.(\lambda_0 - \lambda_2) + (-k_{tH}.C_{H_2} - k_{tS} - k_d).\lambda_2 \quad (41)$$

ix. Moments Balances of Dead Polymer Chains:

$$\frac{d(V.\mu_0)}{dt} = -q_s.\mu_0 + R_{\mu_0}V \quad (42)$$

$$\frac{d(V.\mu_1)}{dt} = -q_s.\mu_1 + R_{\mu_0}.V \quad (43)$$

$$\frac{d(V.\mu_2)}{dt} = -q_s.\mu_2 + R_{\mu_0}V \tag{44}$$

x. Propane Mass Balance:

$$\frac{dm_{Pa}}{dt} = \dot{m_{Pa}} - \dot{m_s}.w_{Pa} \tag{45}$$

where w_{pa} is the propane mass fraction inside the reactor.

xi. Gas Separator Mass Balance:

$$\dot{m_s} = \dot{m_{gas}} + \dot{m_{Pol}} \tag{46}$$

$$\dot{m_{gas}} = (w_{Pe} + w_{pa}).\dot{m_s} \tag{47}$$

$$\dot{m_{rec}} = \dot{m_{gas}} - \dot{m_{purge}} \tag{48}$$

Mass flowrates of recirculation, gas and purge streams are represented by $\dot{m_{rec}}, \dot{m_{gas}}, \dot{m_{purge}}$, respectively. w_{Pe} is the propene mass fraction inside the reactor.

3.3.6. Energy Balance

i. Reactor Energy Balance:

$$\frac{dT}{dt} = \frac{\dot{m}_M.Cp_{Pe}(T_{in}).[T_{in} - T] + Q_{Pol} - [Q_C + \dot{m_{M,c}}Cp_{Pe}(T).[T - T_c]]}{Cp_{Pe}(T).N_{Pe}.MM_{Pe} + Cp_{Pol}\,(T).m_{Pol}} \tag{49}$$

$$\dot{m}_M = \dot{m}_{Pe} + \dot{m}_{Pa}$$

where Cp_l $(l = M,\ Pol)$ are the heat capacities of monomer and polymer and T , T_{in} and T_c are the reactor temperature, inlet reactor temperature and condenser temperature, respectively. The mass flowrate of vapor from the reactor to the condenser is $\dot{m_{M,c}}$. The polymerization heat, Q_{Pol}, and the condensation heat, Q_C, are given by:

$$Q_{Pol} = (-\Delta H).R_{pol}.V \tag{50}$$

$$Q_C = \dot{m_{M,c}}.\lambda(T) \tag{51}$$

The reaction enthalpy is given by $(-\Delta H)$ and the monomer latent heat of condensation is $\lambda(T)$.

ii. Condenser Energy Balance

- In the monomer side:

$$\frac{dT_C}{dt} = \frac{Q_C - Q_E}{m_{M,c}.\,Cp_{Pe}(T_C)} \tag{52}$$

where the exchanged heat in the condenser, Q_E, is given by:

$$Q_E = UA.\,(T_C - T_w) \tag{53}$$

The global heat exchange coefficient is given by UA and $m_{M,c}$ and T_w are the total monomer mass inside the reactor and the water side temperature in the condenser, respectively.

The condensation capacity is limited to the available heat exchange in the condenser. The modeling of this physical limitation is proposed bellow:

$$Q_C = 0; \qquad (Q_E < 0) \tag{54}$$

$$Q_C = \dot{m_{M,c}}.\,\lambda(T); \qquad (Q_C < Q_E) \tag{55}$$

$$Q_C = Q_E; \qquad (Q_C \geq Q_E) \tag{56}$$

- In the water side:

$$\frac{dT_w}{dt} = \frac{\dot{m_w}.\,Cp_w(T_{w,in}).\,[T_{w,in} - T_w] + Q_E}{m_{w,c}.\,Cp_w(T_w)} \tag{57}$$

where $\dot{m_w}$, $m_{w,c}$, $T_{w,in}$ and Cp_w are the mass flowrate of water through the condenser, the total water mass inside the condenser, the inlet temperature of the water stream and heat capacity of water.

3.3.7. Controllers

SILVA (2018) implemented 3 different controllers to the polymerization reactor: (i) a reactor temperature control (TC1) that manipulates the valve placed at the outlet monomer stream to condenser; (ii) a cooling water control (TC2) that manipulates the valve placed at the feed water stream to the condenser; and (iii) a reactor level control (LC) that manipulates the valve placed at the outlet slurry stream to the separator. For the 3 controllers, traditional feedback strategies with proportional and integral actions were used.

Table 3.3.7-1 describes the manipulated variables (MV) and the controlled variables (CV) for each controller and their respective constitutive equations.

Table 3.3.7-1 –Control Strategies (SILVA, 2018).

CONTROLLER	MV	CV	EQUATION	
Reactor Temperature (TC1)	$\dot{m_{M,c}}$	T	$\dot{m_{M,c}} = \dot{m_{M,c,bias}} + k_{p,T}.\left[\left(T - T_{sp}\right) + \frac{1}{\tau_T}.\int\left(T - T_{sp}\right)dt\right]$	(58)
Condenser Temperature (TC2)	$\dot{m_w}$	T_w	$\dot{m_w} = \dot{m_{w,bias}} + k_{p,T_C}.\left[\left(T_C - T_{C,sp}\right) + \frac{1}{\tau_{T_C}}.\int\left(T_C - T_{C,sp}\right)dt\right])$	(59
Reactor Level (LC)	$\dot{m_s}$	V	$\dot{m_s} = \dot{m_{s,bias}} + k_{p,V}.\left[\left(V - V_{sp}\right) + \frac{1}{\tau_V}.\int\left(V - V_{sp}\right)dt\right]$	(60)

Moreover, two additional controllers were implemented in order to control the propane accumulation inside the reactor and to keep constant the rate of monomer added to the reactor, as shown in Table 3.3.7-2. The first controller (AC) controls the monomer purity thourgh manipulation of the gas purge valve. The second controller (FC) controls the monomer inlet flowrate of monomer through manipulation of the monomer make-up valve.

Table 3.3.7-2 – Additional Control Strategies.

CONTROLLER	MV	CV	EQUATION	
Recycled monomer purity (AC)	$\dot{m}_{purge}$	$\dot{w}_{M,Rec}$	$\dot{m}_{purge} = \dot{m}_{purge,bias} + k_{p,wM} \cdot \left[\left(w_{M,Rec} - w_{M,Rec_{sp}}\right) + \frac{1}{\tau_{wM}} \cdot \int \left(w_{M,Rec} - w_{M,Rec_{sp}}\right) dt\right]$	(61)
Monomer inlet mass flow (FC)	$\dot{m}_{M,mkup}$	$\dot{m}_M$	$\dot{m}_{M,mkup} = \dot{m}_{M,mkup,bias} + k_{p,\dot{m}M} \cdot \left[\left(\dot{m}_M - \dot{m}_{M,sp}\right) + \frac{1}{\tau_{\dot{m}M}} \cdot \int \left(\dot{m}_M - \dot{m}_{M,sp}\right) dt\right]$	(62)

3.3.8. Physical Properties

i. Densities (DUTRA, 2012; SILVA, 2018)

The monomer and polymer densities, $\rho_M(T)$ and $\rho_{Pol}(T)$, are expressed in kg/L:

$$\rho_M = -1.0878 \times 10^{-5} T^2 + 4.7376 \times 10^{-3} T + 6.0983 \times 10^{-2} \quad (63)$$

$$\rho_{Pol} = -2.0888 \times 10^{-6} T^2 + 9.5767 \times 10^{-4} T + 8.0950 \times 10^{-1}; \quad (64)$$

ii. Heat Capacities and Latent Heat of Vaporization (DUTRA, 2012; SILVA, 2018):

Given a dimensionless temperature:

$$\Omega(T) = 1 - \frac{T}{364.9} \quad (65)$$

The heat capacities of monomer, polymer and water, $Cp_M(T)$, $Cp_{Pol}(T)$ and $Cp_w(T)$ expressed as, in $cal/(g.°C)$:

$$Cp_M = 1.98685 \times 10^{-3}\Omega^{-1} + 0.646454 - 0.846918\Omega + 1.3177\Omega^2 - 3.00842\Omega^3 + 14.04220\Omega^4 - 17.4783\Omega^5 \quad (66)$$

$$Cp_{Pol} = 0.3669 + 0.00242(T - 273.15) \quad (67)$$

$$Cp_w = 3.6653 - 2.77195 \times 10^{-2} T_w + 1.07756 \times 10^{-4} T_w^2 - 1.87210 \times 10^{-7} T_w^3 \quad (68)$$

The latent heat of condensation of monomer, λ_M, expressed in cal/kg is:

$$\lambda_M = 2.6380 \times 10^7 . \frac{\Omega^{0.37261}}{4.1855 MM_M} \quad (69)$$

iii. Vapor Pressures (PERRY, 1997)

The monomer vapor pressure, P_M^{SAT}, is expressed in bar-a as:

$$P_M^{SAT} = 9.86923310^{-6} \exp 57.263 + \left(-\frac{3382.4}{T}\right) - 5.7707 \ln(T) + 1.0431 \times 10^{-5} T^2) \quad (70)$$

iv. Critical Constants (PERRY, 1997)

The critical point of propylene is relatively low. As the model will be used in a wide range of operating condition, the knowledge about the critical point - above which the monomer cannot exist in the liquid phase – is crucial.

- $T_{crit} = 365{,}5\ K$;
- $P_{crit} = 4{,}63\ MPa$;
- $V_{crit} = 0.118 m^3/kmol$;
- $Z_{crit} = 0.286$.

(71)

3.3.9. Polymer Properties

Although the polymer quality does not constitute a safety issue, modeling of the polymer properties enables the validation of the process model as a whole. Therefore, the weighted average molar mass, M_w, the number average molar mass, M_n, the polydispersity index, PD, the melting index, MI, and the xylene soluble content, XS, are given (DUTRA, 2012; SILVA, 2018):

$$M_w = MM_{Pe} \frac{\mu_2}{\mu_1} \quad (72)$$

$$M_n = MM_{Pe} \frac{\mu_1}{\mu_0} \quad (73)$$

$$PD = \frac{M_w}{M_n} \tag{74}$$

$$\log(MI) = d_1 \log(M_w) + d_2 \tag{75}$$

$$\frac{d(XS)}{dt} = \frac{R_{Pol}}{m_{Pol}}\left(XS^R + k_{xs}\left(\frac{m_{TEA}}{m_{PEEB}} - 1\right) - XS\right) \tag{76}$$

where d_1, d_2, XS^R and k_{xs} are empirical quality parameters.

3.3.10. Parameters and Nominal Conditions

Table 3.3.10-1 and Table 3.3.10-2 show the general parameters and the nominal conditions of the process model, required to perform the simulations.

Table 3.3.10-1 - Parameters of the process model (MATTOS NETO; PINTO, 2001; SILVA, 2018).

Parameter	Symbol	Value	Unit
Hydrogen molar mass	MM_{H_2}	2	g/mol
Propene molar mass	MM_{Pe}	42.08	g/mol
Catalyst molar mass	MM_{Cat}	180	g/mol
Heat exchange coefficient	UA	55000000	$cal/(K.h)$
Reaction heat	ΔH	142000	cal/kg
Universal gas constant	R	1.987	*cal/(mol.K)*
Empirical quality parameter	$d1$	-4.2773;	*dimensionless*
Empirical quality parameter	$d2$	28.1131;	*dimensionless*
Propagation adjustment factor	$a1$	0.3	*dimensionless*
Propagation adjustment factor	$a2$	0.6	*mol/L*
Propagation adjustment factor	$a3$	-0.1	*dimensionless*
Propagation adjustment factor	$a4$	-1.5	*dimensionless*
Empirical quality parameter	XS^R	*3.5*	*%p/p*
Empirical quality parameter	k_{xs}	*4.8*	*%p/p*

Table 3.3.10-2 – Nominal conditions of the process model (MATTOS NETO; PINTO, 2001; SILVA, 2018).

Nominal Conditions	**Symbol**	**Value**	**Unit**
Total monomer mass inside the condenser	$m_{M,c}$	100000	kg
Total water mass inside the condenser	$m_{w,c}$	1000	kg
Reactor inlet temperature	T_{in}	303.15	K
Water inlet temperature at condenser	$T_{w,in}$	303.15	K

Table 3.3.10-3 shows the kinetic model parameters required to perform the simulations.

Table 3.3.10-3 - Kinetics parameters required to perform the simulations (MATTOS NETO; PINTO, 2001; SILVA, 2018).

	Activation Energy $(\boldsymbol{cal/mol})$		**Pre-exponential Factor**		
Step	Symbol	Value	Symbol	Value	Unit
Initiation	$\boldsymbol{E_c}$	500	$\boldsymbol{k_{c0}}$	7000	$\boldsymbol{L/(mol.h)}$
Propagation	$\boldsymbol{E_p}$	500	$\boldsymbol{k_{p0}}$	5000	$\boldsymbol{L/(mol.h)}$
Chain transfer to Monomer	$\boldsymbol{E_{tM}}$	500	$\boldsymbol{k_{tM0}}$	0.01	$\boldsymbol{L/(mol.h)}$
Chain transfer to Hydrogen	$\boldsymbol{E_{tH}}$	700	$\boldsymbol{k_{tH0}}$	15	$\boldsymbol{L/(mol.h)}$
Spontaneous chain transfer	$\boldsymbol{E_{tS}}$	500	$\boldsymbol{k_{tS0}}$	0.01	$\boldsymbol{1/h}$
Deactivation	$\boldsymbol{E_d}$	700	$\boldsymbol{k_{d0}}$	0.002	$\boldsymbol{1/h}$
$\mathbf{T_{ref} = 343.15\ K}$					

Controller tunning were carried out manually or as reported by DUTRA (2012) and SILVA (2018). Table 3.3.10-4 shows the tuning parameters of the controllers.

The operational range of manipulated variables were estimated based on heuristic values for the normal operation condition, while others were based reported by DUTRA

(2012) and SILVA (2018). Table 3.3.10-5 shows the operation ranges of manipulated variables:

Table 3.3.10-4 –Tuning Parameters of the controllers.

Controller	**Setpoint**		**Proportional Gain (K_p)**		**Integral Time (τ_c)**	
Reactor temperature	$\boldsymbol{T_{sp}\,(K)}$	$\mathbf{343.15}$	$\boldsymbol{k_{p,T}\ \left(\frac{kg}{h.K}\right)}$	$\mathbf{10000}$	$\boldsymbol{\tau_T(h)}$	$\mathbf{10}$
Cooling water temperature	$\boldsymbol{T_{w,sp}(K)}$	$\mathbf{340.15}$	$\boldsymbol{k_{p,T_C}\ \left(\frac{kg}{h.K}\right)}$	$\mathbf{1000}$	$\boldsymbol{\tau_{T_C}(h)}$	$\mathbf{0.5}$
Reactor level	$\boldsymbol{V_{sp}(L)}$	$\mathbf{30 \times 10^3}$	$\boldsymbol{k_{p,V}\left(\frac{kg}{L.h}\right)}$	$\mathbf{10}$	$\boldsymbol{\tau_V(h)}$	$\mathbf{10}$
Recycled monomer purity	$\boldsymbol{w_{M,Rec_{sp}}}$	$\mathbf{0.85}$	$\boldsymbol{k_{p,wM}\left(\frac{kg}{h}\right)}$	$\mathbf{-100000}$	$\boldsymbol{\tau_{wM}(h)}$	2
Monomer inlet mass flow	$\boldsymbol{\dot{m}_{M,sp}\ (kg/h)}$	$\mathbf{21000}$	$\boldsymbol{k_{p,\dot{m}M}(*)}$	$\mathbf{-100}$	$\boldsymbol{\tau_{\dot{m}M}\ (h)}$	1
(∗) dimensionless						

Table 3.3.10-5 – Operational ranges of manipulated variables.

Symbol	**Lower Limit (kg/h)**	**Upper Limit (kg/h)**
$\boldsymbol{\dot{m}_{M,c}}$	0	$\mathbf{5 \times 10^4}$
$\boldsymbol{\dot{m}_w}$	0	$\mathbf{1 \times 10^5}$
$\boldsymbol{\dot{m}_s}$	0	$\mathbf{5 \times 10^4}$
$\boldsymbol{\dot{m}_{purge}}$	0	$\mathbf{2 \times 10^4}$
$\boldsymbol{\dot{m}_{M,mkup}}$	0	$\mathbf{3 \times 10^4}$

3.4.Analysis of Model Implementation

3.4.1. Simulation Environment

The model was implemented in MATLAB. Since the polymerization problem has a stiff nature due to the different dynamics of intermediate catalytic species, when compared to the other model states (DUTRA, 2012), the selected ordinary differential equation solver was 'ode15s.m'. This solver is a variable-step, variable-order (VSVO) solver that uses a variable order method based on the numerical differentiation formulas (NDFs) of orders 1 to 5 to integrate the system of differential equations in a time interval, given initial conditions ("Solve stiff differential equations and DAEs — variable order method - MATLAB ode15s", [s.d.]). The error tolerances were set to relative error of 1×10^{-8} and absolute error tolerance of 1×10^{-10}.

3.4.2. Sensitivity Analysis

The implementation of the model described by SILVA (2018) is analyzed in Appendix A with reasonable results and comparable responses regarding previous works. The second model implementation step consists in the validation of the additional control strategies and the inclusion of propane as the monomer impurity. To achieve that goal, process variables were observed when changing the setpoints of the controlled variable.

Figure 3.4.2-1 shows the process behavior when 3 different setpoints for monomer purity in the recycled stream are considered. The red lines show that to increase the monomer purity in the recycled stream (from 0.85 to 0.95) it is necessary to increase the mass flowrate of purge - as one can see in part (a) - and hence reduce the propane accumulation in the reactor. On the other hand, the intensification of the purge implies on less recirculated monomer. Thus, in order to keep the monomer mass flowrate to reactor constant, the make-up flowrate must be increased, as one can see in part (b). As a result

of these changes, purer monomer is injected into the reactor, reducing the propane mass inside the reactor and increasing reaction productivity, as one can see in part (c).

Analogously, the blue and green lines show the opposite behavior when setpoints of lower purity are imposed. Observing the green line that describes the purge mass flowrate, one can notice the slow dynamics to stabilize the flowrate. This can be explained by the fact that a change in purge mass flowrate directly affects the purity of the inlet monomer stream. It takes some time for the complete response of the input change to reach the reactor output and converge to a new stationary point.

Finally, a consistency test was performed to check the control of the inlet monomer flowrate. 10% negative and positive disturbances were applied to the monomer inlet setpoint. Figure 3.4.2-2 shows the responses of manipulated and process variables. As expected, to increase the monomer inlet mass flowrate, the make-up mass flowrate must also be increased. However, this leads to reduction of the residence time in the reactor, which leads to productivity decrease, that results in the increase of the recycled gas. This effect explains the reason why make-up variations that reduce the setpoint of the monomer inlet setpoint exert stronger effects than in the opposite direction.

Having shown the model performance, which is comparable to previous works and consistent with expected behaviors, the model can be considered as valid and useful to perform hazard analysis.

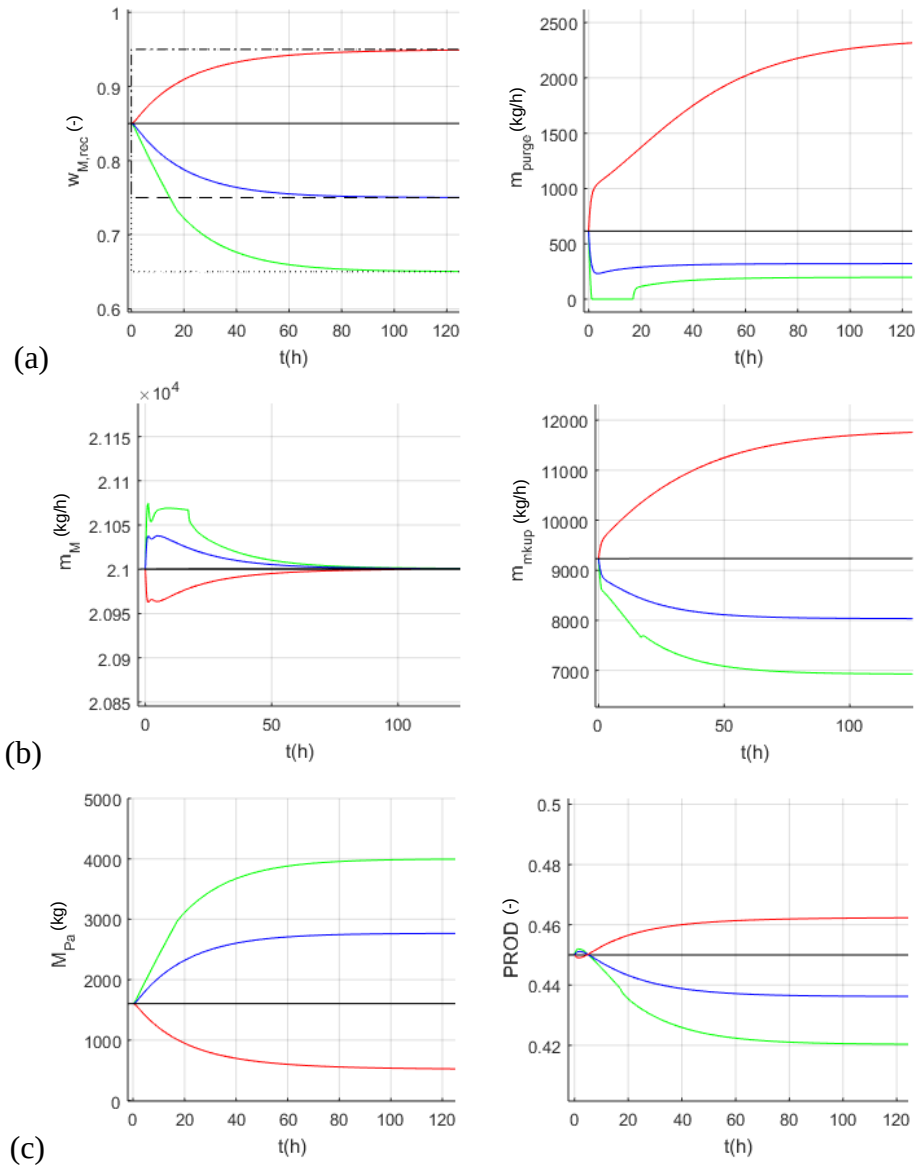

Figure 3.4.2-1 - Process variables behavior for different setpoints of monomer purity in the recycled stream: (a) Monomer purity in the recycled stream (left) and purge mass flowrate (right); (b) Monomer mass flowrate to reactor (left) and monomer make-up mass flowrate (right); (c) Propane mass inside the reactor (left) and Productivity (right).

(___) Original Steady State; (- - -) $w_{M,Rec,SP} = 0.75$; (…..) $w_{M,Rec,SP} = 0.65$; (-.-.) $w_{M,Rec,SP} = 0.95$; (___) Variable trajectory when setpoint is changed to $w_{M,Rec,SP} = 0.95$; (___)+Variable trajectory when setpoint is changed to $w_{M,Rec,SP} = 0.75$; (___)Variable trajectory when setpoint is changed to $w_{M,Rec,SP} = 0.65$;

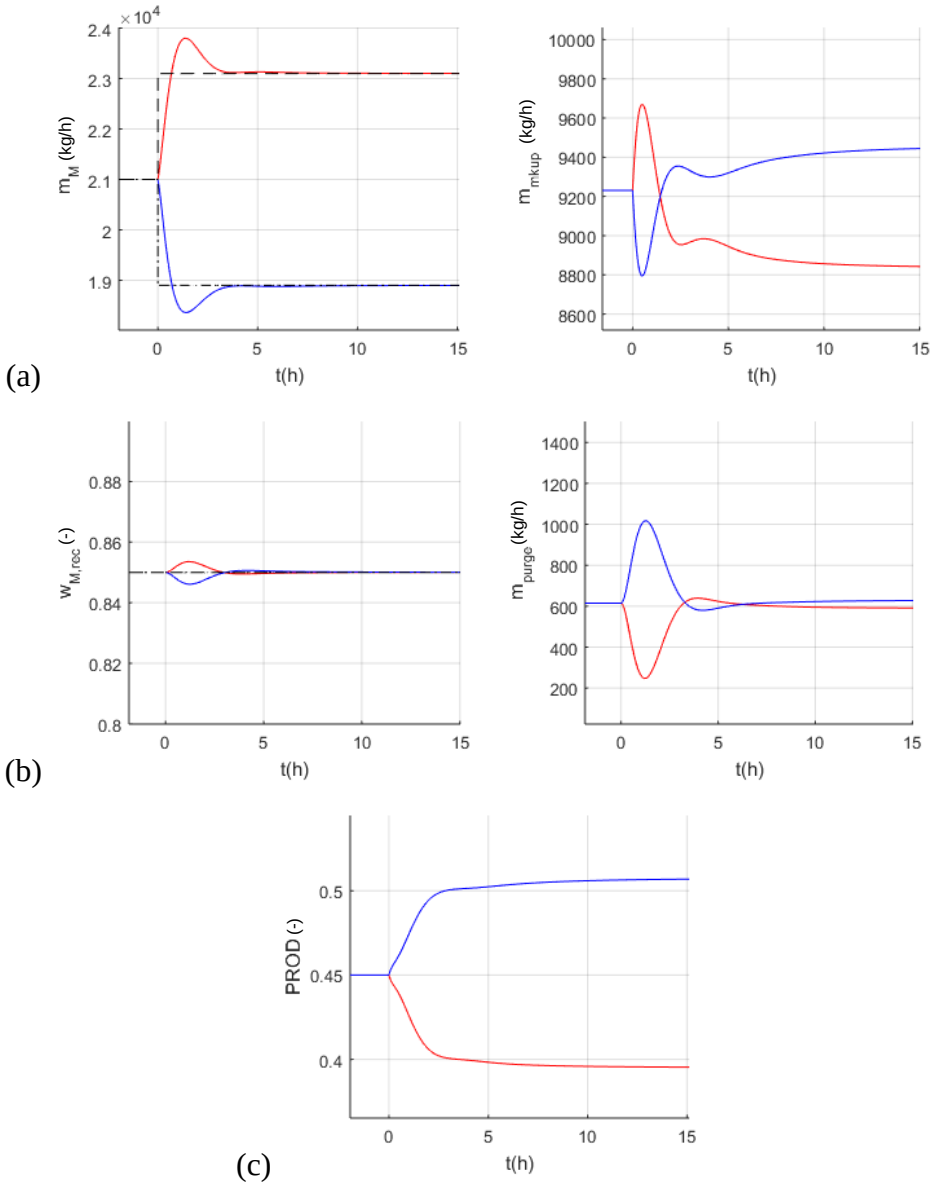

Figure 3.4.2-2 - Process variables behavior for different setpoints of monomer mass flowrate in the recycled stream: (a) Monomer purity in the recycled stream (left) and purge mass flowrate (right); (b)Monomer mass flowrate to reactor (left) and monomer make-up mass flowrate (right); (c) Propane mass inside reactor (left) and Productivity (right).

(- - -) $m_{M,SP} = +10\%$; (-.-.-) $m_{M,SP} = -10\%$; (——) Variable trajectory when setpoint is $+10\%$; (——) Variable trajectory when setpoint is-10%;

3.5.Model Adaptation

As discussed in the literature review, when simulating the model over a wide range of operation conditions, the validity of model parameters and numerical the convergence may be jeopardized. Therefore, it is crucial that model results be checked regarding

consistency. Figure 3.5-1 shows the strategy for numerical simulations used for the proposed safety analysis.

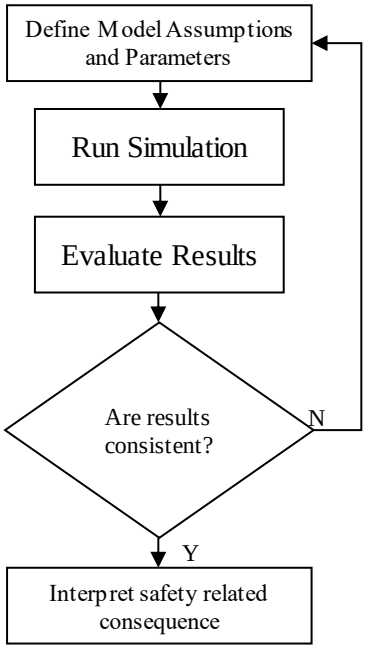

Figure 3.5-1 – Strategy for numerical simulations.

During the model development stage, three different versions of the model were proposed. Each model considered different assumptions and demanded new parameters in order to provide consistent simulation results. This concept is illustrated in Figure 3.5-2.

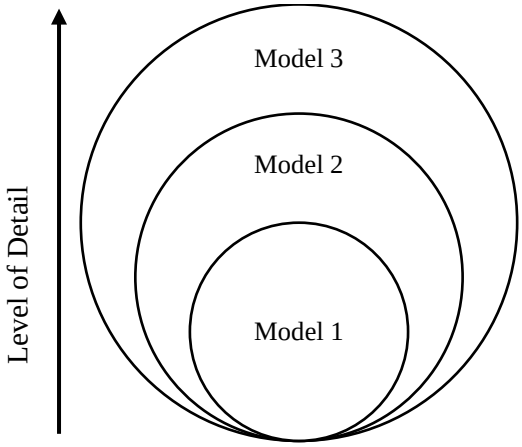

Figure 3.5-2 – Hierarchical structure of Developed Models.

Model 1 is based on previous publications (MATTOS NETO; PINTO, 2001; PRATA et al., 2009; SILVA, 2018) as described in section 3.3 of this Chapter. Propane was considered the main impurity of the inlet monomer stream and the reactor pressure was modeled as a function of temperature.

Model 2 is a first modification of Model 1 and considers the TEA/PEEB ratio effect on the catalyst activity. Figure 3.5-3 shows that the kinetic factor, f_{orig}, elaborated for applications in narrow ranges of operation conditions (SILVA, 2018), can be inconsistent when extrapolation is needed. The proposed adjustments were:

- Introduce a linear approximation up to zero in the region of low TEA concentrations since it is known that TEA (co-catalyst) is needed to activate the catalyst (MALPASS; BAND, 2012);
- Assume a constant behavior of 80% of deactivation in the region of low $PEEB$ concentrations, since it is known that the excess of PEEB jeopardizes mainly the quality of the final product and is not able to kill the reaction (PINTO, 2019a).

The proposed modifications can be seen in Figure 3.5-3, which shows the modified factor, f_{mod}.

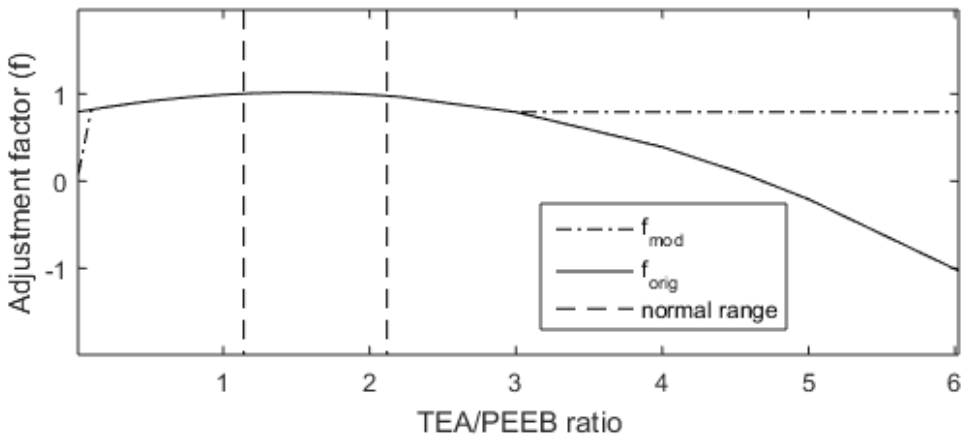

Figure 3.5-3 –Adjustment of the kinetic factor.

Besides, Model 2 considered a limiting flowrate in the compression and condensation unit. It was considered that the normal recycled rate is about 60% of the maximum compression capacity, so that:

$$\dot{m_{M,Rec}}|_{max} = 2 \times 10^4 kg/h \tag{77}$$

Finally, it was also assumed that when the reactor is flooded with liquid, condensation cannot take place. This can lead to very dangerous operation, due to the simultaneous increase of pressure and temperature and should be avoided.

Model 3 is an improvement of Model 2 regarding the thermodynamic behavior of propene, motivated by the fact that the operating temperature, $T_{sp} = 343\,K$ and the propene critical temperature, $T_{crit} = 365.57\,K$ (ANGUS; ARMSTRONG; DE REUCK, 1980) are close. Due to the proximity to the critical temperature, the assumption of liquid-vapor equilibrium during simulations may not be correct in all conditions. Besides, the remaining thermodynamic properties are subject to significant variations in the proximities of the critical point. For this reason, Model 3 was developed to take into account the more precise thermodynamic description of the reaction system.

In the region of liquid-vapor equilibrium, the reactor pressure, $P_{reactor}$, was assumed to be equal to the monomer saturation pressure, P_M^{SAT}, however, the equation was modified in the form (ANGUS; ARMSTRONG; DE REUCK, 1980):

$$\begin{aligned} P_{reactor} &= P_M^{SAT} \\ &= P_{crit} \times \exp((b_1\theta + b_2\theta^{1.5} + b_3\theta^4 + b_4\theta^{4.5})(1-\theta)^{-1}) \end{aligned} \tag{78}$$

where $b_i (i = 1\ to\ 4)$ are auxiliary coefficients and $\theta = (1 - (T/T_c))$.

Outside the region of liquid-vapor equilibrium, the reactor pressure was assumed to follow the modified Virial equation in the form:

$$P_{reactor} = \rho_{Pe} RT[1 + \sum_{i=1}^{21} \psi_i (X)_i \,] \tag{79}$$

where $\psi_i (i = 1\ to\ 21)$ are auxiliary coefficients and $(X)_i$ $(i = 1\ to\ 21)$ are contributory terms that depend on $\tau = T_{crit}/T$ and $\omega = \rho_{Pe}/\rho_{crit}$.

The global density of propene can be obtained as:

$$\rho_{Pe} = \frac{m_{Pe}}{V_{reactor} - \frac{m_{Pol}}{\rho_{Pol}}} \tag{80}$$

where, $V_{reactor}$, is the reactor total volume capacity.

At saturation conditions, the liquid and vapor densities (function of the temperature) are (ANGUS; ARMSTRONG; DE REUCK, 1980):

$$\rho_{Pe,liq} = \rho_{Pe,c} \exp\left[c_7 \theta^{13/6} \sum_{i=1}^{6} c_i \theta^{\frac{i+2}{6}}\right] \tag{81}$$

$$\rho_{Pe,vap} = \rho_{Pe,c} \exp\big([d_1 \theta^{0.5} + d_2 \theta + d_3 \theta^{1.5} + d_4 \theta^2 + d_5 \theta^4 + d_6 \theta^{5.5} + d_7 \theta^9\,](1-\theta)^{-1} + d_8 ln(1-\theta)\big) \tag{82}$$

where $\rho_{Pe,c}$ is the critical density, θ a dimensionless number given by $1 - T/T_c$ and c_i $(i = 1\ to\ 7)$ and d_i $(i = 1\ to\ 8)$ are auxiliary coefficients.

To identify the thermodynamic state, it is necessary to verify two conditions. Above the critical temperature, a supercritical state is assumed to occur. Below the critical temperature,

- subcooled liquid is assumed if $\rho_{Pe} > \rho_{Pe,liq}$;
- overheated vapor is assumed if $\rho_{Pe} < \rho_{Pe,vap}$;
- and liquid-vapor phase equilibrium is assumed if $\rho_{Pe,liq} > \rho_{Pe} > \rho_{Pe,vap}$.

The liquid fraction can be calculated as:

$$x_{liq} = \frac{\rho - \rho_{Pe,vap}}{\rho_{Pe,liq} - \rho_{Pe,vap}} \quad \text{If } \rho_{Pe,liq} > \rho_{Pe} > \rho_{Pe,vap} \quad \text{(Liquid-vapor equilibrium)} \tag{83}$$

$$x_{liq} = 1 \quad \text{If } T > T_c \text{ or } \rho_{Pe} > \rho_{Pe,liq} \quad \text{(Supercritical or subcooled liquid)} \tag{84}$$

$$x_{liq} = 0 \quad \text{If } \rho_{Pe} < \rho_{Pe,vap} \quad \text{(Overheated vapor)} \tag{85}$$

The reactor volume, V, can be obtained as:

$$V = V_{liq} = \frac{m_{Pe} x_{liq}}{\rho_{Pe,liq}} + \frac{m_{Pol}}{\rho_{Pol}} \quad \text{If } \rho_{Pe,liq} > \rho_{Pe} > \rho_{Pe,vap} \text{ or } \rho_{Pe} < \rho_{Pe,vap} \quad \text{(Liquid-vapor equilibrium or overheated vapor)} \tag{86}$$

$$V = V_{reactor} \quad \text{If } T > T_c \text{ or } \rho_{Pe} > \rho_{Pe,liq} \quad \text{(Supercritical or subcooled liquid)} \tag{87}$$

Finally, the slurry composition can be calculated as:

$$w_M = \frac{M_{Pe} + M_{Pa}}{M_{total,liq}} x_{liq} \tag{88}$$

$$w_{Pol} = \frac{M_{Pol}}{M_{total,liq}} \tag{89}$$

$$\rho = \rho_{Pe,liq} . w_M + \rho_{Pol} . w_{Pol} \tag{90}$$

$M_{total,liq}$ is the total liquid mass inside the reactor, where reaction takes place and the slurry density, ρ, is obtained based on the liquid composition.

C_p was also more precisely calculated for the operation near the critical temperature ("NIST Reference Fluid Thermodynamic and Transport Properties Database (REFPROP version 7)", 2019):

$$Cp(\rho_{Pe}, T) = Cp^{id} - R - R\left[\sum_{i=1}^{21} N_i (XC)_i\right]_0^{\omega} + R\left[\frac{(1 + \sum_{i=1}^{21} N_i (XT)_i)^2}{1 + \sum_{i=1}^{21} N_i (X\rho)_i}\right] \tag{91}$$

where $(XC)_i$, $(XT)_i$ and $(X\rho)_i$ are contributory independent terms of the state equation relating $\tau = T_c/T$ and $\omega = \rho_{Pe}/\rho_c$. As one can see, Figure 3.5-5, the heat capacities of saturated liquid, Cp_{liq}, and saturated vapor, Cp_{vap}, increase asymptotically near the critical point. This behavior has been shown experimentally for propylene (NEDUZHII et al., 1972) and also for other products (NOWICKI et al., 2001; REBILLOT; JACOBS, 1998). The densities can also change significantly near the critical point, as shown in Figure 3.5-4. Model parameters required for simulation are presented in Appendix B.

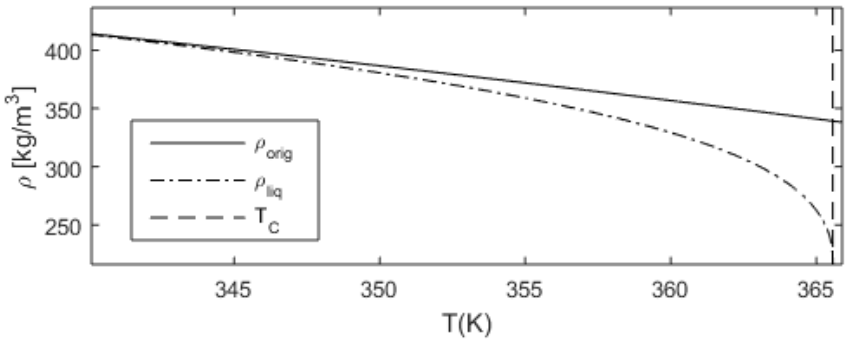

Figure 3.5-4 – Densities of the saturated liquid near the critical temperature.

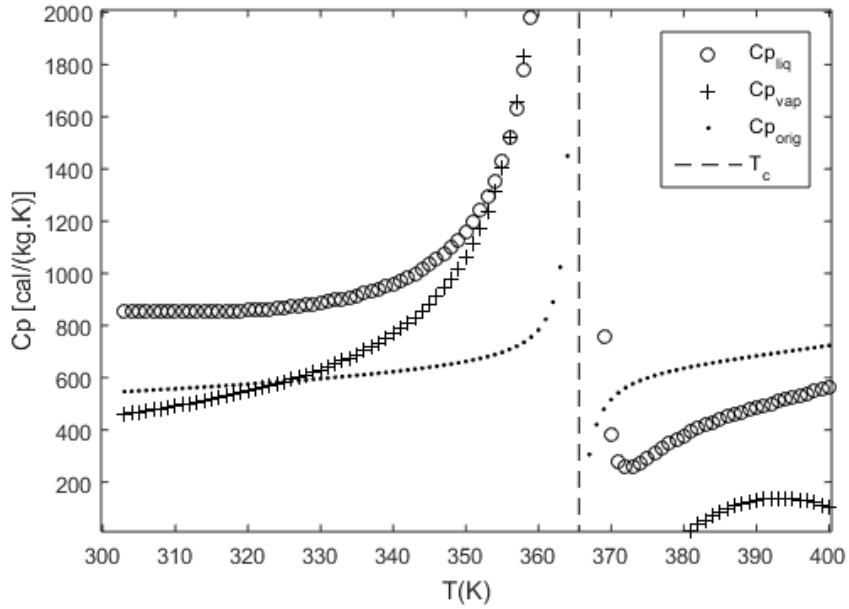

Figure 3.5-5 – Comparison of heat capacity near the critical temperature.

Chapter 4

Hazard Identification Method

4.1. Proposed Approach

As discussed before, one of the most applied methods for hazard identification, used worldwide, is the so-called HAZOP, which must be recognized as an important systematic and practical tool that, when applied by an experienced group, can indeed bring beneficial results regarding safety and operability. Nevertheless, it is also well-known that HAZOP is a “time-consuming”, “labor-intensive” (DUNJÓ et al., 2010) and an experience dependent approach and sometimes it can be overly conservative, once accurate process behavior against process deviations is not available.

As presented in Chapter 2, a lot of effort has been made to automatize hazard analysis. Among the analyzed methods, the Malfunction Procedure (RAONI; SECCHI; DEMICHELA, 2018) proposed the use of simulations in a systematic manner for hazard identification. Although the proposed methodology provides variable deviations from normal condition for sets of process disturbances, the procedure is fundamentally different from the usual HAZOP approach. The Malfunction Procedure assumes the occurrence of malfunctions and uses process simulation to determine the impact of the disturbance on the process variables. Differently, HAZOP starts with a list of process variables and applies the so-called guide words to investigate the causes of process deviations. One must notice that HAZOP is repetitive, because there is a certain correlation among the process variables. This means that, if one is able to simulate and analyze all relevant device malfunctions, each simulation will provide a set of process

variables deviations (RAONI; SECCHI; DEMICHELA, 2018). Figure 4.1-1 illustrates the characteristics of the discussed procedures.

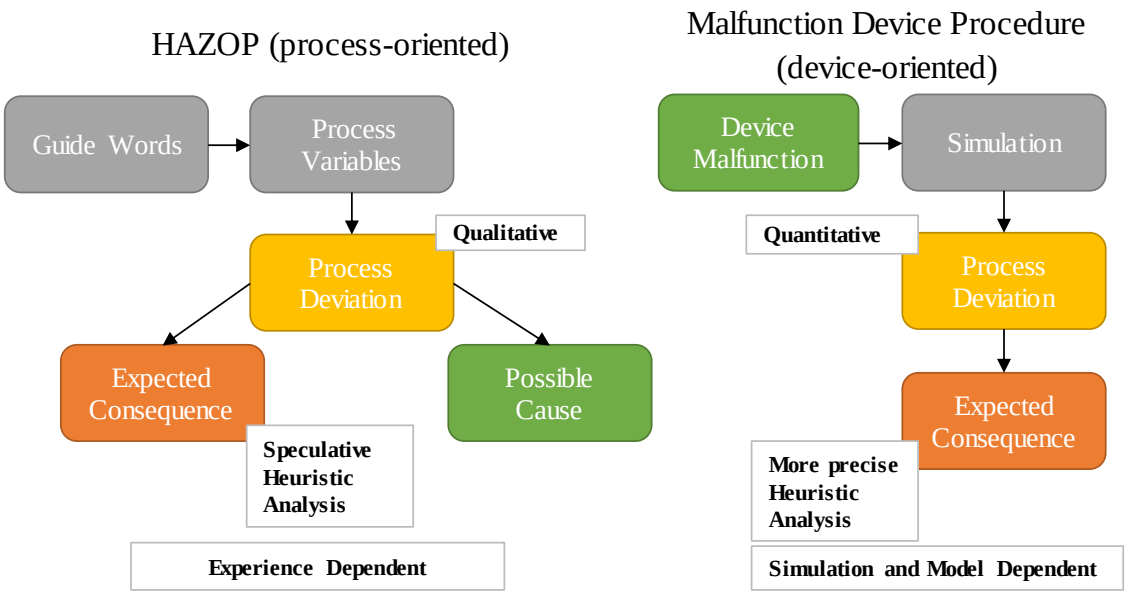

Figure 4.1-1 – Characteristics of the HAZOP and the Malfunction Device procedures.

It is important to emphasize that HAZOP (process-oriented procedure) is well-known for its systematic and disciplined way to identify process deviations and that one cannot assure with device-oriented procedure that all device malfunctions, or at least the main ones, are actually covered in the analysis. In order to tackle this question, a systematic approach based on FMEA methodology is proposed and applied to a general process flow chart as illustrated in Figure 4.1-2 and recorded in Table 4.1-1 where one can obtain a generic list of device malfunctions.

Figure 4.1-2 - Generic Process View.

An important assumption made here is that equipment materials and design conditions have been properly selected and that the plant can be safely operated at

nominal conditions. In that manner, the relevant safety malfunctions are the ones that trigger process trajectories that potentially can exceed the plant design limits.

Table 4.1-1 – Typical Failure Modes of general process streams.

Item	Function	Failure Mode
Input Streams	Add mass to the Process Node	No mass: pump failure, human error (valve inadvertently closed)
		Less mass: control failure, plugging
		More mass: control failure
		Other composition: Off spec raw material
	Add energy to the Process Node	Less energy: inlet temperature disturbance; failure of heat transfer control
		More energy: inlet temperature disturbance, failure of heat transfer control
Output Streams	Remove mass from the Process Node	No mass: pump failure, human error (valve inadvertently closed)
		Less mass: control failure, plugging
		More mass: control failure
	Remove energy from the Process Node	Coupled to mass balance, failure of heat transfer control

At the boundaries of the process node or at the interfaces between different nodes, a malfunction can also take place. Therefore, the process-parameters and devices placed at the boundaries and interfaces of the node must also be considered. Table 4.1-2 describes some process malfunctions related to the boundaries and interfaces that can potentially disturb the process variables.

Table 4.1-2 - Failure Modes of boundaries and interfaces of process nodes.

Item	Function	Failure Mode
Equipment External Walls	Contain mass	Design limits may depend on process parameters and devices. Occurrence of leaks.
	Exchange a limited amount of energy	Less Energy: fouling
Equipment Internal Walls	Contain mass	Design limits may depend on process parameters and devices. Occurrence of leaks.
	Exchange a limited amount of energy	Less Energy: fouling

A systematic approach is proposed for mapping the potential malfunction devices considering that process streams, node boundaries and devices are subjected to failures that can disturb the process as illustrated in Figure 4.1-3. When investigating streams failure modes, part of the devices will be already covered.

The simulation of devices malfunctions can be performed as deviations to the model parameters and the model input conditions, mainly when the device model is not available. After simulating all device malfunctions and building the "Simulation Result Table", a heuristic Hazard Analysis must be performed (RAONI; SECCHI; DEMICHELA, 2018). Particularly to the safety study, it is important to judge if the process variables deviations are sufficiently strong to exceed design limits, leading thus to loss of containment or damage. Thus, one must assure that the necessary process variables are provided as output variables for the malfunction simulations. Nevertheless, the simulations can also provide information about quality, cost and operation issues. Depending on the application, a different set of variables should be selected as the minimum set for further analyses.

In a traditional HAZOP analysis, the process variables used most often to suport process hazard identification are flow, pressure, temperature, level and composition. Other less frequent variables are also used, such as agitation, speed, frequency, voltage, time (relevant for batch processes), among others (CENTER FOR CHEMICAL PROCESS SAFETY, 1992; CROWL; LOUVAR, 2002).

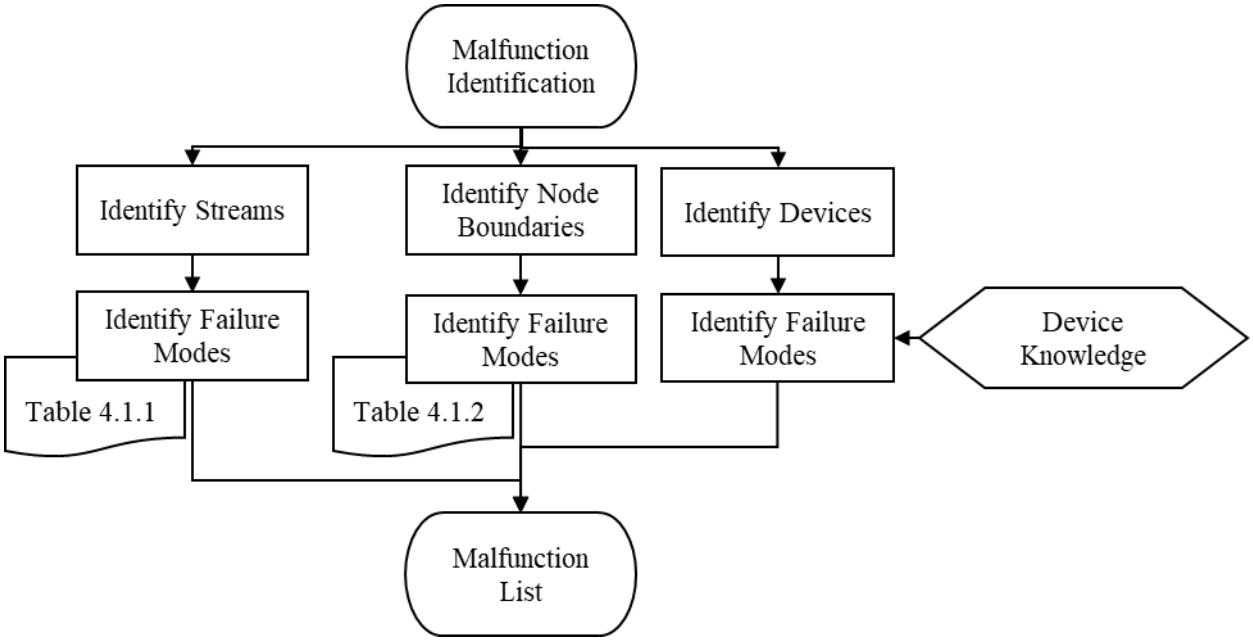

Figure 4.1-3 - Systematic Approach for Device Malfunction Identification.

The selection of the minimum process variables required to analyze the process hazards can be performed with the help of the Generic Master Logic Diagram presented by PAPAZOGLOU and ANEZIRIS (2003). If one considers chemical processes hazards, it generally regards the identification of potencial scenarios of loss of primary content (LOPC) (PAPAZOGLOU; ANEZIRIS, 2003). This considers the loss through the boundary that keeps process substances in their designed space. Knowing that the unexpected realease of substances can cause environmental, personal and asset damages, it is important to characterize the relation between process variables, and factors that can lead to loss of primary content. Figure 4.1-4 shows a simplified version of the event tree

proposed by PAPAZOGLOU and ANEZIRIS (2003) that leads to LOPC. Althought this diagram has been proposed for a qualitative hazard identification procedure, it brings valuable information about how process variables deviations can lead to hazardous scenarios.

It should be observed that vibration, high temperature, over and under pressure are the immediate causes of structural failures. Therefore, these variables are crucial for deeper heuristic analyses.

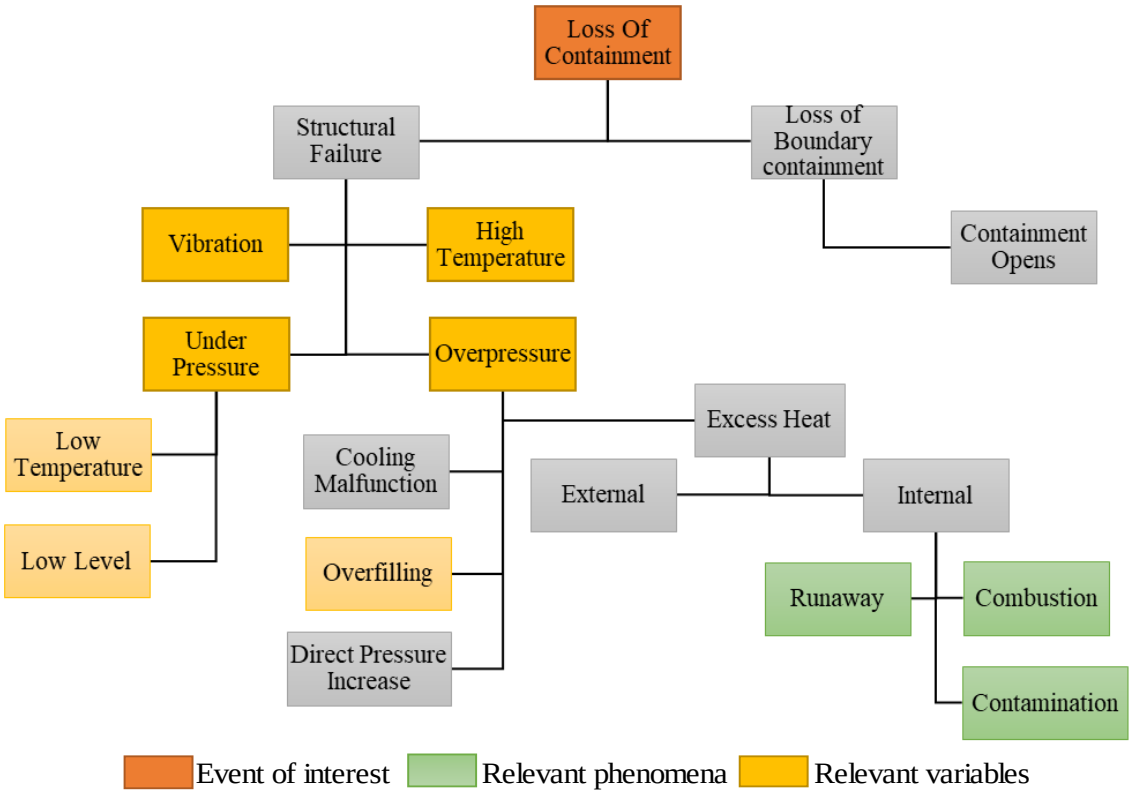

Figure 4.1-4 - Generic Master Logic Diagram. Adapted from PAPAZOGLOU and ANEZIRIS, (2003).

In this scenario, it should be highlighted that the process model should be able to capture undesired behaviors (as runaway reactions, contaminants side reactions, combustion, among others) and the dynamics of all relevant process variables which is not always possible particularly in the first stages of process design and in complex process flowsheets. Modeling the mechanisms of overfilling leading to overpressure, and

low temperature and low level leading to under pressure is also desirable. However, when not available, it is recommended to monitor these variables in order to feed critical analyses of the trajectories of process variables.

It is important to emphasize that the model can also provide other important output variables for the understanding of hazardous scenarios. The selection of the minimum set of output variables does not exclude the possibility of checking other available information, but guides the analyst to identify mechanisms of loss of primary containment, which are relevant for safety analyses. Besides, depending on the process, additional variables should be added to the minimum set of simulation output variables.

Therefore, the proposed approach uses the Malfunction Procedure (RAONI; SECCHI; DEMICHELA, 2018) and contributes with systematic guidelines about (i) the identification of device malfunctions; (ii) the selection of important output variables of simulations; and (iii) the critical phenomena that should be taken into account during modeling steps to allow for complete hazard identification analyses.

Chapter 5

Results and Discussion

5.1.Device Malfunction Identification

As proposed in Chapter 4, all inlet and outlet process streams, node boundaries and interfaces should be eligible to malfunction. Figure 5.1-1 shows all potential process malfunctions, which are highlighted in orange and numbered sequentially. Following the proposed methodology, the failure modes of each device are shown in Table C-1 from Appendix C.

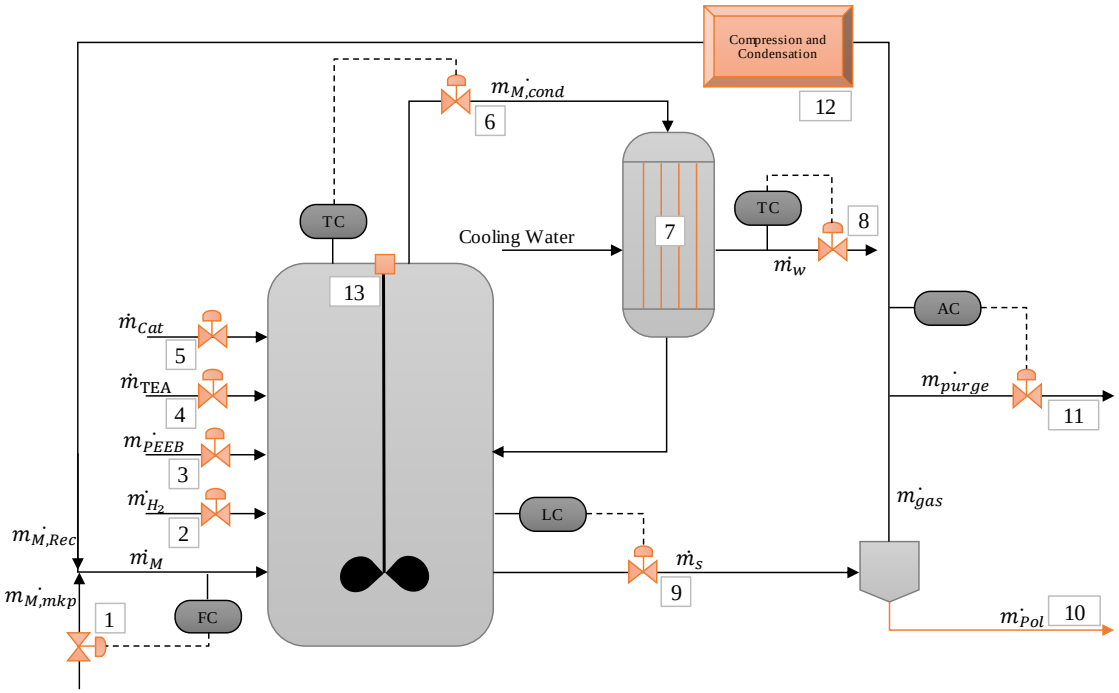

Figure 5.1-1 – Possible candidates for process malfunctions.

5.2.Simulations

5.2.1. Normal Condition

The normal operation condition considered for simulations leads to product grade with $MI = 15\ g \times (10\text{min})^{-1}$, $XS = 7\%\ p/p$ and $Prod = 0.45$, with recycled monomer purity set to 80%. As discussed in Chapter 4, the critical process variables for safety are pressure, temperature and level. Vibration will not be investigated here, since models are not available for vibrations of pumps and compressors. Due to the slow agitator speed, vibration was not considered in the agitator system.

Figure 5.2.1-1 shows the normal operating conditions of the most critical variables for safety.

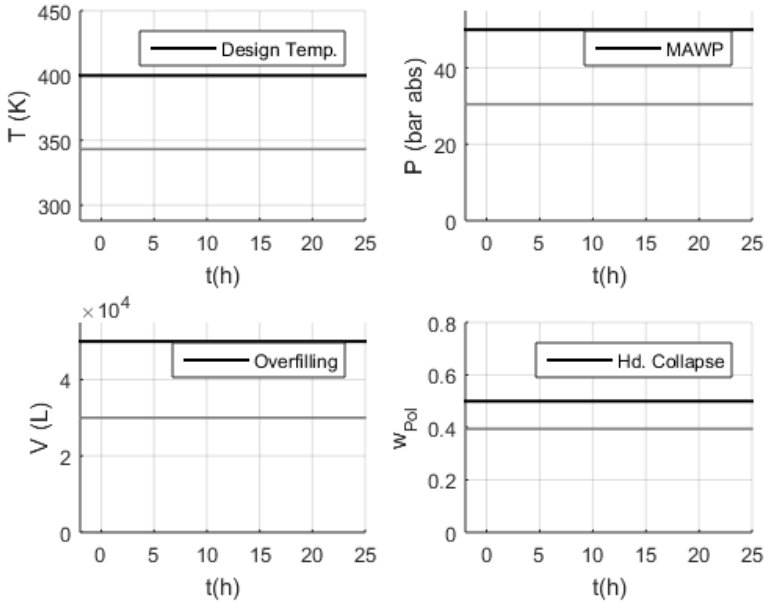

Figure 5.2.1-1 - (—) Normal conditions of the most critical variables for safety.

A critical variable, that is particularly important for this case study, is the polymer mass fraction inside the reactor. As the polymer is in the solid phase, it is crucial that the polymer be kept in suspension in the liquid phase. Experience shows that when polymer mass fraction is higher than 0.5, the hydrodynamic collapse of the suspension can occur.

This phenomenon can cause significant damage to the reactor mechanical components and can lead to loss of primary containment, constituting thus a critical variable for safety (PINTO, 2019b). The maximum allowed limits were defined as follows:

- Volume: the normal operation condition represents 60% of the design limit of 50 m^3.
- Pressure: the normal operation condition represents 60% of the maximum allowed working pressure (MAWP) of 50 bar.
- Temperature: the normal operation condition is approximately 50 K below the design temperature of 400 K.

5.2.2. Malfunction Simulation

The malfunctions, as described in Appendix C, were simulated as step disturbances in the model parameters and model inputs conditions. Figure 5.2.2-1 represents a general disturbance on the evaluated parameter (or input condition), where the dashed colored lines represent disturbances in direction of decreasing parameter (or input condition) normal values and the continuous colored lines indicate disturbances in the direction of increasing values. In all cases, the grey continuous lines represent the normal steady states.

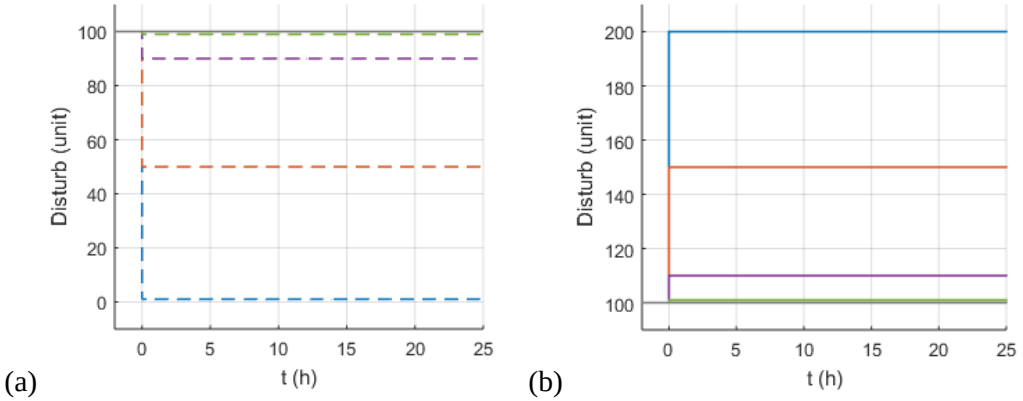

(a) (b)

Figure 5.2.2-1 - General disturbance representation: (a) (- - -) (- - -) (- - -) (- - -) decreasing steps; (b) (—) (—) (—) (—) increasing steps; (—) normal steady state

- **S-1 (No Monomer Make-up flowrate) and S-2 (Lower Monomer Make-up flowrate)**

Four different steps were applied to the monomer make-up flowrate in order to simulate scenarios S-1 and S-2. Freezing the monomer make-up flow at lower values represents the loss of control of the monomer inlet flowrate, leading to immediate increase of residence time and, thus, of monomer conversion. Consequently, the polymer fraction increases and the recovered gas decreases, contributing even more to reduction of monomer feed rates. This creates a self-sustained effect that can lead to hydrodynamic collapse, even after small disturbances of the make-up flow, since the volume control procedure actuates on the slurry valve closing it to keep the volume stable. All models were able to capture this effect, but with different dynamics as one can see in Figure 5.2.2-2 and Figure 5.2.2-3.

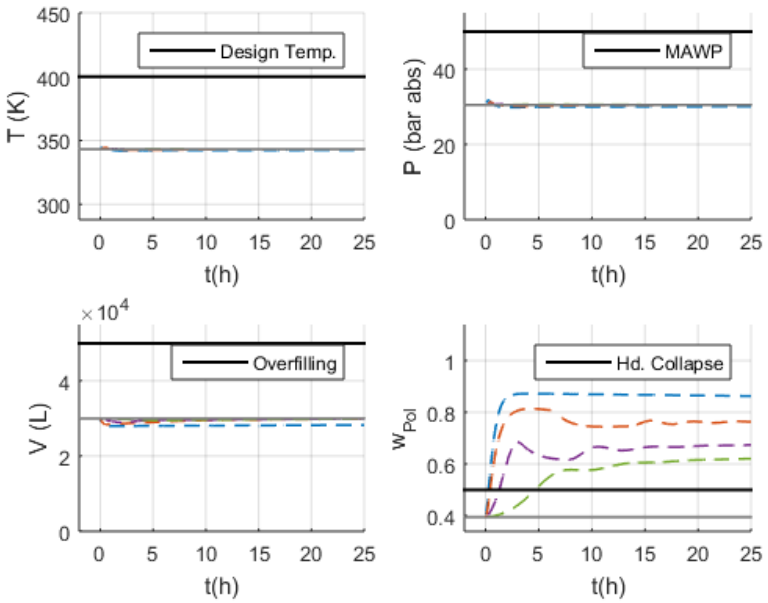

Figure 5.2.2-2 – Behavior of critical variables in scenarios S-1 and S-2 with Models 1 and 2.

Make-up flow: (- - -) No flow; (- - -) 50% of normal flow; (- - -) 90% of normal flow; (- - -) 99% of normal flow; (—) Normal

The slightly different results of temperature and pressure trajectories are related to the different thermodynamic equations when the process approaches the critical point.

Figure 5.2.2-4 shows the behavior of monomer liquid fraction. The reduction of the monomer liquid fraction reduces propene and propane concentrations in the slurry. As the monomer is consumed and its liquid fraction is reduced, the reactor volume decreases even when the slurry valve is already closed as the polymer is denser than its monomer.

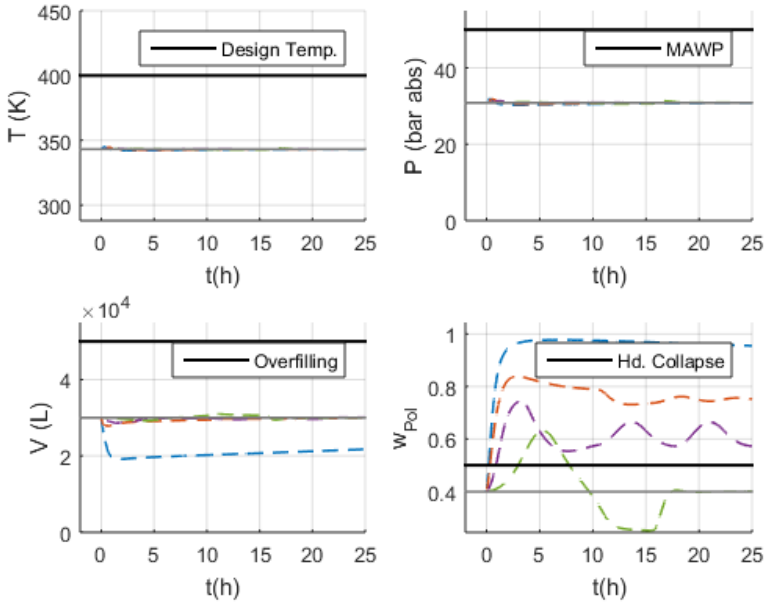

Figure 5.2.2-3 – Behavior of critical variables in scenarios S-1 and S-2 with Model 3.

Make-up flow: (- - -) No flow; (- - -) 50% of normal flow; (- - -) 90% of normal flow; (- - -) 99% of normal flow; (—) Normal.

The oscillatory behavior observed for Model 3, when the make-up flow is reduced to 90% of its normal value, is related to the purge control. After the failure, the slurry valve closes, the propene mass inside reactor decreases, and the purity of the recycled stream decreases, triggering an increasing response of the purge rate, up to the point where the monomer is not recycled anymore. At this condition, the monomer feeding into the reactor is provided only by the fresh monomer stream, which increases the mass of

propene inside the reactor and the monomer purity of the recycled stream. This triggers the opposite effect, reducing the purge and increasing the recycled stream back to reactor, which reduces the propene concentration and closes a cycle of oscillatory behavior. It is believed that the distinct dynamic behavior of Model 3, after the hydrodynamic collapse, is related to modeling the liquid fraction, which depends on the monomer mass inside the reactor and is accounted by the calculation of the slurry composition (which affects the recycled stream composition). It is important to observe, though, that the oscillatory behavior is unreal, as operation is not possible after the hydrodynamic collapse of the slurry stability.

The numerical "wash-out" effect after the hydrodynamic collapse, observed for Model 3, when the make-up flow is reduced to 99% of its normal value, is caused by the increase of the recycle stream flowrate after closing of the purge valve, which leads to reduction of residence time and, hence, to reduction of monomer conversion.

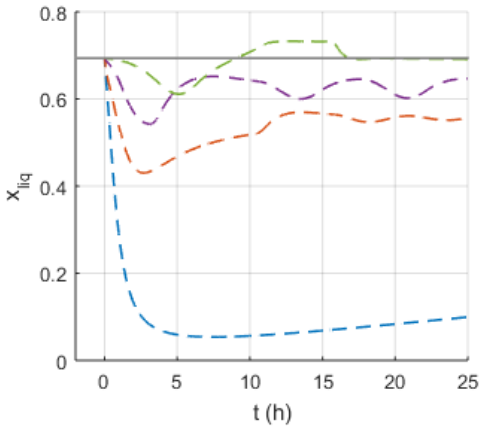

Figure 5.2.2-4 – Behavior of liquid fraction of monomer in scenarios S-1 and S-2 with Model 3

Make-up flow: (- - -) No flow; (- - -) 50% of normal flow; (- - -) 90% of normal flow; (- - -) 99% of normal flow; (—) Normal.

Nevertheless, the event of interest in this analysis is the safety impact of the process variables, which results on hydrodynamic collapse, even when small disturbances are introduced into the make-up flowrate, characterizing this scenario as a potential

hazard for the operation. Models 1 and 2 are able to describe the safety critical behavior, although Model 3 indicates faster dynamic responses until the hydrodynamic collapse. Thus, if dynamic information is desired, the simpler model can underestimate the propagations speed of the potential hazard.

- **S-3 (Higher Monomer Make-up flowrate):**

After increasing the monomer make-up flowrate, one can see in Figure 5.2.2-5 that the residence time decreases and that the unreacted monomer mass flowrate ($\dot{m_{gas}}$) increases, leading to increase of the recycled monomer flowrate sent back to the reactor.

As no limit was imposed on the recycled mass flowrate, $\dot{m_{Rec}}$, the recovered gas is sent back to the reactor, creating the self-sustained increase of the monomer inlet flow rate to the point that it exceeds the reactor output flowrate capacity, leading to overfilling of the reactor, as shown in Figure 5.2.2-6. However, it is known that the recycled gas is compressed and condensed before returning to the reactor. In this circuit, pipelines and equipment have a maximum designed flowrate capacity that limits the maximum recycled mass flowrate to reactor. Figure 5.2.2-7 shows the process behavior when this effect is considered.

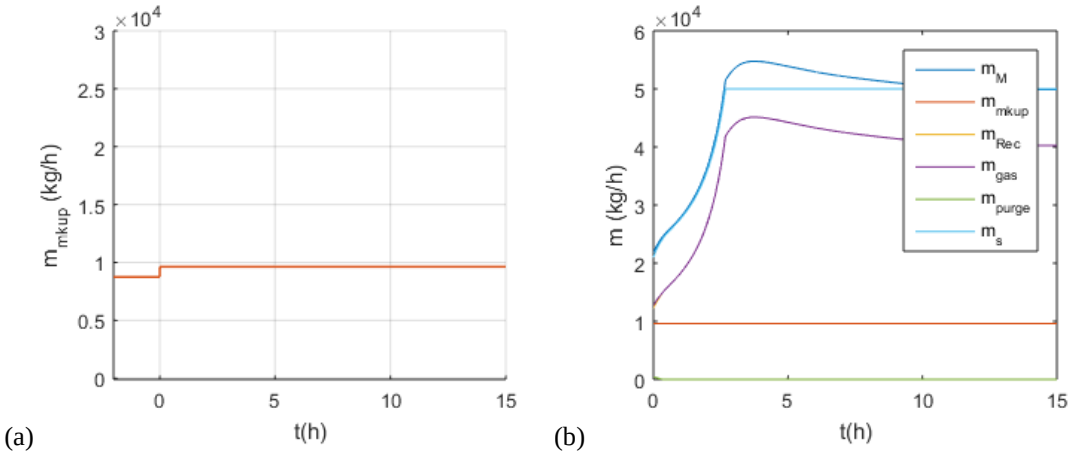

Figure 5.2.2-5 – (a) Make-up flow disturbance (10% increase) and (b) Behavior of other mass flowrates with Model 1.

As a consequence, attaining the maximum recycled flowrate to the reactor, the residence time decreases, the unreacted monomer mass flowrate increases, but the recycled monomer sent back to the reactor becomes limited, which leads to irrelevant safety effects regarding temperature, pressure and level. On the other hand, although the limit of the recycle mass flowrate prevents the reactor from overfilling, it triggers other process hazard: the overload of the compression and condensation unit. As one can see in Figure 5.2.2-8, the recycle flowrate is lower than the gas generation, which in practical terms means the occurrence of the overload of the compressing unit, with possible overpressure. Similar results were obtained with Model 3 as shown in Figure 5.2.2-9.

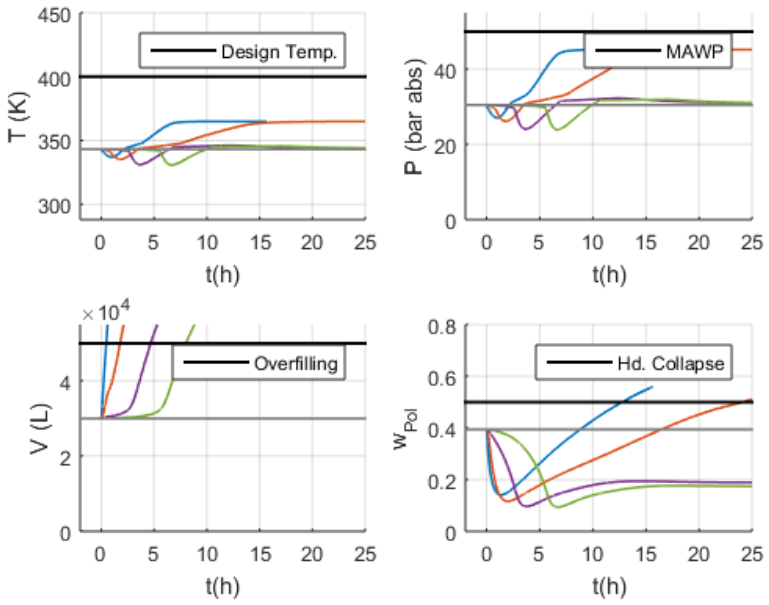

Figure 5.2.2-6 – Behavior of critical variables in scenario S-3 with Model 1

Make-up flow: (—) Maximum flow; (—) 150% of normal flow; (—) 110% of normal flow; (—)101% of normal flow; (—) Normal

In conclusion, in this simulation case, Model 1 leads to wrong understanding of the hazardous scenario, being necessary the increase of the modeling level of detail. Model 2 is sufficient to describe the safety critical scenario, but different dynamic paths are observed when more detailed assumptions are made, as shown with Model 3. Despite

that, the simulations confirm that the analyzed scenario constitutes an import hazard for the process operation.

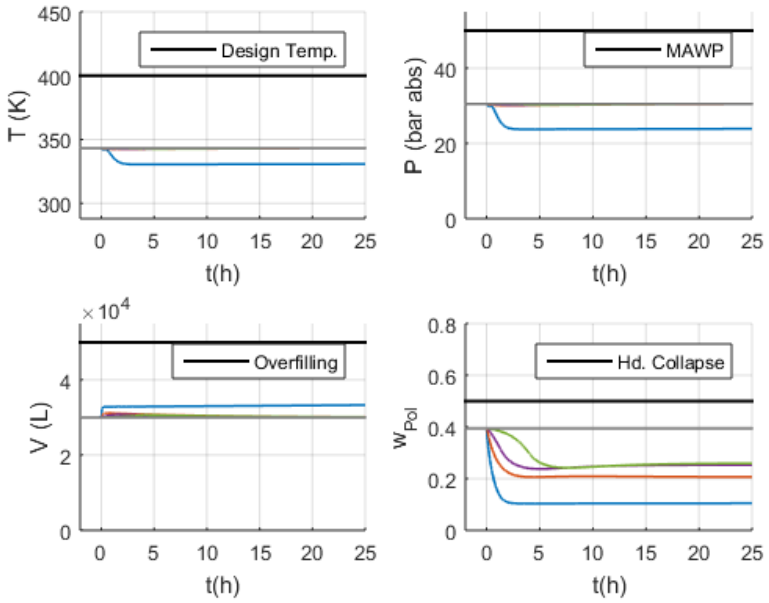

Figure 5.2.2-7 – Behavior of critical variables in scenario S-3 with Model 2.

Make-up flow: (—) Maximum flow; (—) 150% of normal flow; (—) 110% of normal flow; (—)101% of normal flow; (—) Normal

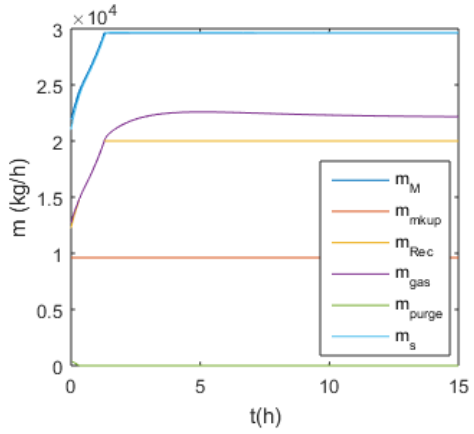

Figure 5.2.2-8 - Mass flowrates after disturbance of +10% on the monomer make-up stream with Model 2.

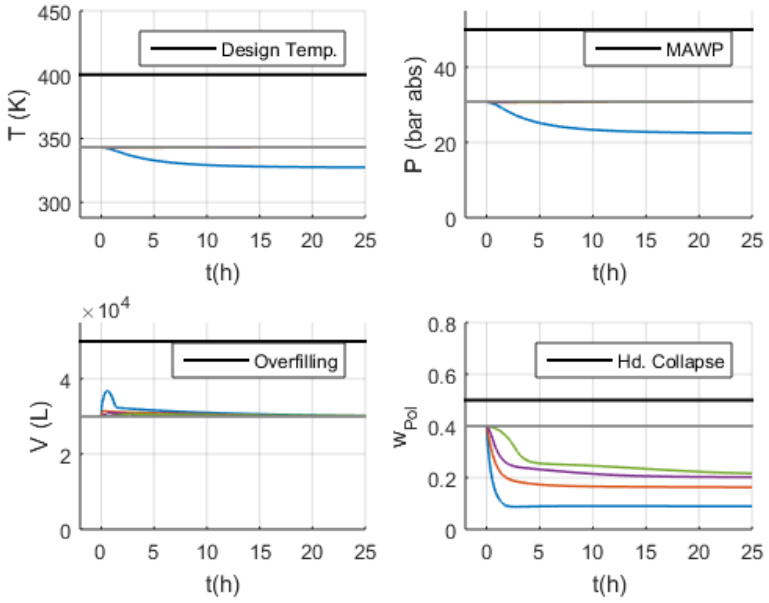

Figure 5.2.2-9 – Behavior of critical variables in scenario S-3 with Model 3.

Make-up flow: (—) Maximum flow; (—) 150% of normal flow; (—) 110% of normal flow; (—)101% of normal flow; (—) Normal

- **S-4 (Composition of the Make-up stream of Monomer out of specification)**

Three different decreasing steps from the normal value of 99% were applied to the monomer make-up purity in order to simulate scenario S-4. As expected, all models show no relevant effect for the safety critical variables. As an example, Figure 5.2.2-10 shows the results obtained with Model 1. Safety is assured through the effective manipulation of the purge valve and control of the monomer purity in the gas stream.

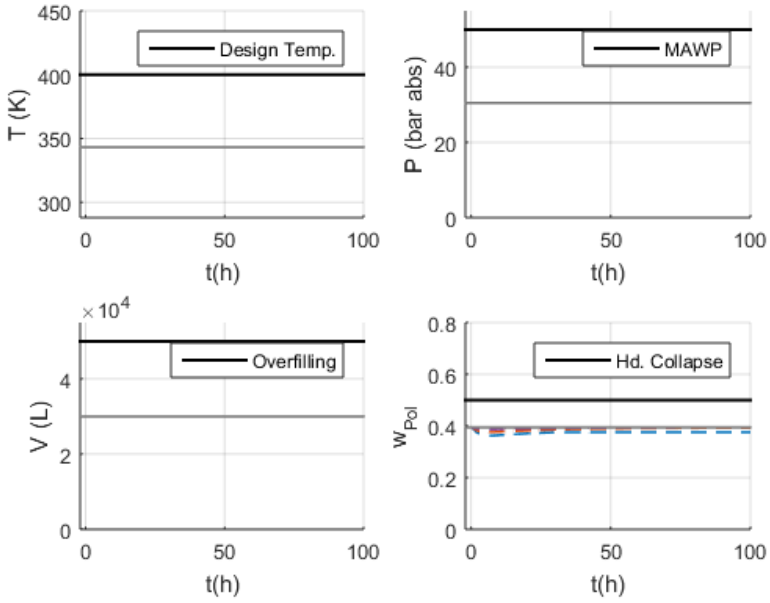

Figure 5.2.2-10 – Behavior of critical variables in scenario S-4 with Model 1.

Monomer purity: (- - -) 85%; (- - -) +90% ; (- - -) 95%; (—) Normal

- **S-5 (Lower inlet Monomer temperature) and S-6 (Higher inlet Monomer temperature)**

Six different steps from the normal operation value were applied to the inlet temperature in order to simulate scenarios S-5 and S-6. As expected, all models showed no relevant effect for the safety critical variables. Figure 5.2.2-11 and Figure 5.2.2-12 show the results obtained with Model 1.

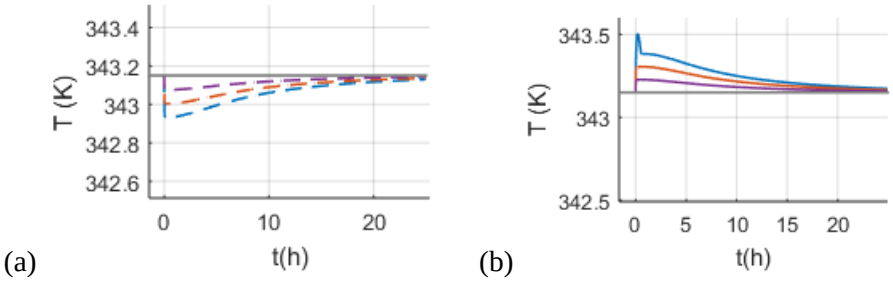

(a) (b)

Figure 5.2.2-11 –Temperature disturbances in scenario (a) S-5; and (b) S-6.

Reactor Inlet Temperature: (- - -) $-15K$; (- - -) $-10K$; (- - -) $-5K$; (—) $+15K$; (—) $+10K$; (—) $+5K$; (—) Normal

The safety is assured through the effective manipulation of process variables control to keep the reactor temperature constant.

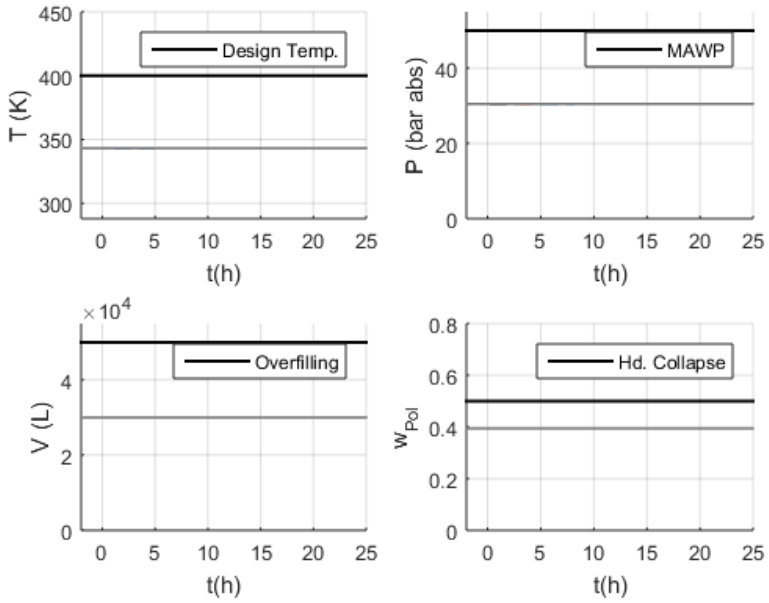

Figure 5.2.2-12 - Behavior of critical variables in scenarios S-5 and S-6 with Model 1.

Reactor Inlet Temperature: (- - -) $-15K$; (- - -) $-10K$; (- - -) $-5K$; (—) $+15K$; (—) $+10K$; (—) $+5K$; (—) Normal

- **S-7 and S-8 (No and Lower Hydrogen feed flowrate) and S-9 (Higher Hydrogen feed flowrate)**

Eight different steps from the normal value were applied to the hydrogen mass flowrate in order to simulate scenarios S-7, S-8 and S-9. The reduction of the inlet hydrogen flowrate increases the polymer fraction inside reaction due to variations on the catalyst activities. No significant differences between dynamic trajectories and new steady states could be seen when different models were used, as one can see in Figure 5.2.2-13 and Figure 5.2.2-14. It is important to emphasize that the increase of the inlet hydrogen flowrate affects the polymer fraction inside reaction on the opposite direction, as one might already expect. However, no relevant effect on the safety critical variables could be observed as shown in Figure 5.2.2-15.

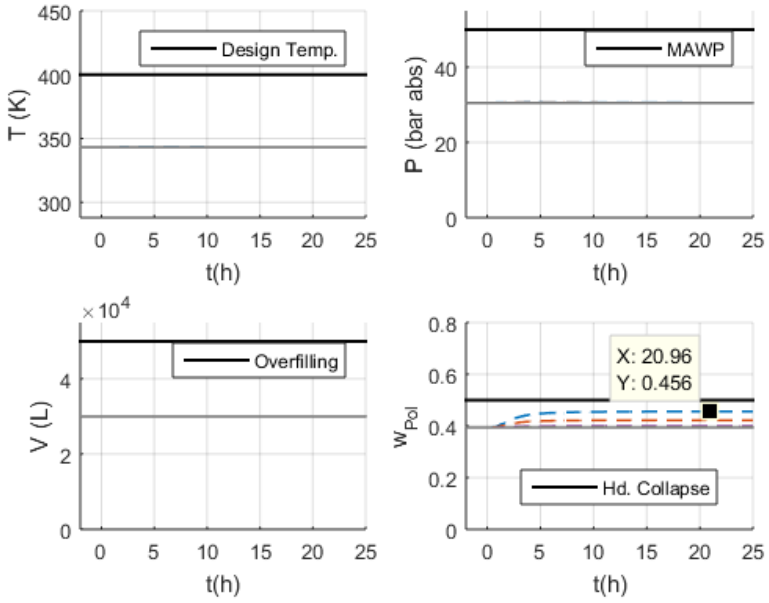

Figure 5.2.2-13- Behavior of critical variables in scenarios S-7 and S-8 with Model 1.

Hydrogen feed flowrate: (- - -) No flow; (- - -) 50% of normal flow; (- - -) 90% of normal flow; (- - -) 99% of normal flow; (—) Normal

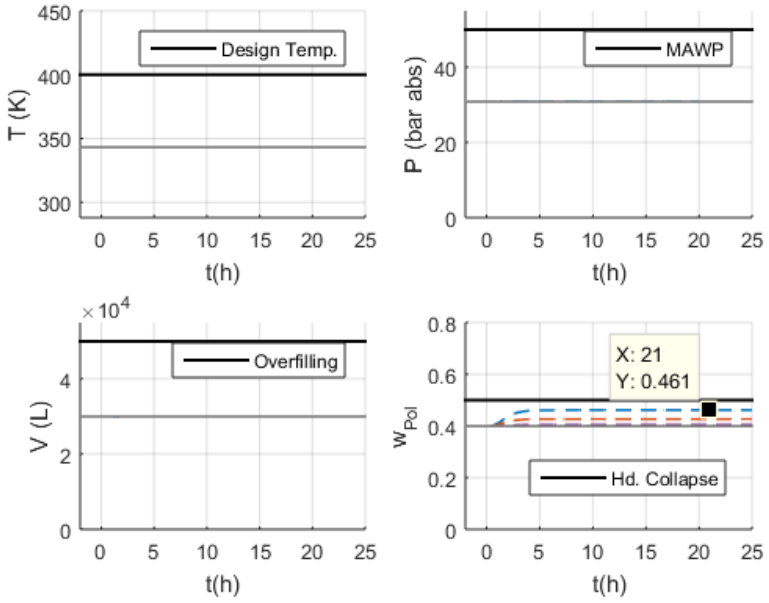

Figure 5.2.2-14- Behavior of critical variables in scenarios S-7 and S-8 with Model 3.

Hydrogen feed flowrate: (- - -) No flow; (- - -) 50% of normal flow; (- - -) 90% of normal flow; (- - -) 99% of normal flow; (—) Normal

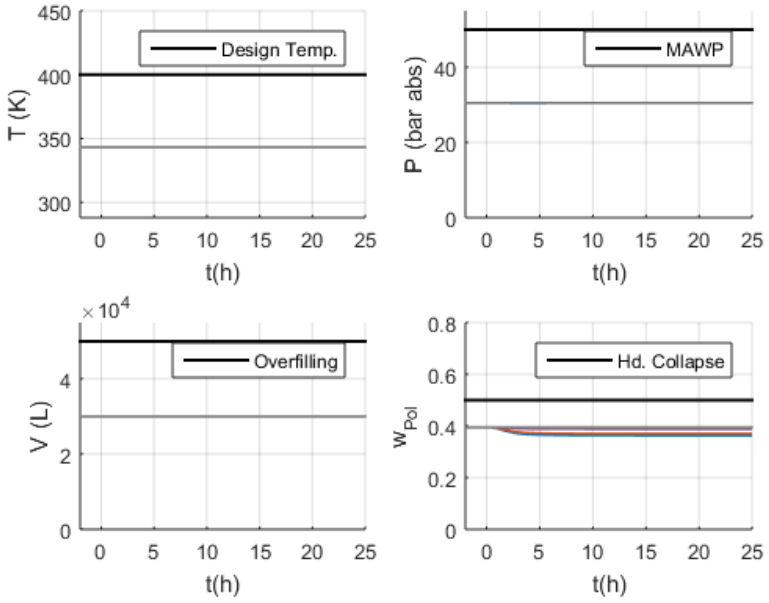

Figure 5.2.2-15 – Behavior of critical variables in scenario S-9 with Model 1.

Hydrogen feed flowrate: (—) Maximum flow; (—) 150% of normal flow; (—) 110% of normal flow; (—)101% of normal flow; (—)Normal

- **S-10 and S-11 (No and Lower PEEB feed flowrate) and S-12 (Higher PEEB feed flowrate)**

Eight different steps from the normal value were applied to the inlet $PEEB$ mass flowrate in order to simulate scenarios S-10, S-11 and S-12. The normal operating ratio between $TEA/PEEB$ represents the optimum point of catalyst activity. Thus, it is expected that any modification on this variable is able to reduce the reaction rate inside the reactor and thus the polymer fraction. Simulation results obtained with Model 1 capture this effect when the $PEEB$ mass flowrate is reduced, but leads to reaction death when feed is interrupted. This effect is not consistent with practical experience, as the interruption of the $PEEB$ feed flowrate is detrimental to polymer quality but does not lead to reaction shutdown. The extrapolation of operating conditions parameter leads to wrong understanding of the physical behavior in this case. Model 2 captures the deactivation

effect related to the reduction of the $PEEB$ feed flowrate, but limits the impact of the disturbance on the reaction rate, which is more consistent with the practical experience. Figure 5.2.2-16 shows the different responses of Model 1 and 2.

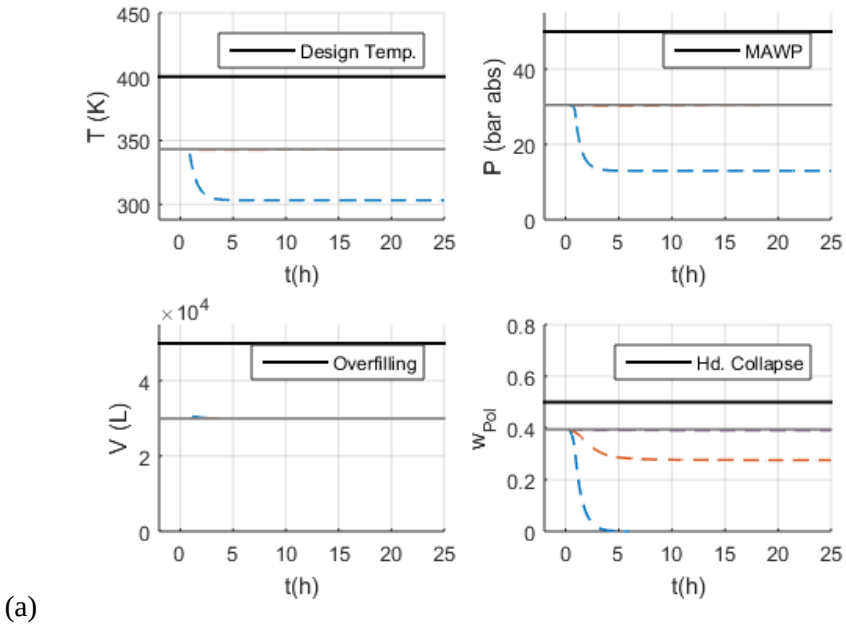

(a)

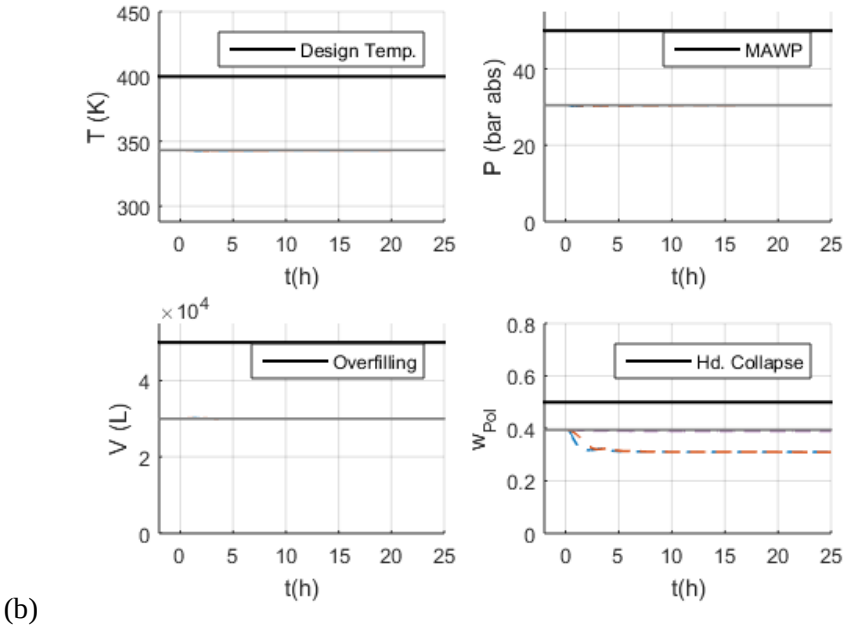

(b)

Figure 5.2.2-16- Behavior of critical variables in scenarios S-10 and S-11 with (a) Model 1; and (b) Model 2.

Inlet PEEB mass flowrate: (- - -) No flow; (- - -) 50% of normal flow; (- - -) 90% of normal flow; (- - -) 99% of normal flow; (—) Normal.

Increasing steps on the $PEEB$ feed flowrate can be captured similarly by the different models and lead to irrelevant effects on the safety critical variables, as shown in Figure 5.2.2-17.

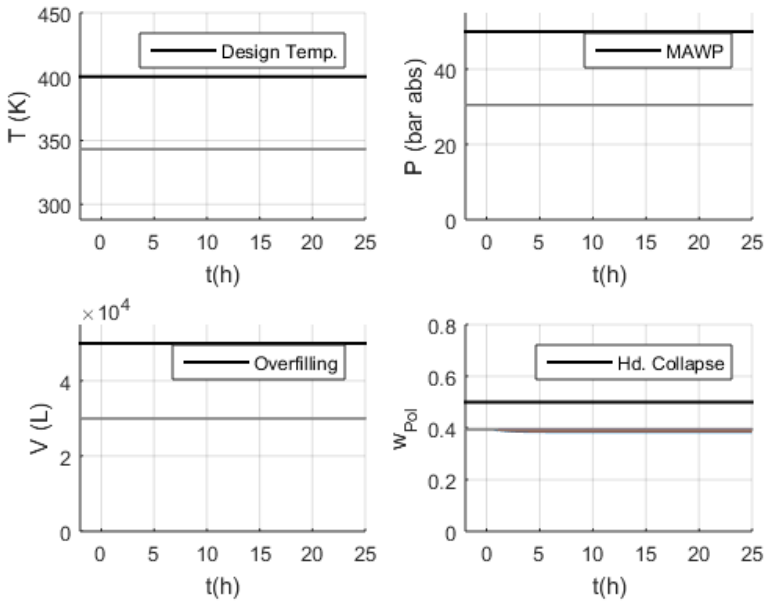

Figure 5.2.2-17 – Behavior of critical variables in scenario S-12 with Model 1.

Inlet PEEB mass flowrate: (—) Maximum flow; (—) 150% of normal flow; (—) 110% of normal flow; (—) 101% of normal flow; (—) Normal.

- **S-13 and S-14 (No and Lower TEA feed flowrate) and S-15 (Higher TEA feed flowrate)**

Eight different steps from the normal value were applied to the TEA inlet mass flowrate in order to simulate scenario S-13, S-14 and S-15. As discussed in the previous simulations, the $TEA/PEBB$ normal operating ratio represents an optimum point of catalyst activity. However, the absence of TEA can lead to complete deactivation of the catalyst system, as TEA is a co-catalyst for the reaction system.

Simulation results obtained with Model 1 are shown in Figure 5.2.2-18 and do not capture the effect of deactivation when the TEA mass flowrate is null. Again, this

limitation is related to the extrapolation of the original operation condition, leading to wrong understanding of the physical behavior. As one can see in Figure 5.2.2-19, when Model 2 is used, the deactivation effect is captured when the TEA flowrate is interrupted. When the reaction does not occur, the gas generation is equivalent to the monomer inlet flowrate. Thus, if the setpoint of the monomer flowrate is higher than the capacity of the recycle system, the compression and condensation unit become overloaded. On the other hand, if the setpoint of the monomer flowrate is lower than the capacity of the recycle system, no safety issue is posed and the monomer is recirculated through the process equipment. Similar results can be obtained with Model 3, as shown in Figure 5.2.2-20, despite the different dynamic trajectories. In conclusion, for scenarios S-13 and S-14, Model 2 is sufficient for description of the safety critical scenarios.

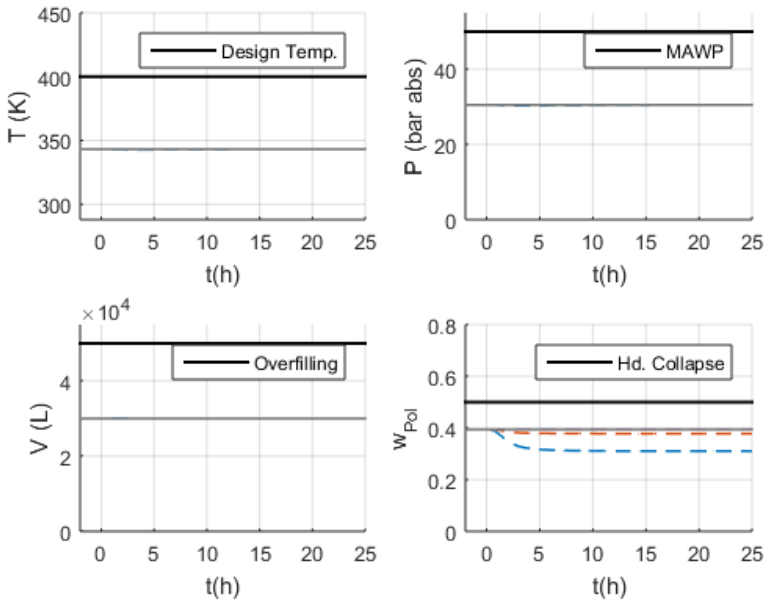

Figure 5.2.2-18 – Behavior of critical variables in scenarios S-13 and S-14 with Model 1.

Inlet TEA mass flowrate: (- - -) No flow; (- - -) 50% of normal flow; (- - -) 90% of normal flow; (- - -) 99% of normal flow; (——) Normal

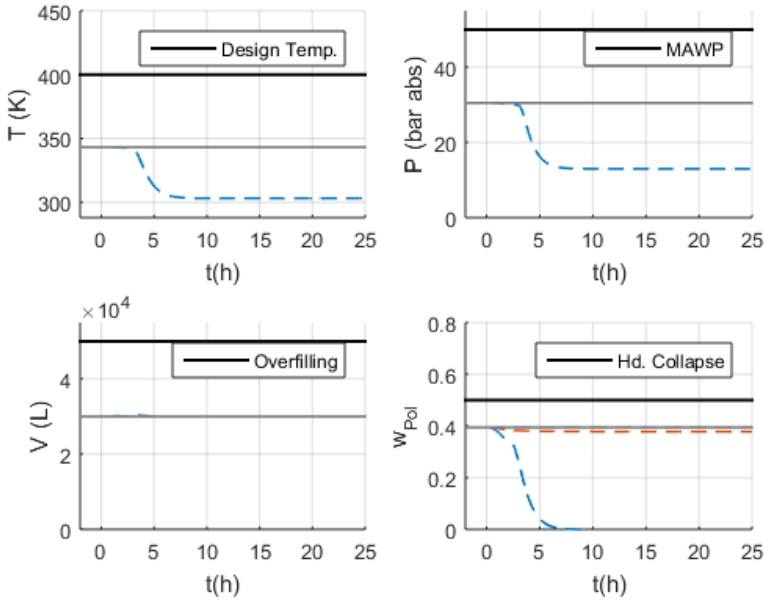

Figure 5.2.2-19 – Behavior of critical variables in scenarios S-13 and S-14 with Model 2.

Inlet TEA mass flowrate: (- - -) No flow; (- - -) 50% of normal flow; (- - -) 90% of normal flow; (- - -) 99% of normal flow; (—) Normal

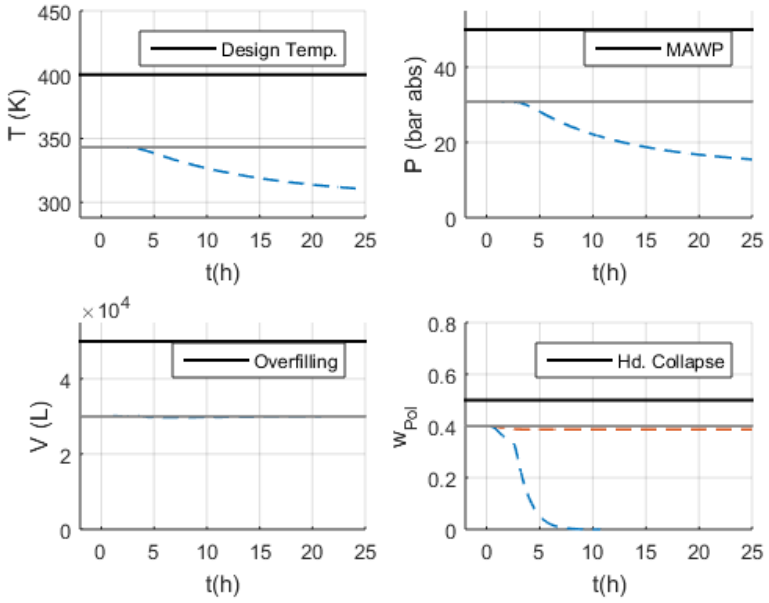

Figure 5.2.2-20 – Behavior of critical variables in scenarios S-13 and S-14 with Model 3.

Inlet TEA mass flowrate: (- - -) No flow; (- - -) 50% of normal flow; (- - -) 90% of normal flow; (- - -) 99% of normal flow; (—) Normal

Regarding the positive steps on the TEA feed flowrate, simulation S-15, all models provide comparable results. The simulation result with Model 1 is shown in Figure 5.2.2-21. The increase of the TEA mass flowrate affects negatively the reaction rate, reducing the polymer fraction inside the reactor, with no relevant safety effect.

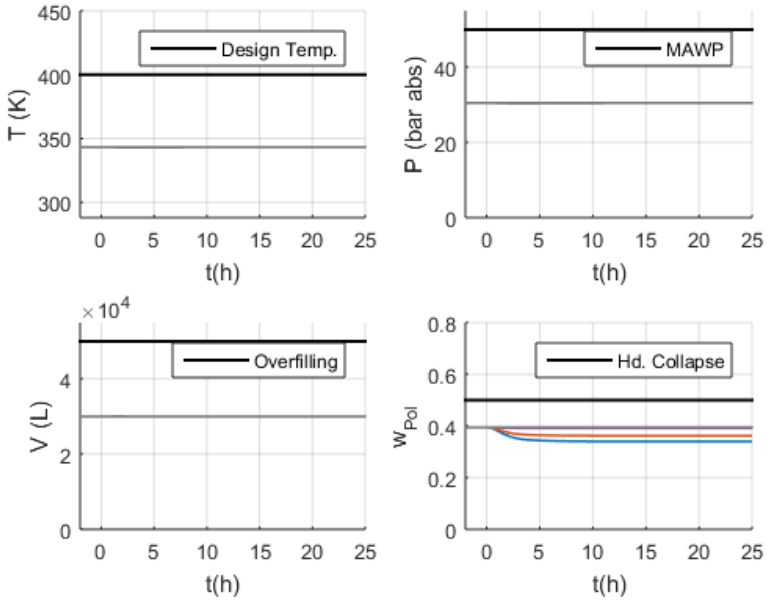

Figure 5.2.2-21 – Behavior of critical variables in scenario S-15 with Model 1.

(—) Maximum flow; (—) 150% of normal flow; (—) 110% of normal flow; (—) 101% of normal flow; (—) Normal

- **S-16, S-17 and S-19 (No and Lower catalyst feed flowrates, and reduced catalyst activity) and S-18 (Higher catalyst feed flowrate)**

Six different steps from the normal value were applied to the inlet catalyst mass flowrate in order to simulate scenarios S-16, S-17 and S-18. Scenario S-19, which represents the reduction of catalyst activity, is similar to S-17. The inlet catalyst mass flowrate significantly affects the reaction rate and the polymer mass fraction inside the reactor. The absence of catalyst drives the reaction rate to zero. As discussed before, when the reaction does not occur, the gas generation becomes equal to the inlet monomer flowrate

and if the setpoint of monomer flowrate is lower than the capacity of the recycle system, no safety issue is posed. On the other hand, if the setpoint of the monomer flowrate is higher than the capacity of the recycle system, overload of the compression and condensation unit may occur, leading to overpressure and significant operation hazards. All models lead to similar results regarding the behavior of the polymer fraction, w_{Pol}, for negative disturbances of the catalyst flowrate as shown in Figure 5.2.2-22.

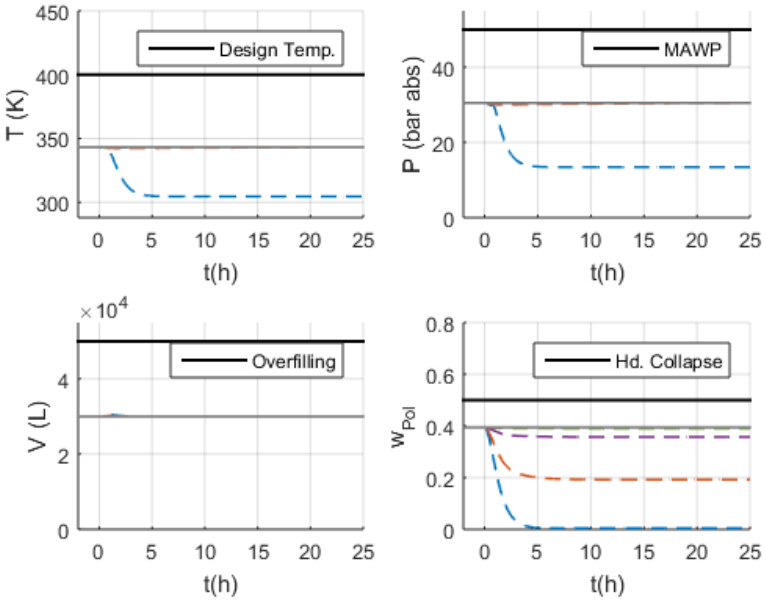

Figure 5.2.2-22 – Behavior of critical variables in scenarios S-16, S-17 and S-19 with Model 1.

Catalyst Inlet flowrate: (- - -) No flow; (- - -) 50% of normal flow; (- - -) 90% of normal flow; (- - -) 99% of normal flow; (—) Normal

The increase of the catalyst mass flowrate leads to increase of polymer mass fraction inside the reactor and can lead to hydrodynamic collapse. For the two higher positive disturbance steps, Model 1 predicted oscillatory behavior, as shown in Figure 5.2.2-23. It can be noticed that the increase of the catalyst feed flowrate leads to increase of the reaction rate and thus reduction of the monomer mass inside reactor. As a result, the purity of the recycle stream decreases and the rate of purge increases, up to the point where the whole generated gas is purged and no recycled monomer is sent back to reactor.

Then, the make-up flowrate increases, in order to keep the monomer inlet flowrate stable. The effect of injecting pure monomer reduces the propane concentration in the reactor and increases monomer purity in the recycled stream. This triggers the actuation of the purge control in the direction of decreasing purge flowrates up to the point that all gas is recycled back to reactor. This fast increase of pure gas sent back to the reactor leads to increase of reaction rates again, increasing the polymer fraction, reducing the propene concentration and generating the observed oscillatory behavior. The described flow responses can be seen in Figure 5.2.2-24, for increase of 50% of the catalyst normal flowrate. The presence of periodic oscillatory responses associated to bulk polypropylene process, when catalyst deactivation and the temperature controller are considered (DA SILVA ROSA; MELO; PINTO, 2012) and unstable behavior with multiple steady-states due to existence of recycle stream (OLIVEIRA et al., 2006) have been reported in the works of DA SILVA ROSA, MELO and PINTO (2012) and OLIVEIRA et al. (2006).

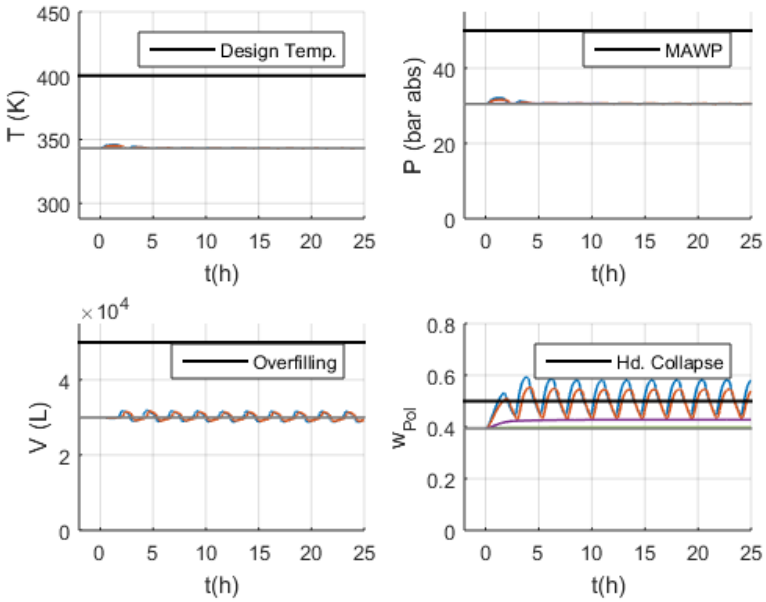

Figure 5.2.2-23 – Behavior of critical variables in scenario S-18 with Model 1.

Inlet catalyst flowrate: (—) Maximum flow; (—) 150% of normal flow; (—) 110% of normal flow; (—) 101% of normal flow; (—) Normal

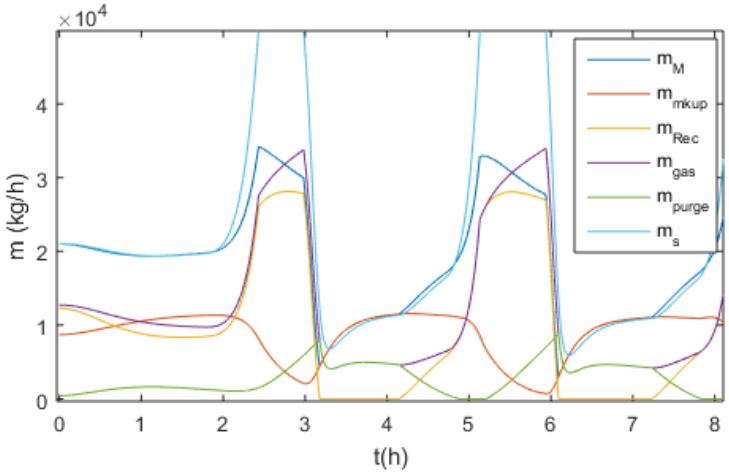

Figure 5.2.2-24 – Mass flowrates after +50% of the inlet catalyst rate with Model 1.

The consideration of a maximum recycle rate capacity, included in Model 2, eliminates this effect as can be seen in Figure 5.2.2-25.

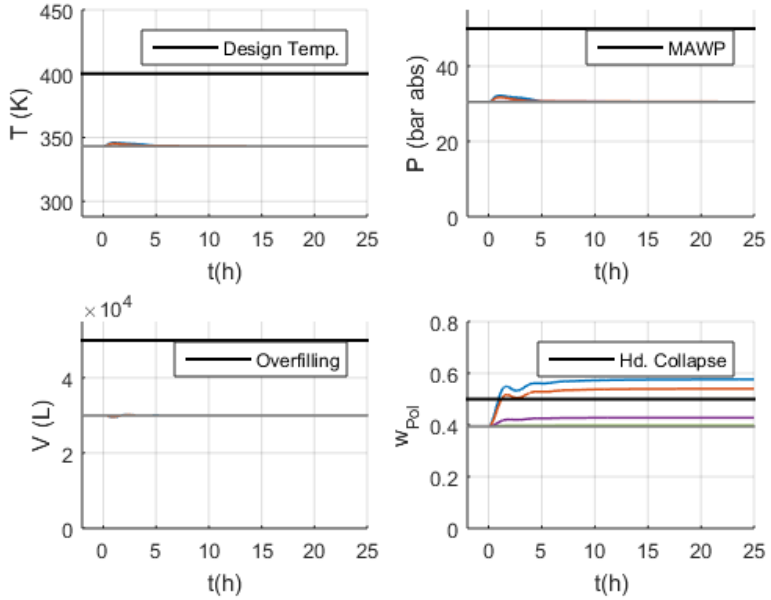

Figure 5.2.2-25 – Behavior of critical variables in scenario S-18 with Model 2.

Inlet catalyst flowrate: (—) Maximum flow; (—) 150% of normal flow; (—) 110% of normal flow; (—) 101% of normal flow; (—) Normal

Results obtained with Model 3 were similar, as one can see in Figure 5.2.2-26, with slightly different dynamic trajectories. Nevertheless, the event of interest in this analysis is the impact of the disturbance on safety, which in all cases resulted on the

hydrodynamic collapse of the suspension when the inlet catalyst flowrate was sufficiently high.

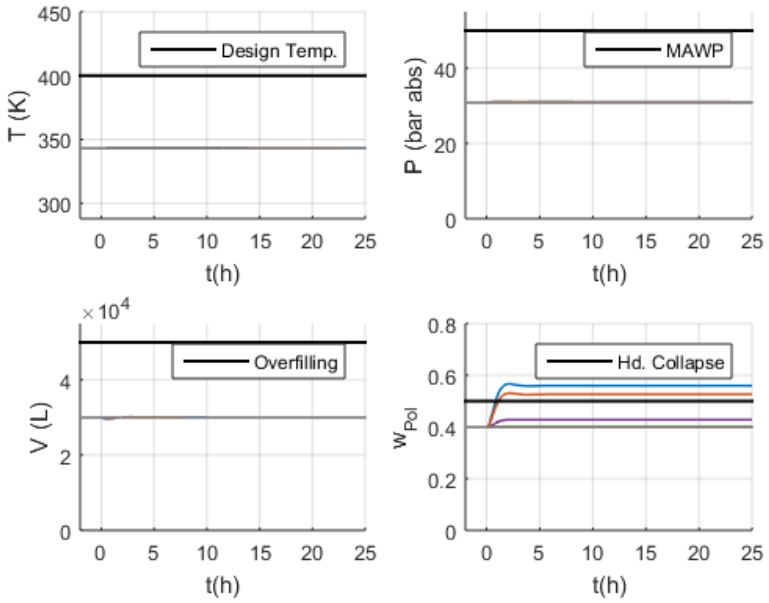

Figure 5.2.2-26 – Behavior of critical variables in scenario S-18 with Model 3.

Inlet catalyst flowrate: (—) Maximum flow; (—) 150% of normal flow; (—) 110% of normal flow; (—) 101% of normal flow; (—) Normal

- **S-20 and S-21 (No and Lower Monomer mass flowrate for heat exchanger) and S-22 (Higher Monomer mass flowrate for heat exchanger)**

Four different steps from the normal value, were applied to the monomer flowrate to the heat exchanger in order to simulate scenarios S-20 and S-21, as shown in Figure 5.2.2-27 for Model 1 (and Model 2) and Model 3. One could expect that the interruption of the vapor flow to the condenser could lead to reaction runaway, with relevant safety effects on maximum allowed reactor temperature and pressure. However, the different models provided comparable results: the fast increase of temperature and pressure, leading the operation to the critical thermodynamic region.

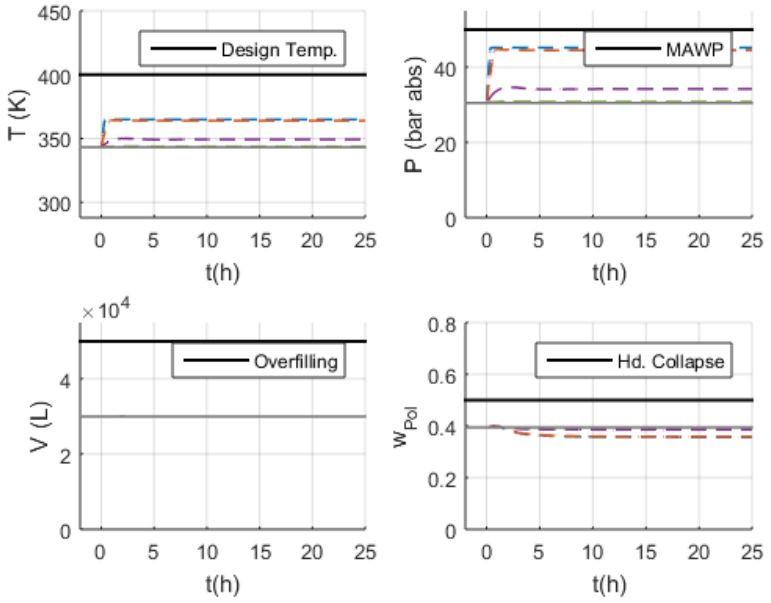

(a)

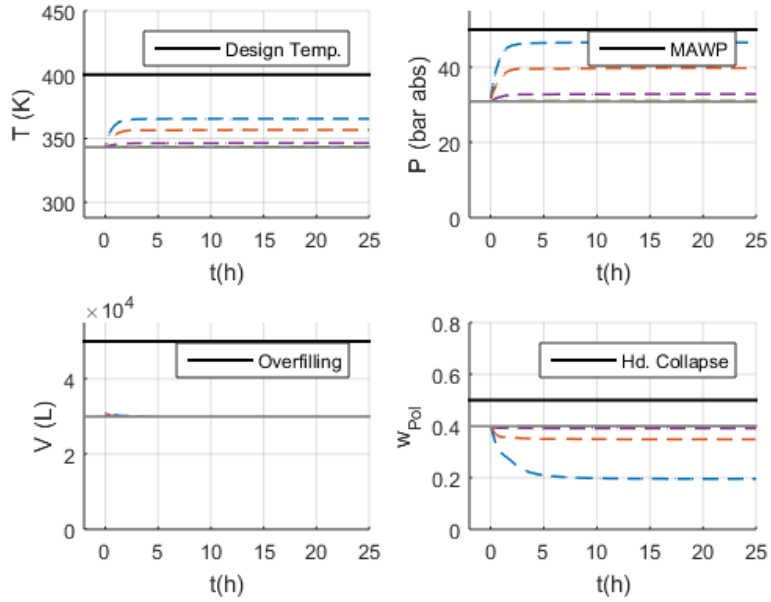

(b)

Figure 5.2.2-27 – Behavior of critical variables in scenarios S-20 and S-21 with (a) Model 1; and (b) Model 3.

Monomer to Condenser mass flowrate: (- - -) No flow; (- - -) 50% of normal flow; (- - -) 90% of normal flow; (- - -) 99% of normal flow; (—) Normal

Although the energy removed through condensation is crucial for the reactor temperature control, the energy term related to the reactor inlet and outlet streams (addition of fresh monomer and removal of hot slurry) is very important for temperature

control. Besides, near the critical point, the heat capacity of saturated liquid and vapor are expected to increase significantly leading to lower temperature increase. These two effects lead to similar simulation results regardless the particular model used to perform the numerical analysis. Despite that, it must be clear that the operation above the critical point poses serious hazards for the process operation and can lead to collapse of the suspension and inefficient removal of the reaction heat.

It can be observed that, after the interruption of the condensate flowrate, the heat release initially increases, reaches a maximum value and then decreases. According to the Arrhenius law, this observation may seem awkward. However, the reduction of the monomer concentration and the consumption of catalyst active sites due to increase of deactivation rate explain this trajectory, as one can see in Table 5.2.2-1. To illustrate this fact, it is necessary to remember that the reaction heat is proportional to the polymerization rate, which is given by:

$$R_{Pol} = k_p C_{Pe} C_{Cat} \quad (92)$$

Table 5.2.2-1 - Polymerization rate term before and after interruption of the condensate flowrate.

		Initial Steady state	**Final Steady State**	**Variation**
$\boldsymbol{k_p}$	Model 1	$\mathbf{5.07 \times 10^3}$	$\mathbf{5.27 \times 10^3}$	+4%
	Model 3	$\mathbf{5.06 \times 10^3}$	$\mathbf{5.211 \times 10^3}$	+3%
$\boldsymbol{C_{Pe}}$	Model 1	**10.05**	**8.78**	-12%
	Model 3	6.86	6.51	-5%
$\boldsymbol{C_{cat}}$	Model 1	$\mathbf{1.86 \times 10^{-4}}$	$\mathbf{1.34 \times 10^{-4}}$	-27%
	Model 3	$\mathbf{1.88 \times 10^{-4}}$	$\mathbf{1.72 \times 10^{-4}}$	-8%

Therefore, although the loss of temperature control through the condenser can significantly increase the reactor temperature and pressure, it does not constitute a safety issue since these variables do not exceed equipment maximum allowed conditions. Nevertheless, attainment of critical conditions can lead to collapse of the suspension and pose significant operation hazards.

Finally, as expected, when the temperature control is lost in the direction of increasing rates of condensate, the reactor temperature and pressure drop. As a result, the contraction of the reaction mass (due to increase of monomer density) increases the concentration of all components in the reactor, leading to small increase of the polymer fraction. Figure 5.2.2-28 exemplifies this behavior.

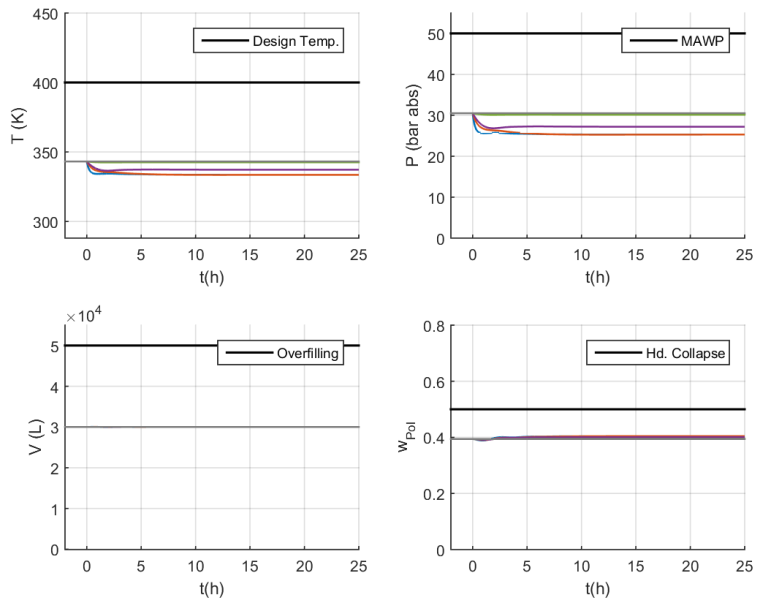

Figure 5.2.2-28 – Behavior of critical variables in scenario S-22 with Model 2.

Monomer to Condenser mass flowrate: (—) Maximum flow; (—) 150% of normal flow; (—) 110% of normal flow; (—) 101% of normal flow; (—) Normal

- **S-23 (Fouling on Heat Exchanger Tubes)**

Four different decreasing steps were applied to the global heat transfer coefficient, UA, in order to simulate scenario S-23. No significant difference between Models 1, 2 and 3 could be observed. Figure 5.2.2-29 shows the results obtained with Model 1 and indicates that, although the reduction of heat exchange capacity can significantly increase reactor temperature and pressure, it does not pose a safety relevant safety problem because the maximum allowed operation conditions are not exceeded, as discussed in the previous simulations. Nevertheless, attainment of the critical point can lead to collapse of the suspension stability and to inefficient removal of the reaction heat.

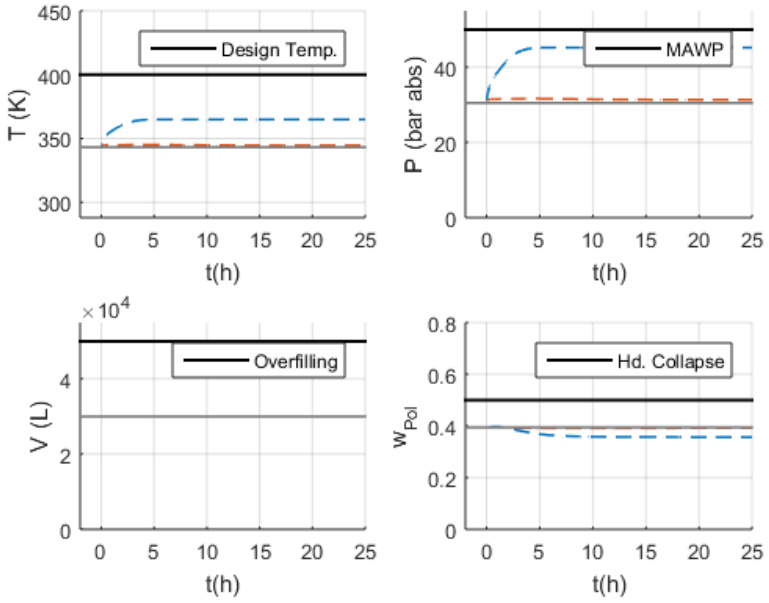

Figure 5.2.2-29 – Behavior of critical variables in scenario S-23 with Model 1.

UA: (- - -) 1% of normal UA; (- - -) 50% of normal UA; (- - -) 90% of normal UA; (- - -) 99% of normal UA; (—) Normal

- **S-24 and S-25 (No and Lower cooling water flowrate to heat exchanger) and S-26 (Higher cooling water flowrate to heat exchanger)**

In order to simulate scenarios S-24, S-25 and S-26, eight different disturbance steps were applied to the water mass flowrate to heat exchanger. When the water flowrate is reduced, the monomer flowrate to condenser increases (reactor temperature control action) and no permanent effect is seen for the critical safety variables, only small disturbances. For lower disturbance steps on the water mass flowrate, an offset for the reactor temperature control occurs, and for the extreme condition of no water flowrate, the maximum allowed temperature (when no heat is removed) can be achieved. Figure 5.2.2-30 shows the results obtained with Model 1. Again, results obtained with the simpler models differ from the ones obtained with Model 3, as shown in Figure 5.2.2-31 but the qualitative analyses can be regarded as similar.

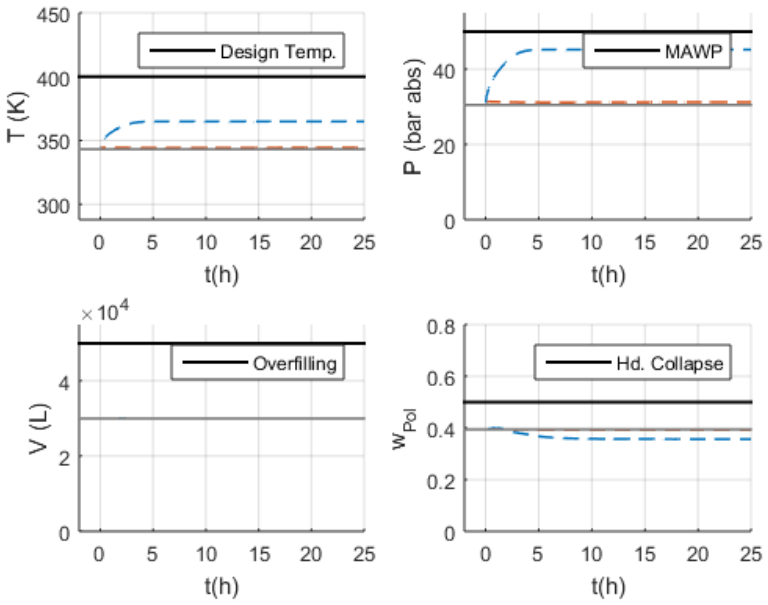

Figure 5.2.2-30 – Behavior of critical variables in scenarios S-24 and S-25 with Model 1.

Water mass flowrate to Condenser: (- - -) No flow; (- - -) 50% of normal flow; (- - -) 90% of normal flow; (- - -) 99% of normal flow; (—) Normal

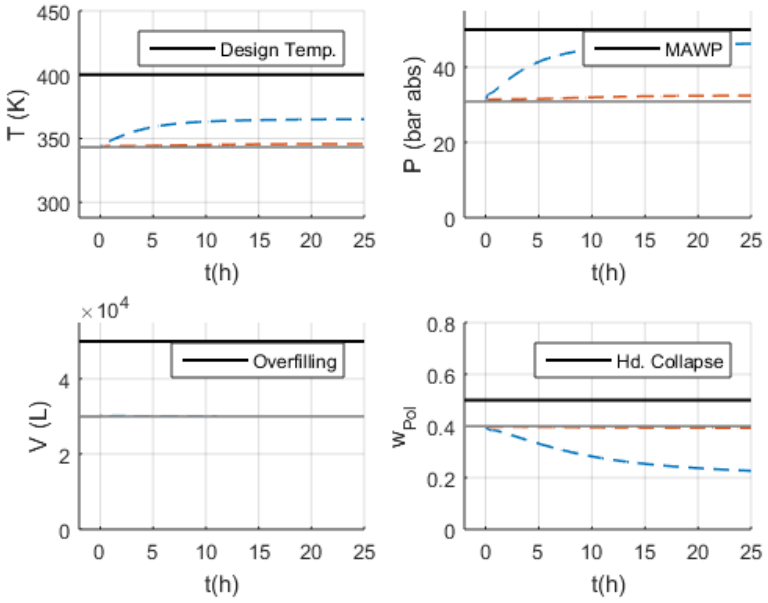

Figure 5.2.2-31 – Behavior of critical variables in scenarios S-24 and S-25 with Model 3.

Water mass flowrate to Condenser: (- - -) No flow; (- - -) 50% of normal flow; (- - -) 90% of normal flow; (- - -) 99% of normal flow; (—) Normal

The increases of the water flowrate cannot significantly affect the critical variables, even for the maximum water flowrate capacity. This occurs because the reactor temperature control effectively acts on the monomer mass flowrate to the heat exchanger, compensating the malfunction of the cooling water system. This effect is exemplified in Figure 5.2.2-32 and Figure 5.2.2-33.

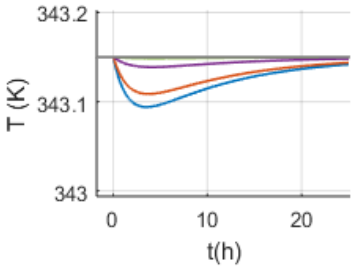

Figure 5.2.2-32 – Effects of temperature disturbance with Model 1.

Water mass flowrate to Condenser: (—) Maximum flow; (—) 150% of normal flow; (—) 110% of normal flow; (—) 101% of normal flow; (—) Normal

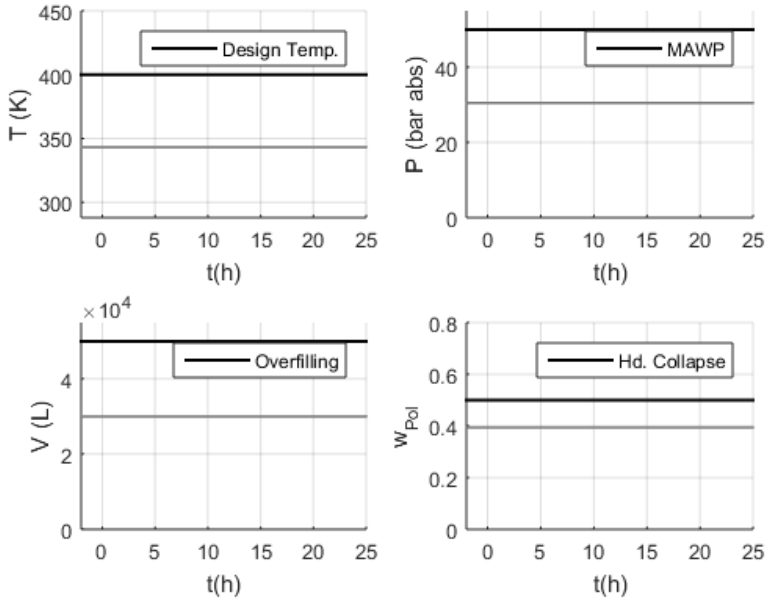

Figure 5.2.2-33 - Behavior of critical variables in scenario S-26 with Model 1.

Water mass flowrate to Condenser: (—) Maximum flow; (—) 150% of normal flow; (—) 110% of normal flow; (—) 101% of normal flow; (—) Normal

- **S-27 (Lower inlet cooling water temperature) and S-28 (Higher inlet cooling water inlet temperature)**

Six different steps from the normal value were applied to the inlet water temperature in order to simulate scenarios S-27 and S-28, as shown in Figure 5.2.2-34. As expected, all models show no relevant effect for the critical safety variables. The stability of the critical safety variables is assured by the effective control actions of the temperature controller to keep reactor temperature and water temperature at their setpoints.

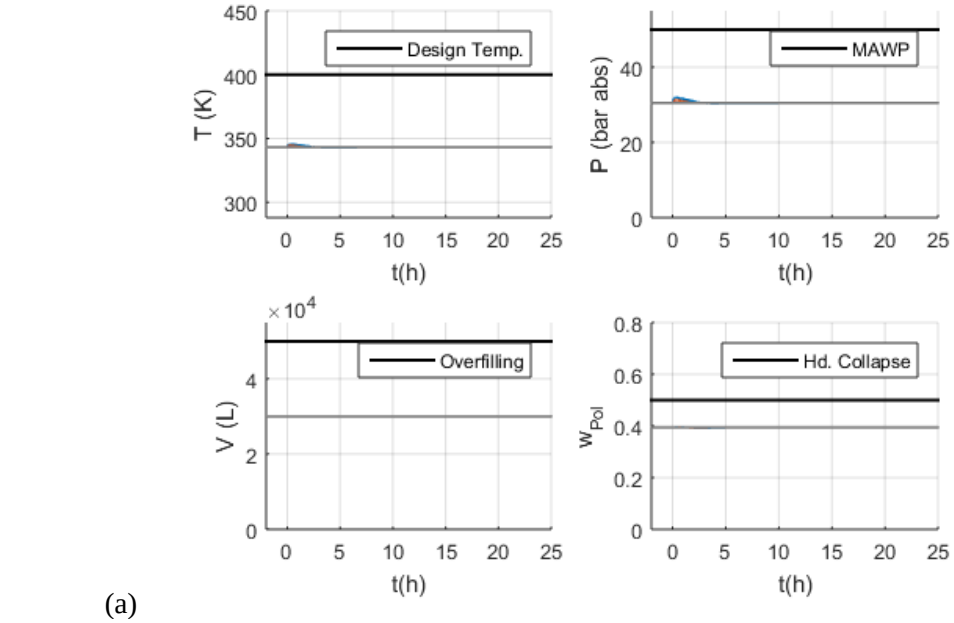

(a)

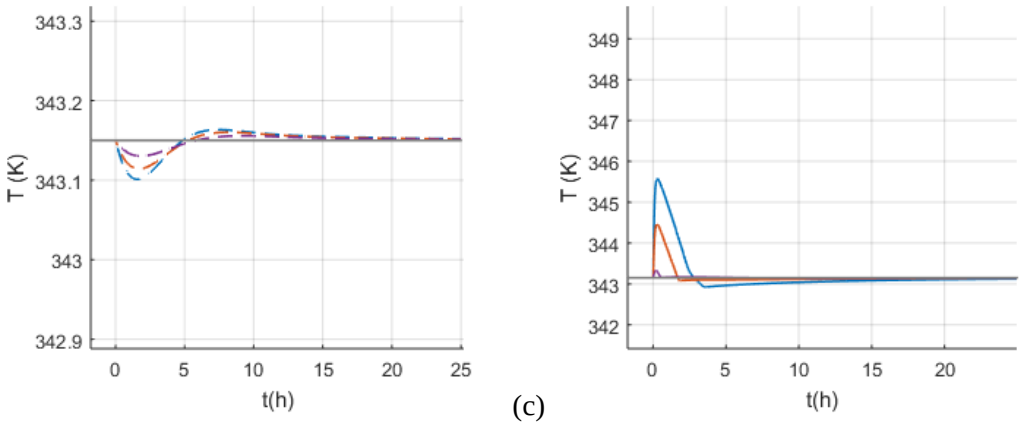

(b) (c)

Figure 5.2.2-34 – (a) Behavior of critical variables in scenarios S-27 and S-28 with Model 1; (b) Effects of temperature disturbance in scenario S-27; (b) Effects of temperature disturbance in scenario S-28.

Inlet water temperature: (- - -) $-15K$; (- - -) $-10K$; (- - -) $-5K$; (—) $+15K$; (—) $+10K$; (—) $+5K$; (—) Normal

- **S-29 and S-30 (No and Lower outlet slurry mass flowrate) and S-31 (Higher outlet slurry mass flowrate)**

Eight different steps from the normal value were applied to the slurry mass flowrate in order to simulate scenarios S-29, S-30 and S-31. All models were able to capture the undesired consequences caused by the loss of level control, either in the

direction of decreasing slurry mass flowrate, which leads to reactor overflow (Figure 5.2.2-35, Figure 5.2.2-36 and Figure 5.2.2-37) or in the direction of increasing outlet slurry flowrate, which leads to reactor running dry (Figure 5.2.2-38). These two effects occur because the inlet flowrates are kept constant and the slurry mass flowrate does not precisely remove the amount of mass that enters the reactor. As a result, mass accumulates inside reactor (the case of lower slurry mass rate than required) or is drained from reactor (the case of higher slurry mass rate than required). The magnitude of the disturbance only affects the time to achieve the final consequence. As a consequence, this poses serious operation hazards.

For all models, reactor overfilling is also followed by hydrodynamic collapse of the suspension, as a result of increasing residence time inside the reactor. For Model 1, no relation between the variations of reactor volume and heat of condensation heat can be observed, resulting on a false safety perception regarding the observed temperature and pressure trajectories. The small disturbances of these variables are related to the accumulation of catalyst, which increases the reaction rates and leads to increase of the heat release. According to Model 2, when the reactor is totally full (liquid phase), the condensation is not possible. The introduction of this assumption, directly affects the temperature and pressure trajectories. Model 2 assumes that pressure is a function of temperature only (vapor pressure), although it is known that the hydraulic expansion of a liquid can lead to overpressuring. This additional modeling feature results on the simultaneous increase of volume and pressure, beyond the allowed maximum limits. It can be observed that the reactor can be overpressured 1.3 times its MAWP before the hydrodynamic collapse can occur, as shown in Figure 5.2.2-37. It can also be seen that the pressure increase is related to the mass accumulation and not to the temperature increase, since the temperature remains stable until the reactor overfilling.

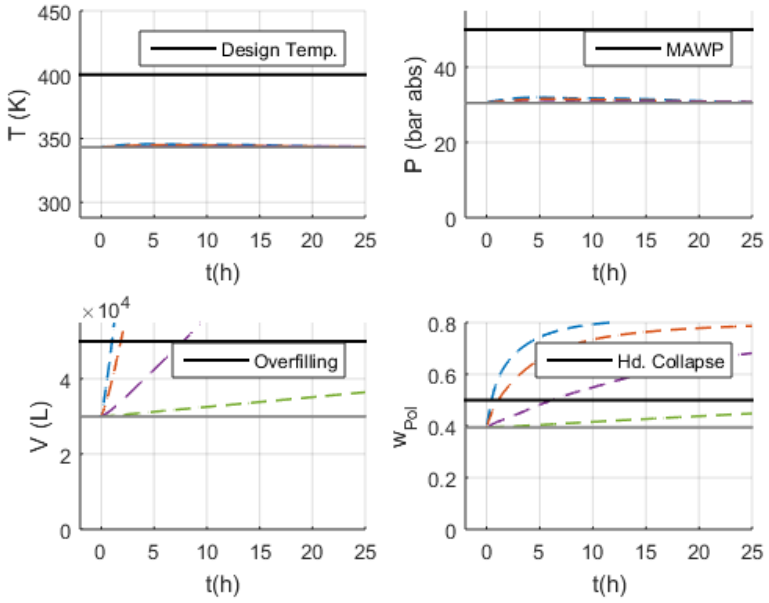

Figure 5.2.2-35 – Behavior of critical variables in scenarios S-29 and S-30 with Model 1.

Slurry mass flowrate: (- - -) No flow; (- - -) 50% of normal flow; (- - -) 90% of normal flow; (- - -) 99% of normal flow; (—) Normal

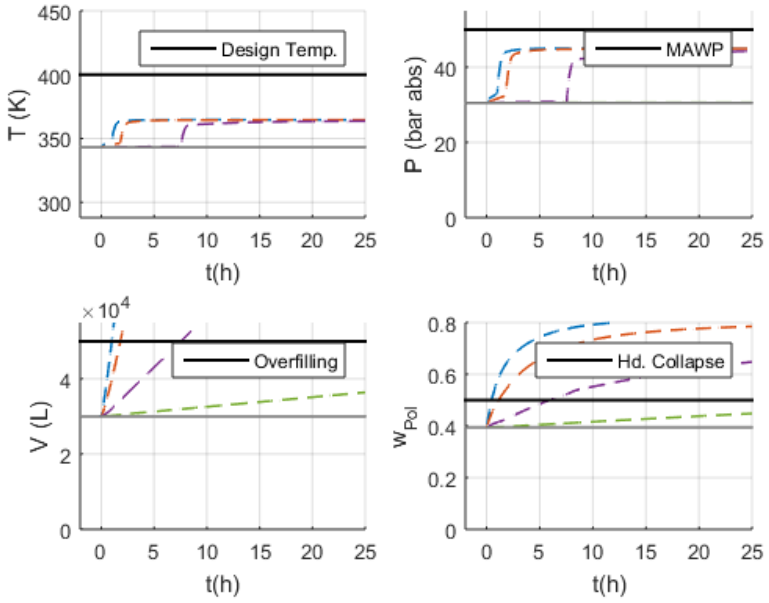

Figure 5.2.2-36 – Behavior of critical variables in scenarios S-29 and S-30 with Model 2.

Slurry mass rate: (- - -) No flow; (- - -) 50% of normal flow; (- - -) 90% of normal flow; (- - -) 99% of normal flow; (—) Normal

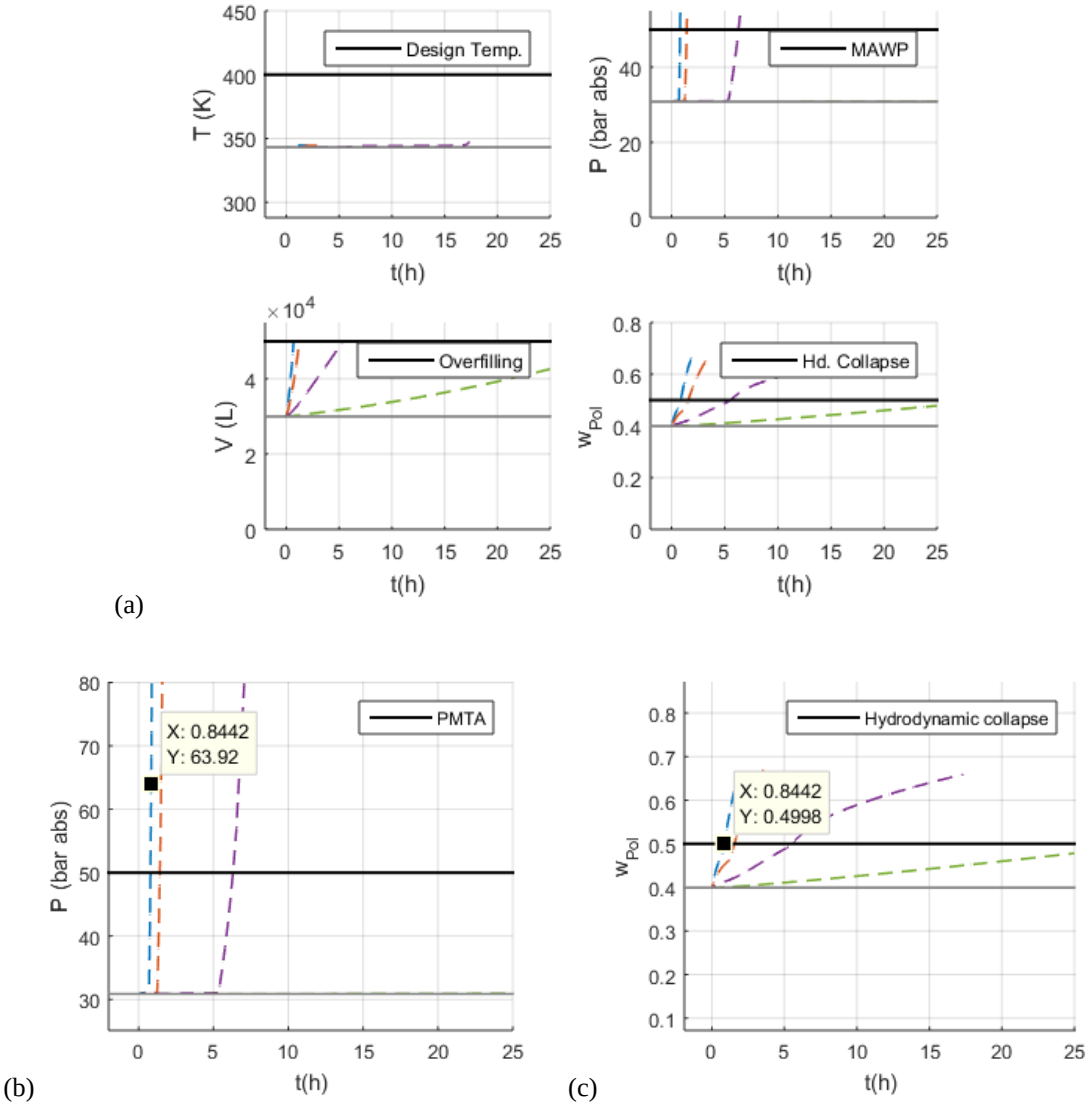

Figure 5.2.2-37 – (a) Behavior of critical variables in scenarios S-29 and S-30 with Model 3; (b) Pressure dynamics for interruption of the slurry mass flowrate; (c) Polymer fraction dynamics for interruption of slurry mass flowrate.

Slurry mass rate: (- - -) No flow; (- - -) 50% of normal flow; (- - -) 90% of normal flow; (- - -) 99% of normal flow; (—) Normal

Regarding the positive steps on the slurry mass flowrate, the consequences are simulated similarly with all models, resulting on drying of the reactor as shown in Figure 5.2.2-38.

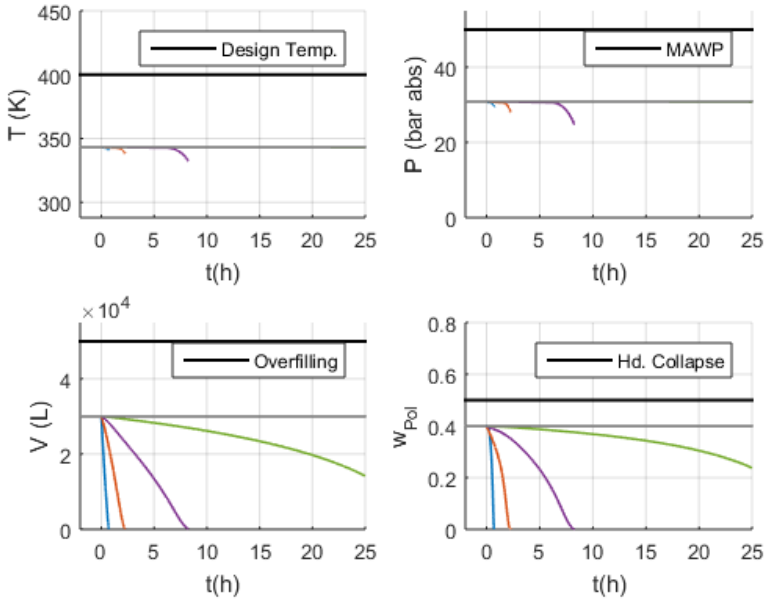

Figure 5.2.2-38 – (a) Behavior of critical variables in scenario S-31 with Model 3.

Water mass flowrate to condenser: (—) Maximum flow; (—) 150% of normal flow; (—) 110% of normal flow; (—) 101% of normal flow; (—) Normal

- **S-32 (Plugging of polymer stream from gas separator)**

Imagine that due to plugging, the polymer stream flow after the separator is reduced to a certain percentage of its normal rate. The excess of polymer that cannot flow through the designed pipeline is returned through the gas line in the monomer recycle stream.

Although this hypothetical scenario can be modeled, it is understood that before exerting any effect on the reactor, the presence of liquid in the compression unit will damage the equipment, which is not designed for liquid handling. In that manner, the return of polymer to reactor was not considered reasonable for computational simulations, as this would lead to operation problems immediately after occurrence.

- **S-33 and S-34 (No and Lower Recycled Monomer Purge flowrate) and S-35 (Higher Recycled Monomer Purge flowrate)**

Six different steps from the normal value were applied to the slurry outlet stream in order to simulate scenarios S-33, S-34 and S-35. The malfunctions on the purge rate mainly influence the polymer fraction inside reactor, since they affect the monomer quality that enters the reactor. For negative steps on the purge rate, propane accumulates inside reactor, reducing the monomer concentration, the reaction rate and thus the polymer fraction, as one can see in Figure 5.2.2-39. The simulation time was increased for these scenarios because this malfunction affects the composition of the recycle stream, which is a function of the reactor variables and modifies the inlet reactor condition, creating a loop effect of slow dynamics. The positive disturbances on the purge mass flowrate exert an opposite effect, leading to increase of monomer concentration, reaction rate and finally the polymer fraction.

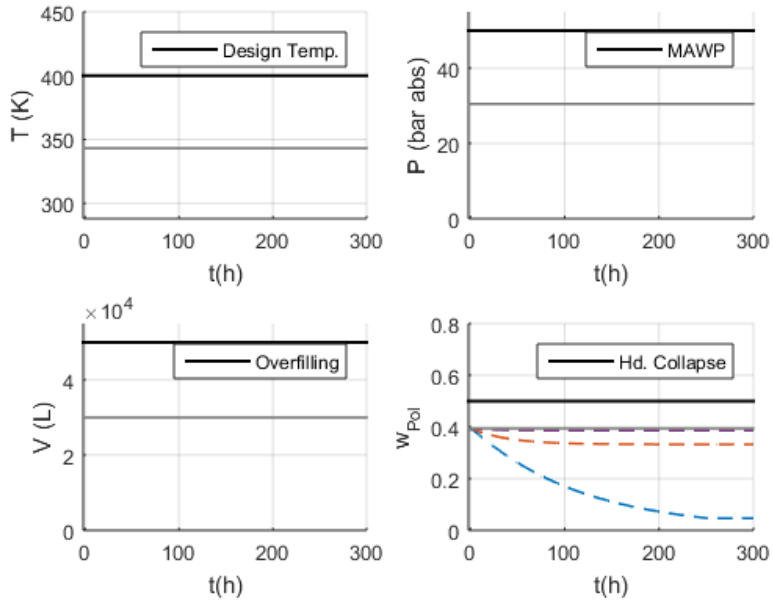

Figure 5.2.2-39 – Behavior of critical variables in scenarios S-33 and S-34 with Model 1.

Purge mass rate: (- - -) No flow; (- - -) 50% of normal flow; (- - -) 90% of normal flow; (- - -) 99% of normal flow; (—) Normal

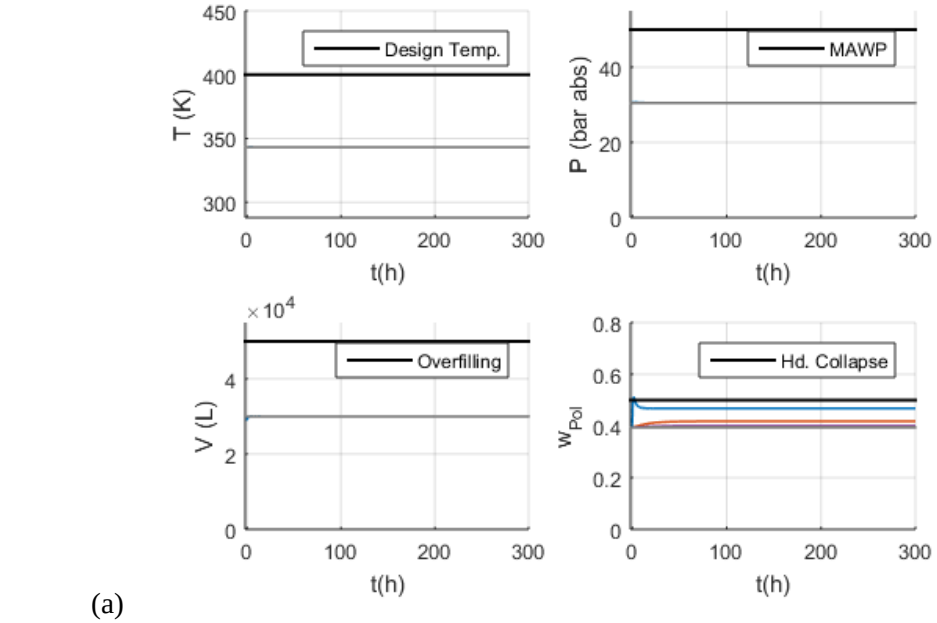

(a)

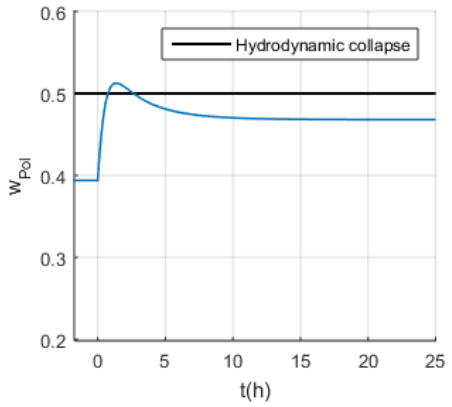

(b)

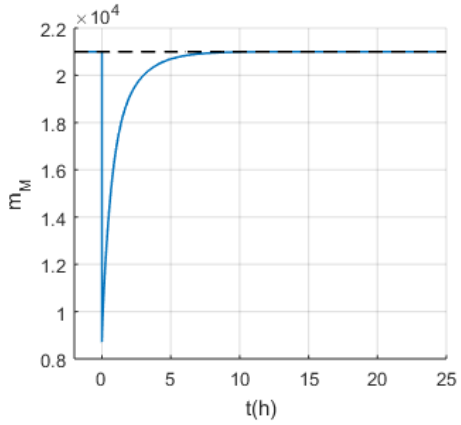

(c)

Figure 5.2.2-40 – (a) Behavior of critical variables in scenario S-35 with Model 1; (b) Effects of the polymer fraction; (c) Effects of the inlet monomer mass flowrate, $\dot{m}_M$

Purge mass flowrate: (—) Maximum flow; (—) 150% of normal flow; (—) 110% of normal flow; (—) 101% of normal flow; (—) Normal

For the sudden and complete opening of the purge valve, the inlet monomer flowrate control is not sufficiently fast to respond to the interruption of the recirculation rate, as one can see in Figure 5.2.2-40. The effect of the reduced inlet flowrate, increases residence time and causes a peek on the polymer fraction, leading to hydrodynamic collapse of the suspension, as one can see in Figure 5.2.2-40. The interesting observation

in this simulation is that changing the inlet monomer flowrate controller parameters can change the safety result. If the integral parameter of monomer inlet control, τ_C, is reduced to 0.1 (dividing by 10 the original value), the behavior presented in Figure 5.2.2-41 can be observed. This case exemplifies the importance of the controller and controller tuning for identifications of process hazards, an issue that has been systematically overlooked in the literature.

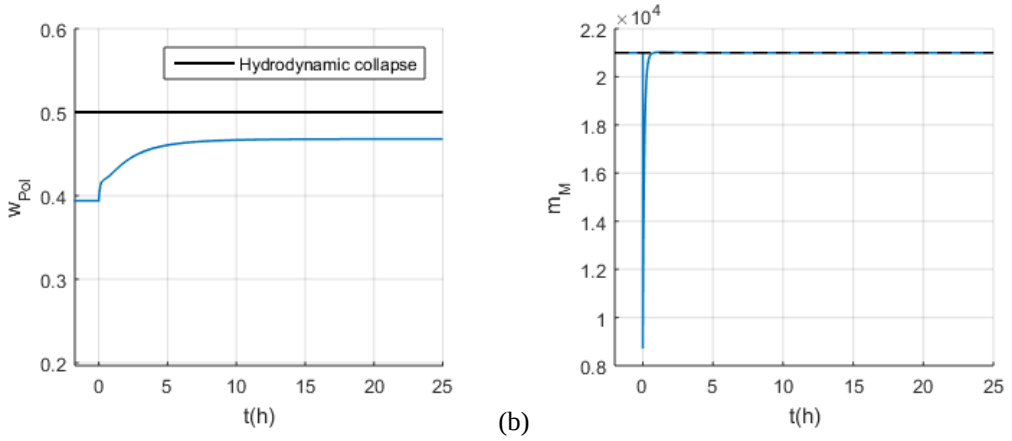

(a) (b)

Figure 5.2.2-41 – (a) Effect of the polymer fraction behavior for $\tau_c = 0.1$; (b) Effect of the monomer inlet mass rate, $\dot{m}_M$ for $\tau_c = 0.1$ with Model 1.

Purge mass flowrate: (▬) Maximum flow

- **S-36 and S-37 (No and Lower Recirculation of Monomer)**

Four different steps from the normal value were applied to the recycled monomer mass flowrate in order to simulate scenarios S-36 and S-37, as one can see in Figure 5.2.2-42.

Recycled monomer mass flowrate mainly affects the polymer fraction inside the reactor, since it affects the monomer quality that enters the reactor. In most cases, the control of the inlet monomer flowrate control is able to deal with the disturbance, except when the recycled stream is suddenly interrupted. As discussed in the previous case, the sudden interruption of the recycled gas stream leads to immediate reduction of the

monomer feed to the reactor inlet stream, increasing the reactor residence time, increasing conversion and leading to the hydrodynamic collapse of the suspension, if the monomer feed rate controller is not properly tuned.

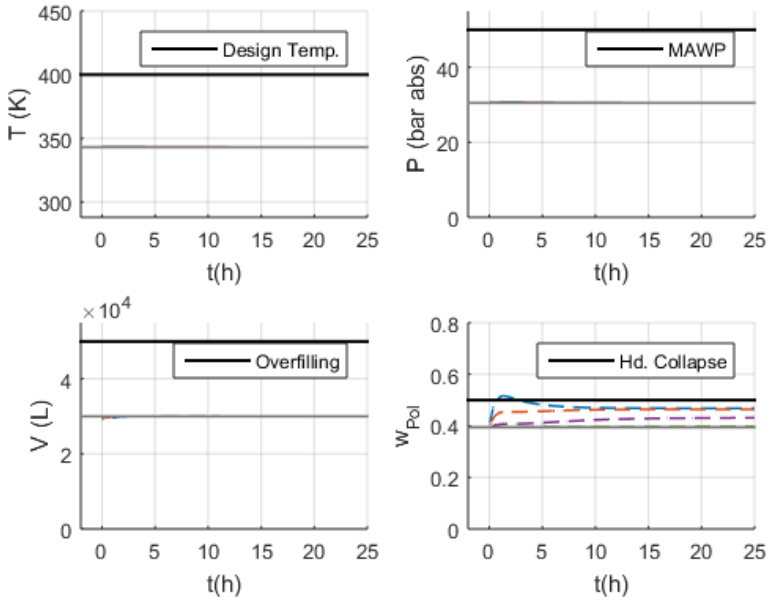

Figure 5.2.2-42 – Behavior of critical variables in scenarios S-36 and S-37 with Model 1.

Purge mass flowrate: (- - -) No flow; (- - -) 50% of normal flow; (- - -) 90% of normal flow; (- - -) 99% of normal flow; (—) Normal

- **S-38 (Agitation Failure)**

The agitation failure can affect the hydrodynamic stability of the liquid suspension. As no sort of control manipulation is normally applied to the agitator, it is considered here that agitator failure can cause accumulation of polymer on the bottom of the reactor and lead to hydrodynamic collapse of the suspension. The model does not take into account the effect of agitation to process variables. Therefore, no simulation was performed.

5.3.Analysis of the Single Failure Approach

In order to validate the hazard identification analysis performed before, the possibility of simultaneous occurrence of multiple failures is investigated. This is an issue that has been

consistently neglected in previous studies. For this analysis, a failure frequency study is performed, starting from the reliability data that can represent the failure probability of devices used in the process simulation step. The data were obtained from two different sources: one based on a generic data resource (CENTER FOR CHEMICAL PROCESS SAFETY, 1989) and the other from the collaboration of different oil and gas companies (NTNU; SINTEF, 2015), as shown in Table 5.3-1.

Table 5.3-1 – Failure data for different devices.

Device	**Failure Mode**	**Failure Rate (h^{-1})**	**Reference**
Electric Centrifugal Pump	Spurious Stop	3.73E-06	OREDA[1], pg. 130
Electric Centrifugal Pump	Failure to Start on Demand	2.08E-06	OREDA[1], pg. 130
Electric Centrifugal Pump	Low Output	9.50E-07	OREDA[1], pg. 131
Electric Centrifugal Pump	High Output	3.30E-07	OREDA[1], pg. 131
Reciprocating Pump (for chemical injection)	Spurious Stop	3.13E-06	OREDA[1], pg. 158
Reciprocating Pump (for chemical injection)	Failure to Start on Demand	0.00E+00	OREDA[1], pg. 158
Reciprocating Pump (for chemical injection)	Low Output	4.72E-05	OREDA[1], pg. 162
Reciprocating Pump (for chemical injection)	High Output	NAD[2]	

1 (NTNU; SINTEF, 2015)

2 NAD = Not Available Data

Device	Failure Mode	Failure Rate (h^{-1})	Reference
Reciprocating Pump (for oil processing)	Spurious Stop	3.13E-06	OREDA[1], pg. 158
Reciprocating Pump (for oil processing)	Failure to Start on Demand	0.00E+00	OREDA[1], pg. 158
Reciprocating Pump (for oil processing)	Low Output	NAD[2]	
Reciprocating Pump (for oil processing)	High Output	NAD[2]	
Electric Centrifugal Compressor	Spurious Stop	3.01E-05	OREDA[1], pg. 70
Electric Centrifugal Compressor	Failure to Start on Demand	1.25E-05	OREDA[1], pg. 70
Electric Centrifugal Compressor	Low Output	2.09E-05	OREDA[1], pg. 71
Control Logic Units	Erratic output	5.21E-06	OREDA[1], pg. 403
Process Control Valves	Critical	1.90E-05	OREDA[1], pg. 489
Analyzers	Catastrophic	2.40E-03	AIChE[3], pg. 152
Transmitter - Level	Critical	1.27E-05	OREDA[1] pg. 391
Transmitter - Flow	All modes	3.63E-06	OREDA[1] pg. 389
Transmitter - Temperature	All modes	3.63E-06	OREDA[1] pg. 398

3 (CENTER FOR CHEMICAL PROCESS SAFETY, 1989)

The failure modes related to human factors (as the undesired closing of manual valves) or plant operability information (as fouling and off spec reagents, for example) were not considered for this analysis due to unavailability of specific plant data. The malfunctions related to control failure were calculated as the sum of failure rates of the three basic elements of the control loop: sensor (transmitter), programmable logic controller and actuator. Although not represented in Figure 5.1-1, it was considered that all inlet flowrates of reagents were controlled by flowrate control loops. Monte Carlo simulations were used aiming to evaluate the possibility of simultaneous failures. For the stochastic model, the following assumptions were made:

- Constant failure rate modeling, which constitutes a reasonable approximation to describe equipment lifetime – after infant mortality and before degradation processes, when the failures occur at higher rates – and for which the exponential distribution is suitable for the calculation of failure probability, given a time interval, Θ, and failure rate, λ (OHRING; KASPRZAK, 2015).

$$P(time\ interval\ [0,\mathrm{t}]\ content\ failure \mid \lambda\} = 1 - \exp(-\lambda \mathrm{t}) \tag{93}$$

This way, the average failure probability in a time interval, Θ, is given by:

$$P_{avg} = \frac{1}{\Theta}\int_0^{\Theta}[1-\exp(-\lambda t))]dt \therefore P_{avg} = 1 - \frac{1}{\lambda\Theta}(1-\exp(-\lambda\Theta)) \tag{94}$$

where Θ characterize the test interval and P_{avg} is the average failure probability between tests.

- Time to failure can be generated at random based on the exponential distribution function for constant failure rates;
- After tests, equipment failure probabilities can be restored;
- Equal criticality level was considered for all devices and the heuristic time interval of one year was applied. An exception was made for the analyzers due to their

high rates of failure. The analyzer probability of failure in a time interval of one year would be 95%, which certainly would jeopardize the operational continuity, justifying a more frequent test interval, which was considered weekly only for this case. Therefore, it seems clear that maintenance programs should be carried out to prevent these failures.

- For each simulation run (one year of operation):
    - Yearly tested equipment can fail independently once per year;
    - Weekly tested equipment can fail independently fifty-two times a year or one time per week;
- Besides that, it was considered that the control failures can occur in the direction of either increasing or decreasing of the manipulated variable (equally probable failure modes).
- After tests, time to failure can be generated at random again.

Before evaluating the possibility of simultaneous malfunctions, it was first checked which malfunctions could be mitigated through the introduction of standby backup systems. The standby system reduces the occurrence probability of a given initiating event and thus, reduces the probability for occurrence of simultaneous failures. In this case, the initiating event rate, λ_{ie}, was calculated as:

$$\lambda_{ie} = \lambda_{device} \times PFD_{backup} \tag{95}$$

where λ_{device} is the failure rate of the operating device and PFD_{backup} is the probability of failure on demand of the backup system.

Table D-1 of Appendix D summarizes the discussed failure data generation for each device malfunction event, corresponding to the malfunction simulations shown before.

In order to evaluate the possibility of simultaneous failure, for each simulation history the minimum time interval between device failures was investigated, during the one-year period, as shown at Figure 5.3-1 below.

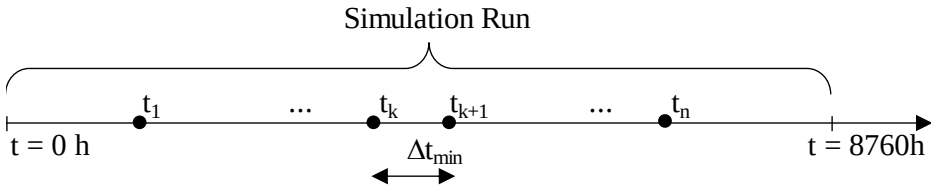

Figure 5.3-1 – Representation of the simulation history.

where $t_k (k = 1 \dots n)$ is the time to failure of the k^{th} failure along the one-year time interval, among n total failures. For each simulation history, $n - 1$ values of Δt were calculated and the possibility of simultaneous failure was assumed when $\Delta t \leq 1h.$, where $\Delta t = t_{k+1} - t_k$. The flowchart shown in Figure 5.3-2 exemplifies the proposed Monte Carlo, MC, algorithm applied to the evaluation of simultaneous failure.

The probability of simultaneous failure, P_{sf}, was obtained by dividing the number of histories with simultaneous failures, n_{sf}, over the total number of histories, N_h.

$$P_{sf} = n_{sf}/N_h \tag{96}$$

The first group of simulations ran $N_h = 1 \times 10^4$ histories each and the results are shown in Table 5.3-2. As discussed before, each simulation history represents one-year operation. The average elapsed time for each simulation was 249s. The second group of simulations ran $N_h = 1 \times 10^5$ histories each. The average elapsed time for each simulation was 7786.16s and the number of histories with simultaneous failure is comparable to the results obtained in the previous group, as presented in Table 5.3-3. From both strategies the average probability of simultaneous failure resulted on approximately 0.56%. In other words, for this case study, in average, 178 years would be necessary for the unit to experience simultaneous failures. Therefore, multiple failures

are expected to occur in less than 1% of the observed failure events, constituting a rare event. This validates the strategy of analyzing single failures during the hazard identification step.

Table 5.3-2 – Probability of simultaneous failure after running 1×10^4 histories per MC simulation.

MC Simulation Reference	n_{sf}	P_{sf}
1	67	0.67%
2	60	0.60%
3	44	0.44%
4	71	0.71%
5	60	0.60%
6	50	0.50%
7	68	0.68%
8	59	0.59%
9	42	0.42%
10	53	0.53%
11	40	0.40%
12	58	0.58%

Table 5.3-3 - Probability of simultaneous failure after running 1×10^5 histories per MC simulation.

MC Simulation Reference	n_{sf}	P_{sf}
13	560	0.56%
14	556	0.56%
15	506	0.51%
16	567	0.57%

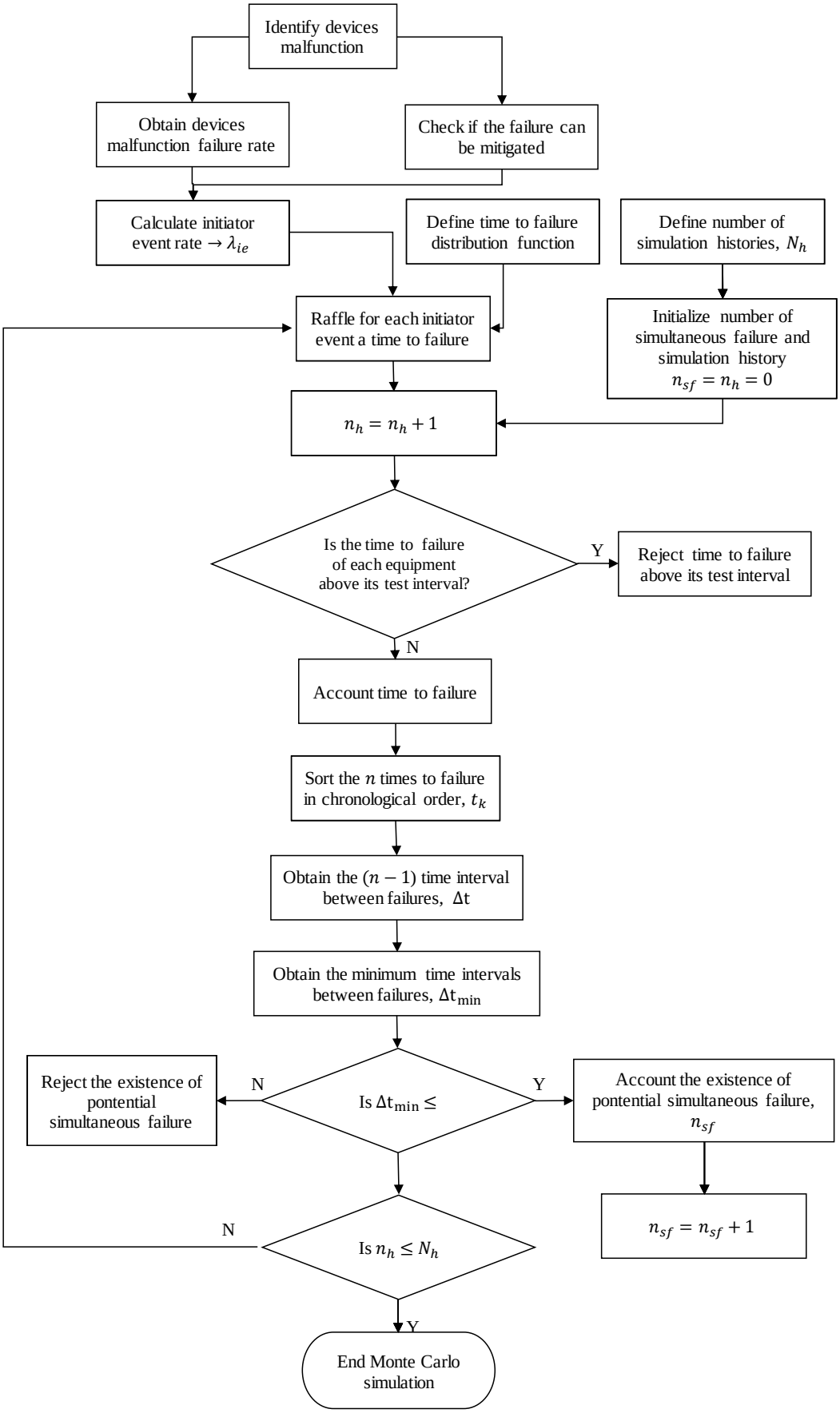

Figure 5.3-2 – Flowchart of the proposed Monte Carlo algorithm.

As the analyzer control loop presents the higher failure rates, the individual contribution of analyzers to the probability of simultaneous failure was investigated by MC simulations with $N_h = 1 \times 10^4$ (Table 5.3-4) and $N_h = 1 \times 10^5$ (Table 5.3-5). Based on Table 5.3-4 and Table 5.3-5, the average contribution of the analyzer to the occurrence of simultaneous failure is approximately equal to 84%. If the probability of simultaneous failure was expressive, it would be strategical to evaluate combinations of the analyzer control loop with other failures, in order to check whether it can aggravate the effect of other individual failures. However, in the present case, it seems more appropriate to implement maintenance programs focused on the prevention of analyzer failures.

Table 5.3-4 – Analyzer contribution for simultaneous failure (1×10^4 histories per MC simulation).

MC Simulation Reference	$n_{sf}\|_{analyzer}$	**Analyzer Contribution to Simultaneous Failure**
6	37	74%
7	60	88%
8	48	81%
9	37	88%
10	43	81%
11	35	88%
12	44	76%

Table 5.3-5 – Analyzer contribution for simultaneous failure (1×10^5 histories per MC simulation).

MC Simulation Reference	$n_{sf}\|_{analyzer}$	**Analyzer Contribution to Simultaneous Failure**
14	473	85%
15	426	84%
16	472	83%

5.4.Safety Considerations after Simulation Results

After the simulations, the impact of the device malfunctions on safety was recorded in Appendix E and the risk related consequence (heuristic analysis from the simulation results) was registered at the “Hazard Analysis Table”.

In summary, the simulation results emphasize the relevance of hydrodynamic collapse of the reaction suspension for the process safety. This undesired consequence is related to different failures, for instance, of the inlet monomer feed control, of the catalyst feed control, of the reactor volume control, of the purge control, of the recycle stream equipment and of the agitator.

With support of the simulations, the thermal runaway of the reaction was investigated, leading the operation to the critical thermodynamic region, which can pose serious hazards for the process operation and can also lead to collapse of the suspension. The direct effect of the thermal runaway on the reactor temperature and pressure were limited below the equipment maximum allowed conditions. Decomposition reactions were not taken into account and should also be investigated as a consequence of the thermal runaway.

The dynamic nature of the simulations, enabled the quantification of threshold values of process disturbances that may lead to hazardous consequences, and the identification of process hazards related to tuning of the process controllers, as the inlet monomer flowrate control leading to collapse of the suspension due to tuning problems. The purge control was also subject of attention related to high failure rates leading to undesired consequences regarding the collapse of the suspension. Despite of that, simultaneous failures were considered rare.

Therefore, preventive and mitigating safety measures must be designed to control the identified hazards. Particularly, monitoring the occurrence of hydrodynamic collapse

of the reaction suspension seems crucial for the process safety. Apart from traditional safety barriers, indirect monitoring of the polymer content in the suspension, on-line soft sensors (COIMBRA et al., 2017) and other technologies should be investigated in order to enhance process safety and reliability.

5.5.Comparison with Traditional HAZOP

In order to provide a comparison benchmark for the computational approach, the HAZOP traditional methodology (human knowledge based) was applied to the same case-study. The HAZOP was performed by two different groups: (a) one composed by a team of four people, consisting of a HAZOP facilitator, a process engineer, a process control engineer and a specialized LIPP-SHAC process specialized engineer; and (b) the other with three people: a HAZOP facilitator, and two process engineers. The first study was developed in two sections of two hours each and the simulation results were not shared with the group, so that the two approaches could be regarded as independent from each other. The second study was performed in one section of three hours and, again, the simulation results were not shared with the group.

The selected *deviations* for the HAZOP application were: Low, No, High, As well as and Reverse Flow; Low and High Temperature; Low and High Pressure; and Low and High Level. The results of this heuristic hazard analysis are shown in Appendix F, distinguishing the main differences between the two HAZOP results.

With the first group, it was possible to perform a more complete analysis, while only a partial analysis was performed with the second group. Therefore, the first study was used as a benchmark for the comparative computational analysis, since both can be regarded as complete approaches. The second study was used to evaluate the variability that is inherent to human-based approaches by comparing the main results obtained with the two different HAZOP studies.

The objective of the performed HAZOP analyses, and of the computational-based analysis, was the identification of potential hazards. The proposed analyses were not focused on designing safeguards or estimating risks.

Using the process-oriented approach, as for the HAZOP analyses, and of the complete study registered fifty-six discussions. On the other hand, through the device-oriented approach, as for the computational based procedure, thirty-seven scenarios were generated. Table 5.5-1 summarizes the main differences observed among the results obtained from the two discussed methods and compares the hazard discussions generated from equivalent causes. This analysis can be examined in detail by comparison between Table E-1 and Table F-1 in Appendix E and Appendix F, respectively.

Table 5.5-1 –Comparison of results obtained with different hazard identification methodologies.

Simulation Reference	**HAZOP Scenario Reference**	**Differences between methods**
S-1 and S-2	1a and 2a	Similar results.
S-3	3a, 8d and 10c	Computational results were more precise: the quantitative analysis, which includes equipment capacity, made more accurate the scenario understanding when compared to the effect of unlimited deviation identified by the HAZOP team.
S-4	4a	Similar results.
S-5 and S-6	Not covered by HAZOP	From the perspective of process deviations, the causes identified for scenarios S-5 and S-6 did not exert significant impact and were regarded as irrelevant discussion.
S-7 and S-8	1h and 2f	HAZOP is more conservative. Both studies understand the hazard occurrence mechanism, but the absence of quantitative information about the process

Simulation Reference	HAZOP Scenario Reference	Differences between methods
		dynamics let HAZOP to overestimate the hazard effects.[4]
S-9	3f	HAZOP was more creative. Based on the computational method, the safety relevant variables were not subject to significant deviations. However, an existing long-term effect not related to the safety critical variables was identified by human experience, when analyzing beyond the immediate effect.
S-10 and S-11	1d and 2d	Similar results.
S-12	3d	Similar results.
S-13	2c	The computational method was more precise. Both studies reached the same conclusion (reaction death), but the explicit quantitative information about flowrates, evidenced a consequent effect of exceeding equipment maximum capacity.
S-14	1c	Similar results.
S-15	3c	Similar results.
S-16	2b	Similar to S-13 versus 2c.
S-17	1b	Similar results.
S-18	3b, 4b, 6e and 8e	HAZOP was more conservative. Both studies understand the hazard occurrence mechanism, but the absence of quantitative information about the process dynamic led HAZOP overestimate the hazard effects.
S-19	4c	Similar results.

4 The HAZOP team was not confident about the final consequence and recommended a kinetic simulation. For that case, the conservative approach was unnecessary, when compared to the simulations.

Simulation Reference	HAZOP Scenario Reference	Differences between methods
S-20 and S-21	1j, 2h, 6b, 6d and 8b	HAZOP was more conservative: Both studies understand the hazard occurrence mechanism, but the absence of quantitative information about the process energy balance and parameter behavior led HAZOP to overestimate the hazard effects.
S-22	3h, 7b, 7c and 9a	Similar results.
S-23	1k	Similar results with slightly different mechanisms.
S-24 and S-25	1i, 2g, 6a and 6c	Similar to S-20 and S-21 versus 1j, 2h, 6b, 6d and 8b.
S-26	3g and 7a	Similar results.
S-27 and S-28	Not covered by HAZOP	From the perspective of the process deviations, the causes identified for scenarios S-27 and S-28 did not exert any significant impact on the process behavior, leading to irrelevant discussion.
S-29 and S-30	1e, 1f, 1g, 2e, 10a and 10b	Similar results.
S-31	3e, 8a and 11a	Similar results.
S-32	Not covered by HAZOP	Reasoning the process in terms of nodes may contribute to overlooking potential hazard sources.
S-33 and S-34	1m, 1n and 2i	Similar results.
S-35	3i	Computational method was more precise. Both studies understand the hazard occurrence mechanism, but the absence of quantitative

Simulation Reference	HAZOP Scenario Reference	Differences between methods
		information about the controller dynamics led HAZOP to underestimate the hazard effects.[5]
S-36	2j	Similar to S-35 versus 3i.
	5a	HAZOP was more creative. Even for the highest level of detail, the models developed were not designed for capturing flow mechanisms related to pressure losses and energy supply from dynamic equipment.
S-37	Not covered by HAZOP	In standard HAZOP studies, limiting the selection of deviations may contribute to overlooking potential hazard sources.
Not covered by device-oriented procedure	1l and 8c	Reasoning the process in terms of variable deviations trigger creative thinking.
Not covered by device-oriented procedure	6f	Reasoning the process in terms of variable deviations trigger creative thinking.

As one can see from Table 5.5-1, the significant higher number of HAZOP scenarios is related to the expressive number (40%) of repetitive discussions (from the perspective of the device malfunction) that were necessary from the perspective of the process variable. For instance, simulation reference S-3 which is related to one device malfunction, was repeated for 3 different process deviations (high flow, high pressure and high level) generated by HAZOP discussions.

5 The HAZOP team was not confident about the final consequence and recommended a kinetic simulation. However, for that case, the non-conservative approach overlooked the potential hazard, when compared to the simulations.

Disregarding the effect of repetitiveness due to different deviations related to the same malfunction and grouping similar scenarios, both analyses, identified 31 different hazard scenarios. Figure 5.5-1 stratifies the main differences observed for both applications.

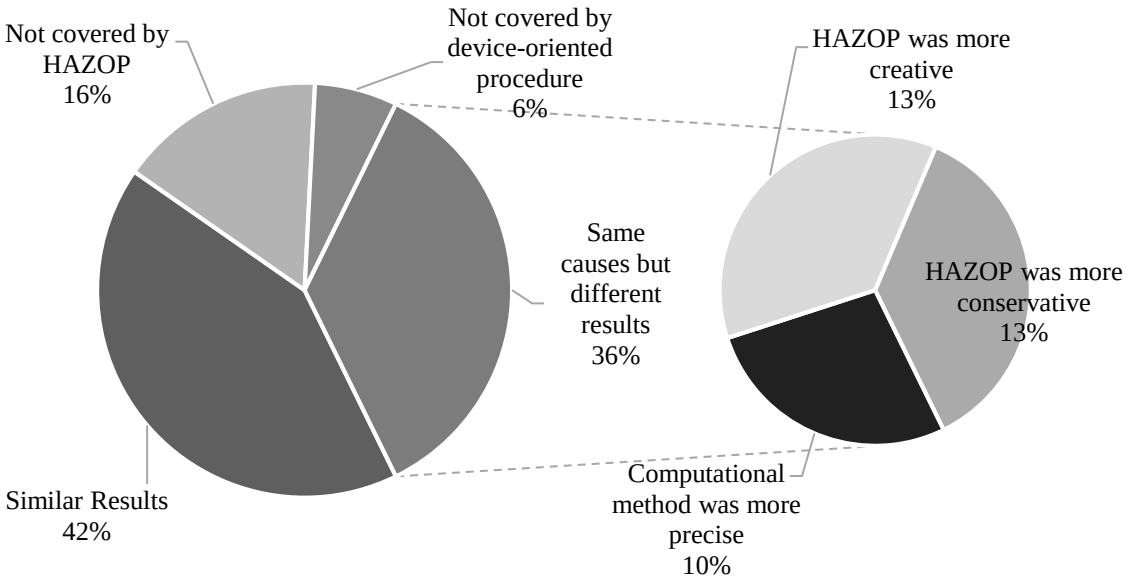

Figure 5.5-1 – Stratified comparison between the standard and the computational based methods.

Approximately half of the discussions achieved the same results. This is an important observation, taking into account the effort needed to develop a robust model that is capable of describing all simulation conditions, as discussed in Chapter 5. Assuming that human based reasoning is able to identify significant part of the existing hazards, the application of the simulation should be perhaps directed to the complex scenarios.

Considering the differences between the systematic structure of both methods, the device-oriented approach used in the computational procedure detected more causes, although many of them were irrelevant, as one can see in simulations S-5, S-6 S-27 and S-28. Those causes were not even discussed during the HAZOP analysis due to the capacity of the group of filtering relevant discussions. On the other hand, the device-

oriented approach was assertive on embracing all process devices, while the process-oriented approach, depending on the scope of HAZOP deviations, can sometimes difficult covering all process devices, as was exemplified in simulation S-37. Nevertheless, the HAZOP method can trigger creative thinking, which was the main reason for the additional causes identified in the heuristic-based study, which was not covered by the computational-based one.

Approximately one third of the discussions started from the same causes but resulted in different safety impacts. When the computational based results were less assertive than the human-based approach, it can be observed that the human-based approach counted on the thinking-together capacity of the team members allowing for correlation of effects beyond the limited result given by the simulation results of the safety-critical variables. However, since no quantitative and dynamic information about the process behavior were available, the HAZOP group has prone to conservative conclusions, which can imply on misdirected resource prioritization and unnecessary investments in posterior process decision-making.

Some important learnings can be extracted from the comparison between the two methods:

- Both HAZOP teams had the perception of being unconservative or conservative when they in fact were (comparing with the simulation results) and would recommend process simulations to check their understandings. In the cases of significant different results, in 60% of the cases the HAZOP team was not confident and recommended the simulation.
- In some cases, the inclusion of a flow model with pressure drop and pressure propagation would be helpful to support understanding the final consequences.

- The HAZOP team creativeness allowed for identification of mid and long-term effects after the failure occurrence. Besides, possible effects regarding restart-up after the failure condition, was discussed. This introduces a relevant aspect that should have been added to the computational based methodology: simulate a malfunction step and, from the malfunction condition, simulate a step back to the normal value.

Finally, comparing the two human-based studies, the variability of the human based approach was verified by comparison between the similar causes from the different HAZOP studies. They differed in mechanism (see discussion 1m versus 1m*), in creativity (see discussion 1c versus 1c*) and also about the understanding of the final scenario (see discussion 3a versus 3a*). This result reinforces the subjective nature of the traditional HAZOP, emphasizing that human factors, as experience, discipline and technical formation can significantly affect the final result of hazard identification analyses.

Chapter 6

Conclusions

The present study investigated the use of a computational-based hazard identification method, discussing the model development, the hazard identification systematic and the simulation results, in order to compare to a traditional human-based procedure.

38 simulation scenarios were identified providing dynamic responses of process critical variables to support precise identification of hazard mechanisms. In the present work the heuristic approach was generally more conservative than the computational-based study which, in some cases, led to overestimation of process hazards. In fewer cases, the human-based study also overlooked some hazard mechanisms.

Nevertheless, it was shown that in almost 50% of the discussed scenarios the human experience was sufficiently precise to identify the process responses when disturbed by malfunctions, especially when scenarios were not safety critical. When the scenario complexity increased and moved nearer safety relevant consequences, the differences between the computational and human-based methods were emphasized. However, for approximately 60% of the cases where major differences were observed between the methodologies, the HAZOP team was able to diagnose that the proposed discussion could be imprecise and were able to recommend a computational analysis to supplement their known limitation.

It is also remarkable that, in some cases, the traditional method boosted human creativity and encouraged the reasoning beyond the immediate relation between cause and consequence. The interpretation of simulation results caused by malfunction devices, somehow limited the extrapolation of consequences. Though, the computational-based

procedure was more systematic and allowed better documentation of hazards, since the simulations enabled the observation of multiple behaviors of state variables, some of which are not usually measured in the real plant, providing better understanding of the critical scenario occurrence mechanism and also dynamic information of process behavior and threshold values for critical deviations.

It was also noticed that, depending on the procedure, different causes could be identified. Thus, it is import to recognize that, although the computational approach is more precise and systematic, it is based on a heuristic identification of malfunctions and still carries the possibility of uncovered hazards.

It was shown that the process-oriented approach was more repetitive and that reasoning the process in nodes (grouping many equipment and pipelines) may contribute to overlooking potential hazard sources. The limitation of the used HAZOP-deviations may also have contributed to this factor. However, reasoning the process in terms of deviations of process variables triggered more creative thinking.

Regarding the human effort to perform the different approaches, the computational-based method and model development depended on the collaboration of different authors (MATTOS NETO; PINTO, 2001; PRATA, 2009; SILVA, 2018), while the HAZOP required a team of few member. Besides, the HAZOP was performed in some couple of hours, while the modeling process to capture all malfunction scenarios and finally the simulations took some months.

By comparing models with different levels of detail, it was observed that, in most cases, the simplest model was able to satisfactorily describe the scenario. Therefore, one could conclude that the level of detail of the model should be adaptable to the demand. In some cases, for example, a flow model with pressure drop would be sufficient to evaluate pressure propagation, since this is an important variable to evaluate process safety.

However, this work did not develop a model to fill this gap and the heuristic analysis was necessary to extrapolate the consequences from the simulation results. Thus, one can notice that a more detailed process model is less dependent on the heuristic approach.

To complement the phenomenological simulation, a frequency approach, using Monte Carlo simulation, was used in the context of hazard identification, to support the evaluation of the probability for occurrence of simultaneous failures in a system of multiple interaction devices. Considering that the case study embraced more than 30 failure modes with different failure rates, Monte Carlo simulations allowed the validation of the proposed procedure, which considered one failure per simulation, as the probability of simultaneous failures was equal to 0,56%. The combination of multiple failures would significantly increase the number of scenarios with no practical relevance for the case study, as demonstrated by Monte Carlo simulations. Besides, it could be observed that the presence of high failure devices increased the probability of simultaneous failures, which, could direct the analysis to more restricted set of possibilities.

In conclusion, one could notice that the modeling process for safety applications constitutes an important time-consuming step, since the assumptions and parameters must cover a wide range of operational conditions. Besides that, simulation tools are process specific and cannot be easily adapted for other processes. Nevertheless, it is true that the simulations can enhance the understanding of mechanisms of hazardous scenarios, avoid conservative decision making and avoid overlooking device failures that can pose serious hazard to the process. Moreover, the obtention of process models can enable other computational applications as optimizations, soft sensors, process predictions among others.

Based on the experience achieved in this work, it could be noticed that human experience and process knowledge can indeed save time from the “low added value

simulations". It is recommended then that, instead of doing a complete computational-based analysis, the scenarios should be evaluated first according to human perception, to discard non critical scenarios, saving some time. When it is not clear if maximum allowed conditions can be exceeded or if the dynamic behavior can introduce additional hazards, then the simulation results can be valuable and support understanding of pre-selected complex scenarios, avoiding under or over estimating the potential hazards.

Finally, this work can be a starting point for other safety applications, regarding:

- Stationary simulation and multiple steady-states analyses in the context of hazard identification, since oscillatory and unstable behavior has been reported for this process (DA SILVA ROSA; MELO; PINTO, 2012; OLIVEIRA et al., 2006) and can complement hazard identification studies (LABOVSKÝ et al., 2007b; ŠVANDOVÁ et al., 2005);
- Risk assessment to each scenario and the design of safety barriers since the present hazard identification study alerted for different hazard situations, mainly related to the hydrodynamic collapse of the reaction suspension, that must be prevented and mitigated;
- Design of a safety-based control layer, since the present hazard study identified different device failures leading to undesired hydrodynamic collapse of the reaction suspension that poses significant risk of process shutdown related to the prevention of this consequence (SOARES; PINTO; SECCHI, 2016);
- Proposal of on-line model-based risk in order to indicate the evolution of the process safety and allow for predictive maintenance and effective decision making that can minimize costs and prevent accidents and losses.

Bibliography

Accident Report Detail | Occupational Safety and Health Administration. Disponível em: <https://www.osha.gov/pls/imis/accidentsearch.accident_detail?id=170662498>. Acesso em: 11 nov. 2019.

ANGUS, S.; ARMSTRONG, B.; DE REUCK, K. M. . **7: Propylene (Propene) - International Thermodynamic Tables of the fluid state**. [s.l: s.n.]. v. 7

BARALDI, P.; ZIO, E. A Combined Monte Carlo and possibilistic approach to uncertainty propagation in event tree analysis. **Risk Analysis**, v. 28, n. 5, p. 1309–1325, 2008.

BARTON, J. A.; NOLAN, P. F. **Runaway Reactions in Batch Reactors**. I Chem. E. Symposium. **Anais**...1989

BAYBUTT, P. A critique of the Hazard and Operability (HAZOP) study. **Journal of Loss Prevention in the Process Industries**, v. 33, p. 52–58, jan. 2015.

BERDOUZI, F. et al. Dynamic simulation for risk analysis: Application to an exothermic reaction. **Process Safety and Environmental Protection**, v. 113, p. 149–163, jan. 2018.

BEVILACQUA, M.; BRAGLIA, M.; GABBRIELLI, R. Monte Carlo simulation approach for a modified FMECA in a power plant. **Quality and Reliability Engineering International**, v. 16, n. 4, p. 313–324, 2000.

BLOM, H. A. P.; STROEVE, S. H.; DE JONG, H. H. Safety risk assessment by monte carlo simulation of complex safety critical operations. **Developments in Risk-Based Approaches to Safety - Proceedings of the 14th Safety-Critical Systems Symposium, SSS 2006**, p. 48–67, 2006.

BOWONDER, B. The Bhopal accident. **Technological Forecasting and Social Change**, v. 32, n. 2, p. 169–182, 1987.

BRITTO, R. R. L. DE. **QUANTITATIVE RISK ASSESSMENT USING MONTE CARLO AND DYNAMIC PROCESS SIMULATION**. [s.l: s.n.]. Disponível em: <http://portal.peq.coppe.ufrj.br/index.php/producao-academica/teses-de-doutorado/2018-1/534-quantitative-risk-assessment-using-monte-carlos-and-dynamic-process-simulation/file>. Acesso em: 25 out. 2018.

CASSON MORENO, V.; SALZANO, E.; KHAN, F. Assessing the Severity of Runaway Reactions. In: **Dynamic Risk Analysis in the Chemical and Petroleum Industry**. [s.l.] Elsevier, 2016. p. 127–138.

CENTER FOR CHEMICAL PROCESS SAFETY. **Guidelines for PROCESS EQUIPMENT RELIABILITY DATA with data tables**. New York: American Institute of Chemical Engineers, 1989.

CENTER FOR CHEMICAL PROCESS SAFETY. **Guideline for Hazard Evaluation procedures**. 2. ed. New York: American Institute of Chemical Engineers, 1992.

CENTER FOR CHEMICAL PROCESS SAFETY. **Chemical Process Quantitative RiskAnalysis**. New York: American Institute of Chemical Engineers, 2000.

CENTER FOR CHEMICAL PROCESS SAFETY. **Layer of Protection Analysis: Simplified Process Risk Assessment**. New York: American Institute of Chemical Engineers, 2001.

CERRUTI, L. **Historical and Philosophical Remarks on Ziegler-Natta Catalysts: A Discourse on In-dustrial CatalysisAn International Journal for the Philosophy of Chemistry**. [s.l: s.n.].

COIMBRA, J. C. et al. On-line dynamic data reconciliation in batch suspension polymerizations of methyl methacrylate. **Processes**, v. 5, n. 3, 1 set. 2017.

CROWL, D.; LOUVAR, J. **Chemical Process Safety: Fundamentals with Applicattions**. 2. ed. [s.l: s.n.].

DA SILVA ROSA, I.; MELO, P. A.; PINTO, J. C. **Bifurcation analysis of the bulk**

propylene polymerization in the LIPP process. Macromolecular Symposia. **Anais**...set. 2012

DANKO, M. et al. Integration of process control protection layer into a simulation-based HAZOP tool. **Journal of Loss Prevention in the Process Industries**, v. 57, p. 291–303, jan. 2019.

DEMICHELA, M.; BALDISSONE, G.; CAMUNCOLI, G. Risk-Based Decision Making for the Management of Change in Process Plants: Benefits of Integrating Probabilistic and Phenomenological Analysis. **Industrial & Engineering Chemistry Research**, v. 56, n. 50, p. 14873–14887, 20 dez. 2017.

DUNJÓ, J. et al. Hazard and operability (HAZOP) analysis. A literature review. **Journal of Hazardous Materials**, v. 173, n. 1–3, p. 19–32, 15 jan. 2010.

DURGA RAO, K. et al. Dynamic fault tree analysis using Monte Carlo simulation in probabilistic safety assessment. **Reliability Engineering and System Safety**, v. 94, n. 4, p. 872–883, 2009.

DUTRA, J. C. S. **CONTROLE DE PROCESSOS BASEADO EM ESQUEMAS DE RECONFIGURAÇÃO**. [s.l.] Universidade Federal do Rio de Janeiro, COPPE, 2012.

DUTRA, J. C. S. et al. Control of Bulk Propylene Polymerizations Operated with Multiple Catalysts through Controller Reconfiguration. **Macromolecular Reaction Engineering**, p. 201–216, 2014.

EIZENBERG, S.; SHACHAM, M.; BRAUNER, N. Combining HAZOP with dynamic simulation—Applications for safety education. **Journal of Loss Prevention in the Process Industries**, v. 19, n. 6, p. 754–761, nov. 2006.

FENTON, N.; NEIL, M. **Risk Assessment and Decision Analysis With Bayesian Networks**. [s.l.] CRC Press, 2013.

FENTON, N.; NEIL, M.; MARQUEZ, D. Using Bayesian networks to predict software defects and reliability. **Proceedings of the Institution of Mechanical Engineers, Part**

O: Journal of Risk and Reliability, v. 222, n. 4, p. 701–712, 11 dez. 2008.

FUJITA, M. et al. Thermal hazard evaluation of runaway polymerization of acrylic acid. **Process Safety and Environmental Protection**, v. 129, p. 339–347, set. 2019.

GONZÁLEZ DAN, J. R. et al. Monte Carlo simulation as a tool to show the influence of the human factor into the quantitative risk assessment. **Process Safety and Environmental Protection**, v. 102, p. 441–449, 2016.

GORDON, R. P. E. The contribution of human factors to accidents in the offshore oil industry. **Reliability Engineering and System Safety**, v. 61, n. 1–2, p. 95–108, 1998.

GRAF, H.; SCHMIDT-TRAUB, H. Process hazard identification during plant design by qualitative modelling, simulation and analysis. **Computers & Chemical Engineering**, v. 23, p. S59–S62, jun. 1999.

GRAF, H.; SCHMIDT-TRAUB, H. Early hazard identification of chemical plants with statechart modelling techniques. **Safety Science**, v. 36, n. 1, p. 49–67, out. 2000.

GUSTIN, J. L.; LAGANIER, F. Understanding vinyl acetate polymerization accidents. **Organic Process Research and Development**, v. 9, n. 6, p. 962–975, nov. 2005.

GYENES, Z.; CARSON, P. **Runaway reactions. Part 2 Causes of Accidents in selected CSB case historiesThe European Commission's science and knowledge service**. [s.l: s.n.].

HU, J.; ZHANG, L.; LIANG, W. Opportunistic predictive maintenance for complex multi-component systems based on DBN-HAZOP model. **Process Safety and Environmental Protection**, v. 90, n. 5, p. 376–388, set. 2012.

ICHEME. **Loss Prevention Bulletin - Improving process safety by sharing experience**. [s.l: s.n.]. Disponível em: <www.icheme.org/humanfactors>. Acesso em: 11 nov. 2019.

ISIMITE, J.; RUBINI, P. A dynamic HAZOP case study using the Texas City refinery

explosion. **Journal of Loss Prevention in the Process Industries**, v. 40, p. 496–501, mar. 2016.

JANOŠOVSKÝ, J. et al. The role of a commercial process simulator in computer aided HAZOP approach. **Process Safety and Environmental Protection**, v. 107, p. 12–21, abr. 2017.

JANOŠOVSKÝ, J. et al. Software approach to simulation-based hazard identification of complex industrial processes. **Computers & Chemical Engineering**, jun. 2018.

JOSEPH, G.; KASZNIAK, M.; LONG, L. Lessons after Bhopal: CSB a catalyst for change. **Journal of Loss Prevention in the Process Industries**, v. 18, n. 4–6, p. 537–548, jul. 2005.

KAMINSKY, W. **Polyolefins: 50 years after Ziegler and Natta I - Polyethylene and Polypropyle**. [s.l: s.n.]. v. 258

KELLY, D. L.; SMITH, C. L. Bayesian inference in probabilistic risk assessment—The current state of the art. **Reliability Engineering & System Safety**, v. 94, n. 2, p. 628–643, fev. 2009.

KHAKZAD, N.; KHAN, F.; PALTRINIERI, N. On the application of near accident data to risk analysis of major accidents. **Reliability Engineering & System Safety**, v. 126, p. 116–125, jun. 2014.

KLETZ, T. **What went wrong? Case histories of process plant disasters and how they could have been avoided**. [s.l.] Elsevier Inc., 2009.

LABOVSKÁ, Z. et al. Model-based hazard identification in multiphase chemical reactors. **Journal of Loss Prevention in the Process Industries**, v. 29, p. 155–162, maio 2014.

LABOVSKÝ, J. et al. Mathematical model of a chemical reactor-useful tool for its safety analysis and design. **Chemical Engineering Science**, v. 62, n. 18–20, p. 4915–4919, 2007a.

LABOVSKÝ, J. et al. Model-based HAZOP study of a real MTBE plant. **Journal of Loss Prevention in the Process Industries**, v. 20, n. 3, p. 230–237, 2007b.

LAWLEY, H. G. Operability studies and hazard analysis. **Chemical Engineering Progress**, v. 70, p. 45–56, 1974.

LUO, Z. H.; SU, P. L.; WU, W. Industrial loop reactor for catalytic propylene polymerization: Dynamic modeling of emergency accidents. **Industrial and Engineering Chemistry Research**, v. 49, n. 22, p. 11232–11243, 17 nov. 2010.

LYONDELLBASELL. **Optimized Ziegler-Natta Catalysts for Bulk PP Processes**. Disponível em: <https://www.lyondellbasell.com/globalassets/products-technology/technology/bulk-pp-processes.pdf?id=13745>. Acesso em: 15 nov. 2019.

MADDAH, H. A. Polypropylene as a Promising Plastic: A Review. **American Journal of Polymer Science**, v. 6, n. 1, p. 1–11, 2016.

MALPASS, D. B.; BAND, E. I. **Introduction to Industrial Polypropylene**. [s.l: s.n.].

MANNAN, S. **Lees' Process Safety Essentials: Hazard Identification, Assessment and Control**. 1. ed. [s.l.] Elsevier Inc., 2014.

MARKOWSKI, A. S. et al. Uncertainty aspects in process safety analysis. **Journal of Loss Prevention in the Process Industries**, v. 23, n. 3, p. 446–454, maio 2010.

MATTOS NETO, A. G.; PINTO, J. C. Steady-state modeling of slurry and bulk propylene polymerizations. **Chemical Engineering Science**, v. 56, n. 13, p. 4043–4057, 2001.

MCCOY, S. A.; ZHOU, D.; CHUNG, P. W. H. State-based modelling in hazard identification. **Applied Intelligence**, v. 24, n. 3, p. 263–279, jun. 2006.

MELO JUNIOR, P. A. **Dinâmica e Estabilidade de Reatores Tubulares de Polimerização com Reciclo Title**. [s.l: s.n.].

NEDUZHII, I. A. et al. **Thermodynamic and Transport Properties of Ethylene and Propylene**. Washington, D.C: National Bureau of Standards Department of Commerce, 1972.

NEIL, M. et al. Modelling dependable systems using hybrid Bayesian networks. **Reliability Engineering & System Safety**, v. 93, n. 7, p. 933–939, jul. 2008.

NIST Reference Fluid Thermodynamic and Transport Properties Database (REFPROP version 7). Disponível em: <https://webbook.nist.gov/cgi/fluid.cgi?ID=C115071&Action=Page>. Acesso em: 24 jun. 2019.

NOWICKI, A. W. et al. Heat capacity and turbidity near the critical point of succinonitrile-water. **Journal of Chemical Physics**, v. 114, n. 10, p. 4625–4633, 2001.

NTNU; SINTEF. **OREDA: Offshore and Onshore Reliability Data Volume 1 - Topside Eqipment**. 6. ed. [s.l.] OREDA Participants, 2015.

OHRING, M.; KASPRZAK, L. The Mathematics of Failure and Reliability. In: **Reliability and Failure of Electronic Materials and Devices**. [s.l.] Elsevier, 2015. p. 181–248.

OLIVEIRA, A. G. et al. Steady-state behavior of slurry and bulk propylene polymerization. **Polymer Reaction Engineering**, v. 11, n. 2, p. 155–176, 2006.

OUELLETTE, R. J.; RAWN, J. D. **Organic Chemistry: Structure, Mechanism, and Synthesis**. [s.l: s.n.].

PAPAZOGLOU, I. .; ANEZIRIS, O. . Master Logic Diagram: method for hazard and initiating event identification in process plants. **Journal of Hazardous Materials**, v. 97, n. 1–3, p. 11–30, fev. 2003.

PARMAR, J. C.; LEES, F. P. The propagation of faults in process plants: Hazard identification for a water separator system. **Reliability Engineering**, v. 17, n. 4, p. 303–314, jan. 1987a.

PARMAR, J. C.; LEES, F. P. The propagation of faults in process plants: Hazard identification. **Reliability Engineering**, v. 17, n. 4, p. 277–302, jan. 1987b.

PASMAN, H. **Risk Analysis and Control for Industrial Processes - Gas, Oil and Chemicals**. [s.l: s.n.].

PASMAN, H. J.; ROGERS, W. J.; MANNAN, M. S. Risk assessment: What is it worth? Shall we just do away with it, or can it do a better job? **Safety Science**, v. 99, p. 140–155, nov. 2017.

PASMAN, H. J.; ROGERS, W. J.; MANNAN, M. S. How can we improve process hazard identification? What can accident investigation methods contribute and what other recent developments? A brief historical survey and a sketch of how to advance. **Journal of Loss Prevention in the Process Industries**, v. 55, p. 80–106, set. 2018.

PERRY, R. H. **PERRY'S CHEMICAL ENGINEERS' HANDBOOK**. 7. ed. [s.l: s.n.].

PINTO, J. C. **Personal communications with J.C. Pinto, 03/22/2019**, 2019a.

PINTO, J. C. **Personal communications with J.C. Pinto, 01/21/2019**, 2019b.

POSCH, D. W. **Applied Plastics Engineering Handbook: Processing, Materials, and Applications**. 2. ed. NY, USA: [s.n.].

PRATA, D. M. **Reconciliação robusta de dados para monitoramento em tempo real**. [s.l.] Universidade Federal do Rio de Janeiro, COPPE, 2009.

PRATA, D. M. et al. Nonlinear dynamic data reconciliation and parameter estimation through particle swarm optimization: Application for an industrial polypropylene reactor. **Chemical Engineering Science journal**, v. 64, n. 4, p. 21–22, set. 2009.

RAMÍREZ, P. A. P.; UTNE, I. B. Use of dynamic Bayesian networks for life extension assessment of ageing systems. **Reliability Engineering & System Safety**, v. 133, p. 119–136, jan. 2015.

RAMZAN, N.; COMPART, F.; WITT, W. Methodology for the generation and evaluation of safety system alternatives based on extended Hazop. **Process Safety Progress**, v. 26, n. 1, p. 35–42, mar. 2007.

RAONI, R.; SECCHI, A. R.; DEMICHELA, M. Employing process simulation for hazardous process deviation identification and analysis. **Safety Science**, v. 101, p. 209–219, 1 jan. 2018.

REBILLOT, P. F.; JACOBS, D. T. Heat capacity anomaly near the critical point of aniline-cyclohexane. **Journal of Chemical Physics**, v. 109, n. 10, p. 4009–4014, 1998.

ROSA, I. DA S. **Análise Dinâmica e de estabilidade de Reatores Tubulares de Polimerização de Propeno do tipo LOOP**. [s.l.] Universidade Federal do Rio de Janeiro, COPPE, 2013.

SELIGMANN, B. J. et al. A blended hazard identification methodology to support process diagnosis. **Journal of Loss Prevention in the Process Industries**, v. 25, n. 4, p. 746–759, 2012.

SHACHAM, M.; BRAUNER, N.; CUTLIP, M. B. Open architecture modelling and simulation in process hazard assessment. **Computers & Chemical Engineering**, v. 24, n. 2–7, p. 415–421, jul. 2000.

SHAMIRI, A. et al. **The influence of Ziegler-Natta and metallocene catalysts on polyolefin structure, properties, and processing abilityMaterials**MDPI AG, , 2014.

SILVA, J. DOS S. **OTIMIZACÃO DA TRANSIÇÃO DE GRADES NA POLIMERIZACÃO EM MASSA DO PROPENO**. [s.l.] Universidade Federal do Rio de Janeiro, COPPE, 2018.

SIU, N. O.; KELLY, D. L. Bayesian parameter estimation in probabilistic risk assessment. **Reliability Engineering & System Safety**, v. 62, n. 1–2, p. 89–116, out. 1998.

SOARES, R. M.; PINTO, J. C.; SECCHI, A. R. An optimal control-based safety system

for cost efficient risk management of chemical processes. **Computers & Chemical Engineering**, v. 91, p. 471–484, ago. 2016.

Solve stiff differential equations and DAEs — variable order method - MATLAB ode15s. Disponível em: <https://www.mathworks.com/help/matlab/ref/ode15s.html>. Acesso em: 15 nov. 2019.

ŠVANDOVÁ, Z. et al. Steady States Analysis and Dynamic Simulation as a Complement in the Hazop Study of Chemical Reactors. **Process Safety and Environmental Protection**, v. 83, n. 5, p. 463–471, set. 2005.

TIAN, W.; DU, T.; MU, S. HAZOP analysis-based dynamic simulation and its application in chemical processes. **Asia-Pacific Journal of Chemical Engineering**, v. 10, n. 6, p. 923–935, nov. 2015.

VAIDHYANATHAN, R.; VENKATASUBRAMANIAN, V. Digraph-based models for automated HAZOP analysis. **Reliability Engineering & System Safety**, v. 50, n. 1, p. 33–49, jan. 1995.

VEN, S. VAN DER. **Polypropylene and other Polyolefins: Polymerization and Characterization**. [s.l.] Elsevier, 1990. v. 53

VENART, J. E. S. Flixborough: The explosion and its aftermath. **Process Safety and Environmental Protection**, v. 82, n. 2 B, p. 105–127, 2004.

VENKATASUBRAMANIAN, V.; VAIDHYANATHAN, R. A knowledge-based framework for automating HAZOP analysis. **AIChE Journal**, v. 40, n. 3, p. 496–505, mar. 1994.

WU, J. et al. An integrated qualitative and quantitative modeling framework for computer-assisted HAZOP studies. **AIChE Journal**, v. 60, n. 12, p. 4150–4173, dez. 2014.

Appendix A Verification of Model Implementation

Variations in $\dot{m_{H_2}}$, $\dot{m_{Cat}}$ and in the relation $\dot{m_{TEA}}/\dot{m_{PEEB}}$ from the steady-state condition where $MI = 15\ g.(10\ \text{min})^{-1}$, $XS = 7\%p/p$ and productivity (defined as the ratio between the mass flowrate of polymer and inlet mass flowrate of monomer: $\dot{m_M}\ /\dot{m_{Pol}}$), $Prod = 0{,}45$ were discussed by SILVA (2018), considering temperature dynamics, control loops and additive effects to the catalyst activity.

Using the same control strategy described by SILVA (2018) and neglecting the presence of propane and the recirculation stream, comparable results were obtained, as one can see in Figure A-. The red, blue and green lines represent the process behavior for step variations in the catalyst mass flowrate, hydrogen mass flowrate and TEA/PEEB ratio ($\dot{m_{TEA}}/\dot{m_{PEEB}}$), respectively, when t = 0. For these inputs, the continuous lines are related to the increase of 10% of the respective original condition while the dashed lines are related to the decrease of 10% of the respective original condition.

As expected, the catalyst mass flowrate directly affects the productivity and MI. The availability of catalyst in the reaction medium affects the concentration of catalyst active species and, thus, the monomer conversion and the molar mass distribution. The stereospecificity of the polymer depends hardly on the $TEA/PEEB$ ratio so that the catalyst mass flowrate does not significantly influence the XS content.

As a chain transfer agent, the hydrogen mass flowrate directly affects MI, but inversely affects the productivity. The concentration of hydrogen in the reaction medium affects the rate of chain transfer influencing the length of polymer chains and also the

monomer conversion. As discussed before, the chain transfer agent has no significant influence on the stereospecificity of the polymer and, thus, does not affect the XS content.

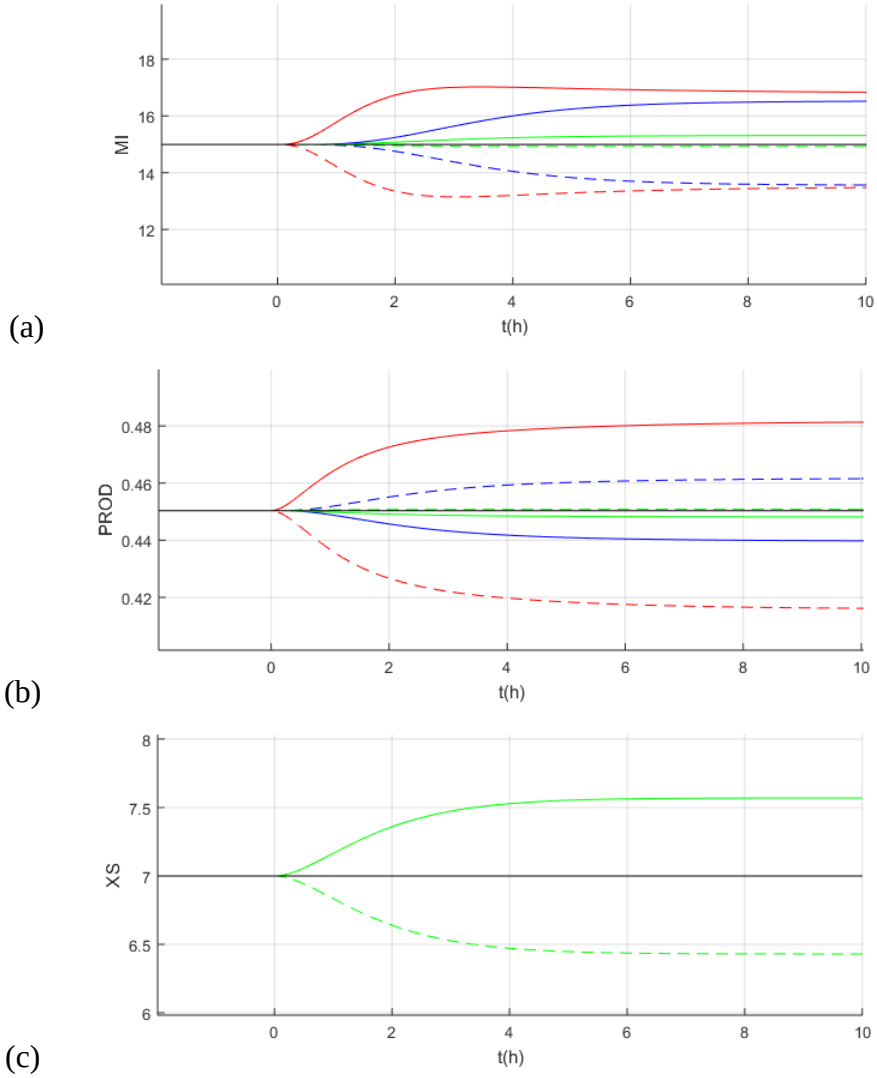

Figure A-1 – Effect on process variables caused by changing input conditions: (a) Melting Index ($g.(10min)^{-1}$); (b) Productivity; (c) Xylene Soluble content (%p/p)

(——) Original Steady State; (——) +10% Catalyst mass feed; (- - -) -10% Catalyst mass feed; (——)+10% Hydrogen mass feed; (- - -) -10% Hydrogen mass feed; (——)+10% TEA/PEEB ratio; (- - -) -10% TEA/PEEB ratio;

Finally, one can see that the $TEA/PEEB$ ratio is capable of significantly changing the XS content, with minor effects on MI and XS content. The relation between catalyst, co-catalyst and Lewis bases changes the polymer stereospecificity and can control the polymer isotacticity. As TEA and $PEEB$ play a secondary role on the propagation rate,

the monomer conversion and the molar mass distribution do not significantly change when $TEA/PEEB$ ratio changes.

SILVA (2018) also presented the influence of manipulated variables after an increase of 10% on the catalyst mass feed. This disturbance was also simulated, resulting on comparable trajectories of the controlled and manipulated variables.

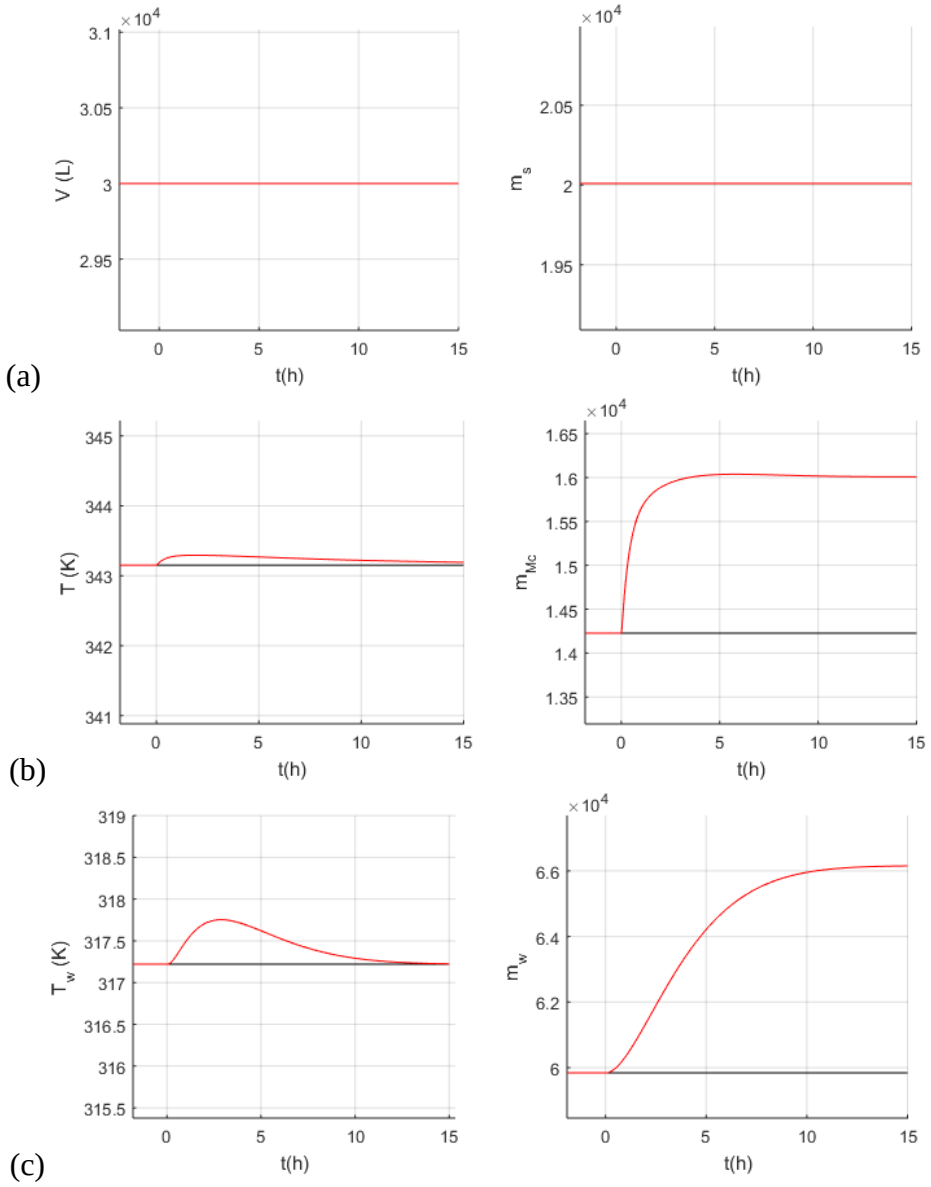

Figure A-2 - Effect on the controlled and manipulated variables caused by changing catalyst mass feed rate

(___) Original Steady State; (___) +10% Catalyst mass feed rate;

With the increment on the catalyst mass feed rate, no significant effect on volume was seen, which is reasonable because it represents a small amount of mass when compared to the monomer feed. On the other hand, both reactor and water temperatures were disturbed due to activation of the reactor, but controllers increased both the rate of condensation and mass flowrate of water, returning the temperatures to the desired setpoints (or original steady states).

Finally, a disturbance in the catalyst mass feed rate was simulated considering reactor temperature setpoint increase (+3°C). The red and green-lines represent the process behavior after catalyst mass feed rate variation, and the addition of simultaneous temperature setpoint increase, respectively. For both, the continuous lines are related to the increase of 10% in the catalyst mass feed rate while the dashed lines are related to the decrease of 10% in the catalyst mass feed rate.

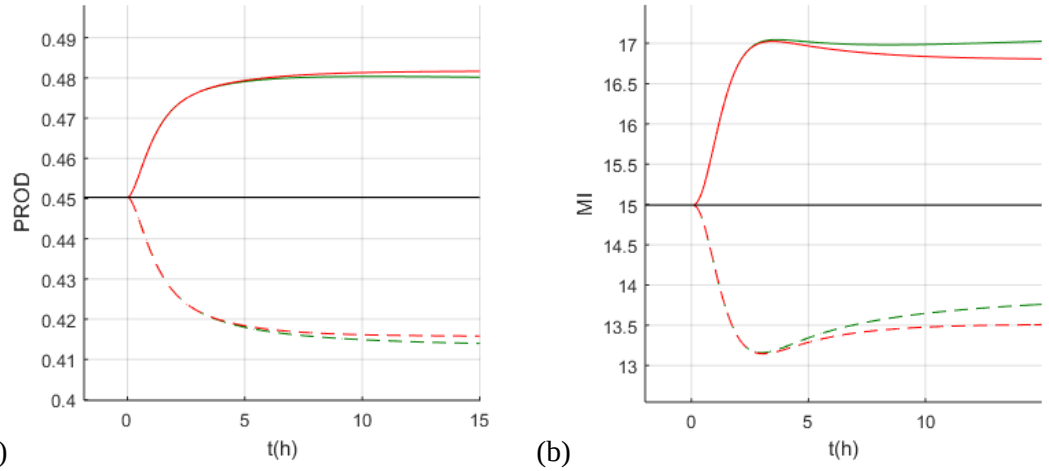

(a) (b)

Figure A-3 - Effect on the process variables caused by changing input conditions: (a) Melting Index ($g.(10min)^{-1}$); (b) Productivity;

(——) Original Steady State; (——) +10% Catalyst mass feed rate; (- - -) -10% Catalyst mass feed rate; (——) +10% Catalyst mass feed rate and +3°C in T_{sp}; (- - -) -10% Catalyst mass feed rate and +3°C in T_{sp}

The reactor temperature setpoint increase exerted a major influence on MI, which may be related to the increase of reaction rates, affecting the chain transfer reactions remaining reaction steps. The temperature setpoint effect on productivity, as shown by SILVA (2018), was not significant. Figure A-, Figure A-2 and Figure A-3 validate the first model implementation step, since reasonable results and comparable responses regarding previous works could be obtained.

Appendix B Thermodynamic Parameters for Model Development

The data presented in this appendix are based on the publications of ANGUS, ARMSTRONG and DE REUCK (1980)

Table B-1 – Numerical Values and Contributory terms of the equation of state for calculation of properties.

i	b_i	c_i	d_i	ψ_i	$(X)_i$	$(X\rho)_i$	$(XT)_i$	$(XC)_i$
1	-6.55352	-6.74467	-4.49239	0.186248	$\omega\tau$	$2\omega\tau$	0	0
2	0.957646	104.1707	-217.979	-1.29261	$\omega\tau^2$	$2\omega\tau^2$	$-\omega\tau^2$	$2\omega\tau^2$
3	-4.74703	-361.099	-22.7582	-0.0541	$\omega\tau$^3	$2\omega\tau^3$	$-2\omega\tau^3$	$6\omega\tau^3$
4	1.193142085086	570.3992	143.8328	1.013803	ω^2	$3\omega^2$	ω^2	0
5		-439.539	53.11794	-2.12123	$\omega^2\tau$	$3\omega^2\tau$	0	0

i	b_i	c_i	d_i	ψ_i	$(X)_i$	$(X\rho)_i$	$(XT)_i$	$(XC)_i$
6		135.5082	-1.09856	1.526272	$\omega^2\tau^2$	$3\omega^2\tau^2$	$-\omega^2\tau^2$	$\omega^2\tau^2$
7		-1.32312	26.01365	-0.25522	$\omega\hat{}3\ \tau\hat{}2$	$4\omega^3\ \tau^2$	$-\omega^3\tau^2$	$2\omega^3\ \tau^2/3$
8			-223.582	1.314788	$\omega^3\tau^3$	$4\omega^3\tau^3$	$-2\omega^3\tau^3$	$2\omega^3\tau^3$
9				-0.04565	$\omega^4\tau^{-1}$	$5\omega^4\tau^{-1}$	$2\omega^4\tau^{-1}$	$\omega^4\tau^{-1}/2$
10				0.09266	ω^4	$5\omega^4$	ω^4	0
11				0.102015	$\omega^4\tau$	$5\omega^4\tau$	0	0
12				-2.2931	$\omega^4\tau^3$	$5\omega^4\tau^3$	$-2\omega^4\tau^3$	$3\omega^4\ \tau^3/2$
13				1.251448	$\omega^5\tau^3$	$6\omega^5\tau^3$	$-2\omega^5\tau^3$	$6\omega^5\tau^3/5$

i	b_i	c_i	d_i	ψ_i	$(X)_i$	$(X\rho)_i$	$(XT)_i$	$(XC)_i$
14				-0.28104	$\omega^6\tau^3$	$7\omega^6\tau^3$	$-2\omega^6\tau^3$	$\omega^6\tau^3$
15				0.022766	$\omega^7\tau^3$	$8\omega^7\tau^3$	$-2\omega^7\tau^3$	$6\omega^7\tau^3/7$
16				-0.23516	$\omega^2\tau^5E$	$(3+a)\omega^2\tau^5\,E$	$-4\omega^2\tau^5E$	$10A_1\tau^5E/\alpha$
17				0.220999	$\omega^4\tau^5\,E$	$(5+a)\omega^4\tau^5E$	$-4\omega^4\tau^5E$	$10A_2\tau^5E/\alpha$
18				0.336805	$\omega^6\tau^3E$	$(7+a)\omega^6\tau^3E$	$-2\omega^6\tau^3E$	$3A_3\tau^3E/\alpha$
19				-0.02102	$\omega^8\tau^3E$	$(9+a)\omega^8\tau^3E$	$-2\omega^8\tau^3E$	$3A_4\tau^3E/\alpha$
20				0.029849	$\omega^{10}\tau^3E$	$(11+a)\omega^{10}\,\tau^3E$	$-2\omega^{10}\tau^3E$	$3A_5\tau^3E/\alpha$
21				0.000285	$\omega^{14}\tau^4E$	$(15+a)\omega^{14}\tau^4E$	$-3\omega^{14}\tau^4E$	$6A_7\tau^4E/\alpha$

where:

- $E = \exp(\alpha\omega^2)$
- $a = 2\alpha\omega^2$
- $\alpha = -1$

Table B-2 – Auxiliary Terms

j	A_j
1	1
2	$\omega^2 - A_1/\alpha$
3	$\omega^4 - 2A_2/\alpha$
4	$\omega^6 - 3A_3/\alpha$
5	$\omega^8 - 4A_4/\alpha$
6	$\omega^{10} - 5A_5/\alpha$
7	$\omega^{12} - 6A_6/\alpha$

Appendix C Possible Failure Modes of Process Devices

Table C-1– Possible Failure Modes.

Item	Description	Function	Failure Mode	Simulation Reference
1	Monomer Make-Up stream	Add fresh monomer to the reactor	No mass: pump failure, valve inadvertently closed	S-1
			Less mass: control failure, plugging	S-2
			More mass: control failure	S-3
			Other composition: off spec raw material (more propane)	S-4
		Add energy to the reactor	Less Energy: lower inlet temperature	S-5
			More Energy: higher inlet temperature	S-6
2	Hydrogen feed stream	Add hydrogen to the reactor	No mass: valve inadvertently closed	S-7
			Less mass: control failure	S-8
			More mass: control failure	S-9

Item	Description	Function	Failure Mode	Simulation Reference
3	PEEB feed stream	Add additive (PEEB) to the reactor	No mass: pump failure, valve inadvertently closed	S-10
			Less mass: control failure, plugging	S-11
			More Mass: control failure	S-12
4	TEA feed stream	Add additive (TEA) to the reactor	No mass: pump failure, valve inadvertently closed	S-13
			Less mass: control failure, plugging	S-14
			More mass: control failure	S-15
5	Catalyst feed stream	Add catalyst to the reactor	No mass: pump failure, valve inadvertently closed	S-16
			Less mass: control failure, plugging	S-17
			More mass: control failure	S-18
			Other composition: off spec raw material (reduced activity)	S-19
6	Condensation stream	Condensate reactor vapors	No mass: valve inadvertently closed	S-20
			Less mass: control failure, plugging	S-21
			More mass: control failure	S-22
7	Heat exchanger tubes	Exchange energy	Less energy: fouling	S-23

Item	Description	Function	Failure Mode	Simulation Reference
8	Cooling water stream	Add cooling water to heat exchanger	No mass: valve inadvertently closed	S-24
			Less mass: control failure	S-25
			More mass: control failure	S-26
		Remove energy from the reactor	Less energy: higher inlet temperature	S-27
			More energy: lower inlet temperature	S-28
9	Slurry outlet stream	Remove mass from the Reactor	No mass: pump failure, valve inadvertently closed	S-29
			Less mass: control failure, plugging	S-30
			More mass: control failure	S-31
10	Polymer outlet stream	Remove polymer from reactor (in the gas separator)	Less mass: plugging	S-32
11	Recycled monomer purge stream	Remove recycled monomer from the Reactor	No mass: valve inadvertently closed	S-33
			Less mass: control failure	S-34
			More mass: control failure	S-35
12	Compression and condensation unit	Send back the recycled monomer to the reactor	No mass: unit failure (valve inadvertently closed, compressor failure)	S-36
			Less mass: compressor reduced capacity	S-37

Item	Description	Function	Failure Mode	Simulation Reference
13	Agitator	Keep reactor mass and temperature homogeneous	No agitation: motor failure	S-38

Appendix D Failure rates of devices

Table D-1 – Failure rates for device malfunctions as considered in the simulations.

Simulation Reference	**Description**	**Failure Mode**	$\boldsymbol{\lambda_{device}}$ $\boldsymbol{(h^{-1})}$	**Failure can be mitigated?**	$\boldsymbol{PFD_{backup}}$	$\boldsymbol{\lambda_{ie}}$ $\boldsymbol{(h^{-1})}$	**Test interval, Θ** $\boldsymbol{(h)}$	**Average failure probability,** $\boldsymbol{P_{avg}}$
S-1	Monomer make-up stream	No mass: pump failure, valve inadvertently closed	2.08E-06	Stand-by pump with automatic start-up	9.06E-03	1.88E-08	8760	0.008%
S-2	Monomer make-up stream	Less mass: control failure, plugging	2.79E-05	No	1.00E+00	2.79E-05	8760	11.268%
S-3	Monomer make-up stream	More mass: control failure	2.79E-05	No	1.00E+00	2.79E-05	8760	11.268%
S-4	Monomer make-up stream	Other composition: raw material off spec (more propane)	NAD	No	NA	NA	NA	NA
S-5	Monomer make-up stream	Less energy: inlet temperature lower	NAD	No	NA	NA	NA	NA

Simulation Reference	Description	Failure Mode	λ_{device} (h^{-1})	Failure can be mitigated?	PFD_{backup}	λ_{ie} (h^{-1})	Test interval, Θ (h)	Average failure probability, P_{avg}
S-6	Monomer make-up stream	More energy: inlet temperature higher	NAD	No	NA	NA	NA	NA
S-7	Hydrogen feed stream	No mass: valve inadvertently closed	NAD	No	NA	NA	NA	NA
S-8	Hydrogen feed stream	Less mass: control failure	2.79E-05	No	1.00E+00	2.79E-05	8760	11.268%
S-9	Hydrogen feed stream	More mass: control failure	2.79E-05	No	1.00E+00	2.79E-05	8760	11.268%
S-10	PEEB feed stream	No mass: pump failure, valve inadvertently closed	3.13E-06	Stand-by pump with automatic start-up	1.36E-02	4.25E-08	8760	0.019%
S-11	PEEB feed stream	Less mass: control failure, plugging	2.79E-05	No	1.00E+00	2.79E-05	8760	11.268%
S-12	PEEB feed stream	More mass: control failure	2.79E-05	No	1.00E+00	2.79E-05	8760	11.268%
S-13	TEA feed stream	No mass: pump failure, valve inadvertently closed	3.13E-06	Stand-by pump with	1.36E-02	4.25E-08	8760	0.019%

Simulation Reference	Description	Failure Mode	λ_{device} (h^{-1})	Failure can be mitigated?	PFD_{backup}	λ_{ie} (h^{-1})	Test interval, Θ (h)	Average failure probability, P_{avg}
				automatic start-up				
S-14	TEA feed stream	Less mass: control failure, plugging	2.79E-05	No	1.00E+00	2.79E-05	8760	11.268%
S-15	TEA feed stream	More mass: control failure	2.79E-05	No	1.00E+00	2.79E-05	8760	11.268%
S-16	Catalyst feed stream	No mass: pump failure, valve inadvertently closed	3.13E-06	Stand-by pump with automatic start-up	1.36E-02	4.25E-08	8760	0.019%
S-17	Catalyst feed stream	Less mass: control failure, plugging	2.79E-05	No	1.00E+00	2.79E-05	8760	11.268%
S-18	Catalyst feed stream	More mass: control failure	2.79E-05	No	1.00E+00	2.79E-05	8760	11.268%
S-19	Catalyst feed stream	Other composition: raw material off spec (reduced activity)	NAD	No	NA	NA	NA	NA
S-20	Condensation stream	No mass: valve inadvertently closed	NAD	No	NA	NA	NA	NA

Simulation Reference	Description	Failure Mode	λ_{device} (h^{-1})	Failure can be mitigated?	PFD_{backup}	λ_{ie} (h^{-1})	Test interval, Θ (h)	Average failure probability, P_{avg}
S-21	Condensation stream	Less mass: control failure, plugging	2.79E-05	No	1.00E+00	2.79E-05	8760	11.268%
S-22	Condensation stream	More mass: control failure	2.79E-05	No	1.00E+00	2.79E-05	8760	11.268%
S-23	Heat exchanger tubes	Less energy: fouling	NAD	No	NA	NA	NA	NA
S-24	Cooling water stream	No mass: valve inadvertently closed	NAD	No	NA	NA	NA	NA
S-25	Cooling water stream	Less mass: control failure	2.79E-05	No	1.00E+00	2.79E-05	8760	11.268%
S-26	Cooling water stream	More mass: control failure	2.79E-05	No	1.00E+00	2.79E-05	8760	11.268%
S-27	Cooling water stream	Less energy: inlet temperature higher	NAD	No	NA	NA		
S-28	Cooling water stream	More energy: inlet temperature lower	NAD	No	NA	NA		

Simulation Reference	Description	Failure Mode	λ_{device} (h^{-1})	Failure can be mitigated?	PFD_{backup}	λ_{ie} (h^{-1})	Test interval, Θ (h)	Average failure probability, P_{avg}
S-29	Slurry Outlet Stream	No mass: pump failure, valve inadvertently closed	3.73E-06	Stand-by pump with automatic start-up	9.06E-03	3.38E-08	8760	0.015%
S-30	Slurry outlet stream	Less mass: control failure, plugging	3.69E-05	No	1.00E+00	3.69E-05	8760	14.556%
S-31	Slurry outlet stream	More mass: control failure	3.69E-05	No	1.00E+00	3.69E-05	8760	14.556%
S-32	Polymer outlet stream	Less mass: plugging	NAD	No	NA	NA	NA	NA
S-33	Recycled monomer purge stream	No mass: valve inadvertently closed	NAD	No	NA	NA	NA	NA
S-34	Recycled monomer purge stream	Less mass: control failure	2.43E-03	No	1.00E+00	2.43E-03	168	17.881%
S-35	Recycled monomer purge stream	More mass: control failure	2.43E-03	No	1.00E+00	2.43E-03	168	17.881%

Simulation Reference	**Description**	**Failure Mode**	$\boldsymbol{\lambda_{device}}$ $(\boldsymbol{h^{-1}})$	**Failure can be mitigated?**	$\boldsymbol{PFD_{backup}}$	$\boldsymbol{\lambda_{ie}}$ $(\boldsymbol{h^{-1}})$	**Test interval, Θ** $(\boldsymbol{h})$	**Average failure probability,** $\boldsymbol{P_{avg}}$
S-36	Compression and condensation unit	No mass: unit failure (valve inadvertently closed, compressor failure)	3.01E-05	Stand-by compressor with automatic start-up	5.27E-02	1.58E-06	8760	0.691%
S-37	Compression and condensation unit	Less mass: compressor reduced capacity	9.50E-07	Stand-by compressor with automatic start-up	5.27E-02	5.01E-08	8760	0.022%
S-38	Agitator	No agitation: motor failure	NAD	No	NA	NA	NA	NA

Appendix E Hazard Analysis from Simulation Results

Table E-1 – Hazard Analysis Table from Simulation Results.

Simulation Reference	Failure Mode	Risk Related Consequence (Heuristic Analysis)
S-1 and S-2	No/Less flow at monomer make-up stream: pump failure, valve inadvertently closed, control failure	Self-sustaining reduction of monomer feed that results on the hydrodynamic collapse, even for small disturbances (decrease) in the make-up flow. Assets damage and possibility of LOPC.
S-3	More flow at monomer make-up stream: control failure	Self-sustaining increase of monomer feed that results on the overload and overpressure of the compression unit, even for small disturbances (increase) in the make-up flow. Possibility of exceeding MAWP with LOPC.
S-4	Other composition at monomer make-up stream: off spec raw material (more propane)	No relevant effect of the safety critical variables.
S-5 and S-6	Less/More energy at monomer make-up stream: inlet temperature lower/higher	No relevant effect of the safety critical variables.
S-7 to S-9	No/Less/More flow at hydrogen feed stream: valve inadvertently closed, control failure	Small disturbances on the polymer fraction with no relevant effect of the safety critical variables.

Simulation Reference	Failure Mode	Risk Related Consequence (Heuristic Analysis)
S-10 to S-12	No/Less/More flow at PEEB feed stream: pump failure, valve inadvertently closed, control failure, plugging	Small disturbances on the polymer fraction with no relevant effect of the safety critical variables.
S-13	No flow at TEA feed stream: pump failure, valve inadvertently closed.	Deactivation of reaction that can result on the overload and overpressure of the compression unit, if the $m_{\dot{M},SP}$ greater than recycled monomer system capacity. Possibility of exceeding MAWP with LOPC.
S-14 and S-15	Less/More flow at TEA feed stream: control failure and plugging	Small decrease of polymer content with no relevant effect of the safety critical variables.
S-16	No flow at Catalyst feed stream: pump failure, valve inadvertently closed	Deactivation of reaction that can result on the overload and overpressure of the compression unit, if the $m_{\dot{M},SP}$ greater than recycled monomer system capacity. Possibility of exceeding MAWP with LOPC.
S-17 and S-19	Less flow at catalyst feed stream: control failure, plugging OR Other composition at catalyst feed stream: raw material off spec (reduced activity)	Small decrease of polymer content with no relevant effect of the safety critical variables.
S-18	More flow at catalyst feed stream: control failure	Increase on reaction conversion that results on the hydrodynamic collapse.

Simulation Reference	Failure Mode	Risk Related Consequence (Heuristic Analysis)
S-20 and S-21	No/Low flow at condensation stream: valve inadvertently closed, control failure, plugging	Reactor temperature and pressure increase but still bellow maximum allowed equipment limits (inherent safer design). No relevant effect of the safety critical variables.
S-22	More flow at condensation stream: control failure	Small reduction of temperature, pressure and increase of polymer fraction with no relevant effect of the safety critical variables.
S-23	Less energy through heat exchanger tubes: fouling	Significant increase of reactor temperature and pressure increase but still bellow maximum allowed equipment limits (inherent safer design). No relevant effect of the safety critical variables.
S-24 and S-25	No/Low flow at cooling water stream: valve inadvertently closed, control failure	Reactor temperature and pressure increase but still bellow maximum allowed equipment limits (inherent safer design). No relevant effect of the safety critical variables.
S-26	More flow at cooling water stream: control failure	No relevant effect of the safety critical variables.
S-27 and S-28	Less/More energy at cooling water stream: inlet temperature disturbance	Disturbances on reactor temperature with no relevant effect of the safety critical variables.
S-29 and S-30	No/Less flow at slurry outlet stream: pump failure, valve inadvertently closed, control failure, plugging	Reactor overfilling with overpressure above MAWP followed by hydrodynamic collapse. Equipment damage with structural failure and LOPC.

Simulation Reference	Failure Mode	Risk Related Consequence (Heuristic Analysis)
S-31	More flow at slurry outlet stream: control failure	Reactor running dry with possibility of damage of liquid operating downstream equipment.
S-32	Less flow at polymer outlet stream: plugging	Sending polymer to the compression unit. Damage of the compression unit equipment.
S-33 and S-34	No/ Less flow at recycled monomer purge stream: valve inadvertently closed, control failure	No relevant effect of the safety critical variables
S-35	More flow at recycled monomer purge stream: control failure	Sudden reduction of monomer inlet rate, increasing reactor residence time and leading to the hydrodynamic collapse.
S-36	No flow through compression and condensation unit: unit failure (compressor failure, valve inadvertently closed, etc)	Sudden reduction of monomer inlet rate, increasing reactor residence time and leading to the hydrodynamic collapse.
S-37	No Agitation: motor failure	Polymer accumulation in the bottom of reactor that resulting on the hydrodynamic collapse.

Appendix F Traditional HAZOP Discussion

Table F-1 – HAZOP Discussion Results.

Deviation	Cause	Consequence	Scenario Reference
Low Flow	Monomer inlet flow control failure reducing make-up injection	Increase of reactor residence time and accumulation of the other reactants, including catalyst. Consequent increase of the slurry viscosity with possibility of hydrodynamic collapse. The increase the slurry viscosity can accelerate fouling on slurry pipe internal surface, with the possibility of premature saturation of level control actions. See discussion for scenario 1g.	1a
		Reduction of reactions conversion. Quality issues. Not safety relevant.	1b

Deviation	Cause	Consequence	Scenario Reference
	Catalyst inlet flow control failure reducing catalyst injection	The accumulation of monomer due to reaction deactivation could lead to an increase of reaction rate, when the catalyst flow is reestablished. Consequently, a fast release of energy with temperature and pressure rise exceeding maximum allowed conditions cannot be neglected. Observation: The final consequence was conservatively considered. For a more accurate result the group would recommend a simulation of the kinetic model.	1b* [6]
	TEA inlet flow control failure reducing TEA injection	Reduction of reactions conversion. Quality issues (less severe than scenario 1b). Not safety relevant.	1c
		The accumulation of monomer due to reaction deactivation could lead to an increase of reaction rate, when the TEA flow is reestablished. Consequently, a fast release of energy with temperature and pressure rise exceeding maximum allowed conditions cannot be neglected.	1c* [6]

[6] Discussions performed by a second HAZOP team that differ from the original group.

Deviation	Cause	Consequence	Scenario Reference
		Observation: The final consequence was conservatively considered. For a more accurate result the group would recommend a simulation of the kinetic model.	
	PEEB inlet flow control failure reducing PEEB injection	Only quality issues. Not safety relevant.	1d
	Level control failure reducing slurry valve opening at the reactor outlet stream	Increase of reactor level and, consequently, its residence time. The mass accumulation inside reactor may lead to overpressure of equipment. LOPC cannot be neglected.	1e
		Increase of reactor level sending liquid to condenser. Interruption of latent heat exchange with mass accumulation inside reactor. The thermal expansion of liquid will lead to overpressure of equipment. LOPC cannot be neglected.	1e* (6)
		Increase of reactor level and, consequently, the residence time, increasing the slurry viscosity with possibility of hydrodynamic collapse. Equipment damage and LOPC cannot be neglected.	1f
	Partial Plugging of slurry outlet line	Premature saturation of level control actions. See discussion for scenarios 1e and 1f.	1g

Deviation	Cause	Consequence	Scenario Reference
	Hydrogen inlet flow control failure reducing Hydrogen injection	Increase of polymer chain length leading to quality issues and increasing slurry viscosity. Possibility of hydrodynamic collapse cannot be neglected, although is not fully expected. Observation: The final consequence was conservatively considered. For a more accurate result the group would recommend a simulation of the kinetic model.	1h
		The increase the slurry viscosity can accelerate fouling on slurry pipe internal surface and jeopardize level and temperature measurement, with possibility of premature failure of level and temperature control actions. See discussion for scenarios 1g and 1j.	1h* (6)
	Water temperature control failure reducing cooling water valve opening	Depending on the magnitude of failure, this may lead to the saturation of reactor temperature control actions. See discussion for scenario 1j.	1i

Deviation	Cause	Consequence	Scenario Reference
	Reactor temperature control failure reducing valve opening to condenser	Increase of reactor temperature leading to runaway reaction. Abrupt rise of conversion and slurry viscosity with possibility of hydrodynamic collapse. Significant pressure increase associated to the temperature rise may exceed equipment maximum allowed conditions. LOPC cannot be neglected.	1j
		Same discussion but with the following observation: The final consequence was conservatively considered. For a more accurate result the group would recommend a simulation of the kinetic model due to proximity to critical temperature.	1j* (6)
	Fouling on condenser tubes	Reduction of heat exchange capacity, resulting on reduction of energy efficiency. Not safety relevant.	1k
	Partial Plugging of gas pipeline from separator due to polymer dragging	See discussion for scenario 8c.	1l
	Recycled monomer purity control failure reducing purge valve opening	Accumulation of propane can deactivate catalyst system resulting on reduced conversion. Quality issues. Not safety relevant. ----------	1m, 1m* (6)

Deviation	Cause	Consequence	Scenario Reference
	Partial Plugging of purge pipeline due to polymer dragging	The accumulation of propane (inert) can increase pressure, but with no relevant impact for safety [6].	1n
No Flow	Monomer inlet flow control failure closing make-up valve	With no make-up flow, propane concentration inside reactor will increase. Besides, monomer feed rate will decrease and thus the reactor residence time will increase and the accumulation of the other reactants, including catalyst will occur. Consequent rise of the slurry viscosity with possibility of hydrodynamic collapse. Observation: It is not expected that the increase of propane concentration inside reactions will significantly affect catalyst activity since for this scenario, the catalyst activity remains stable.	2a
	Catalyst inlet flow control failure interrupting catalyst feed	Reaction death. Not safety relevant.	2b
	TEA inlet flow control failure interrupting TEA feed	Reactions death. Not safety relevant.	2c

Deviation	Cause	Consequence	Scenario Reference
	PEEB inlet flow control failure interrupting PEEB feed	Only quality issues. Not safety relevant.	2d
	Level control failure closing slurry valve at the reactor outlet stream	See discussion for scenarios 1e and 1f.	2e
	Hydrogen inlet flow control failure interrupting hydrogen feed	See discussion for scenarios 1h.	2f
	Water temperature control failure closing cooling water valve	See discussion for scenario 1j.	2g
	Reactor temperature control failure closing valve to condenser	See discussion for scenarios 1j.	2h
	Recycled monomer purity control failure closing purge valve	See discussion for scenarios 1m and 1n.	2i

Deviation	Cause	Consequence	Scenario Reference
	Compression and condensation unit failure	Interruption of monomer recycled stream back to reactor. See discussion for scenario 3i.	2j
High Flow	Monomer inlet flow control failure increasing make-up injection	The increase of propene concentration inside reactor reducing the purge rate will trigger a cumulative increasing effect on the monomer mass rate to reactor reducing residence time and thus reactions conversion. Besides, the saturation of level control actions is possible, leading to reactor overfilling and overpressure. LOPC cannot be neglected.	3a
		The level control will open the slurry valve reducing residence time and thus monomer conversion. This may overload the compression unit with over pressure	3a* (6)
	Catalyst inlet flow control failure increasing catalyst injection	Increase of propagation reactions rate with possible saturation of reactor temperature control actions leading to reactor temperature increase and runaway reactions. Abrupt rise of conversion and slurry viscosity with possibility of hydrodynamic collapse. Significant pressure increase associated to the temperature rise may exceed equipment maximum allowed conditions. LOPC cannot be neglected. Observation: The increase of catalyst flow has negligible effects to the residence time due its magnitude compared to monomer flow.	3b

Deviation	Cause	Consequence	Scenario Reference
	TEA inlet flow control failure increasing TEA injection	Reduction of reaction conversion. Quality issues. Not safety relevant.	3c
	PEEB inlet flow control failure increasing PEEB injection	Reduction of reaction conversion. Quality issues. Not safety relevant.	3d
	Level control failure increasing slurry valve opening at the reactor outlet stream	Level reduction leading to reaction dry running.	3e
		By running dry agitator sealing can be damaged leading to leakages.	3e* (6)
	Hydrogen inlet flow control failure increasing hydrogen injection	Decrease of polymer chain length leading to quality issues and increasing the polymer dragging to the recovered gas system. This situation can accelerate plugging of gas pipe lines. See discussion for scenarios 1l and 1n.	3f
	Water temperature control failure increasing cooling water valve opening	Decrease of reactor temperature and dropping conversion. Possibility of reaction death. Not safety relevant.	3g

Deviation	Cause	Consequence	Scenario Reference
	Reactor temperature control failure increasing valve opening to condenser	Decrease of reactor temperature and dropping conversion. Possibility of reaction death. Not safety relevant.	3h
	Recycled monomer purity control failure increasing purge valve opening	Reduction of recycled monomer sent back to reactor. Increase of propene and decrease of propane concentration leading to propagation reaction increase. Polymer chain length will increase and thus the viscosity. Only quality issues. Not safety relevant. Observation: Although it is not expected the hydrodynamic collapse due to purge failure, the group would recommend a simulation of the kinetic model to confirm this evaluation.	3i
Other Flow (Contamination)	Monomer Off-spec (more propane)	Monomer purity control at the recycled stream will adjust purge rate in order to keep stable operation. Not safety relevant.	4a
	Catalyst Off-spec (more active)	See discussion for scenario 3b.	4b
	Catalyst Off-spec (less active)	See discussion for scenario 1b.	4c
	Inner Leakage at Condenser	Water pressure is lower than reactor pressure. Contamination of cooling water system is possible. But no safety relevant effect to the reactor system.	4d

Deviation	Cause	Consequence	Scenario Reference
Reverse Flow	Compression and condensation unit failure	Make-up monomer sent to compression unit, reducing monomer flow to reactor. See discussion for scenario 1a.	5a
High temperature	Water temperature control failure reducing cooling water valve opening	See discussion for scenario 1i.	6a
	Reactor temperature control failure reducing valve opening to condenser	See discussion for scenario 1j.	6b
	Water temperature control failure closing cooling water valve	See discussion for scenario 2g.	6c
	Reactor temperature control failure closing valve to condenser	See discussion for scenario 2h.	6d
	Catalyst inlet flow control failure increasing catalyst injection	See discussion for scenario 3b.	6e

Deviation	Cause	Consequence	Scenario Reference
	Condensation unit failure	Abrupt increase of reactor temperature with runaway reaction. Rise of conversion and slurry viscosity with possibility of hydrodynamic collapse. Significant pressure increase associated to the temperature rise may exceed equipment maximum allowed conditions. LOPC cannot be neglected.	6f
Low Temperature	Water temperature control failure increasing cooling water valve opening	See discussion for scenario 3g.	7a
	Reactor temperature control failure increasing valve opening to condenser	See discussion for scenario 3h.	7b
	Reaction Death	See discussion for scenario 3h.	7c
High Pressure	Level control failure reducing slurry valve opening at the reactor outlet stream	See discussion for scenario 1e.	8a
	Reactor temperature control failure reducing valve opening to condenser	See discussion for scenario 1j.	8b

Deviation	Cause	Consequence	Scenario Reference
	Partial Plugging of gas pipeline from separator due to polymer dragging	Pressure increase at separator and back pressure propagation may exceed equipment maximum allowed conditions. LOPC cannot be neglected. Observation: The final consequence was conservatively considered. For a more accurate result, the group would recommend a simulation of a flowing model.	8c
	Monomer inlet flow control failure increasing make-up injection	See discussion for scenario 3a.	8d
	Catalyst inlet flow control failure increasing catalyst injection	See discussion for scenario 3b.	8e
Low Pressure	Low Temperature	Reducing temperature will reduce pressure. See discussion for "Low Temperature" scenarios.	9a
High Level	Level control failure reducing slurry valve opening at the reactor outlet stream	See discussion for scenarios 1e and 1f.	10a

Deviation	Cause	Consequence	Scenario Reference
	Partial Plugging of slurry outlet line	See discussion for scenario 1g.	10b
	Monomer inlet flow control failure increasing make-up injection	See discussion for scenario 3a.	10c
	Plugging of polymer outlet from separator	Sending slurry to compression system may damage compressor.	10d* (6)
Low Level	Level control failure increasing slurry valve opening at the reactor outlet stream	See discussion for scenario 3e.	11a